

**Herschel/Planck**  
Consolidated Report on  
Mission Analysis  
Issue 3.1  
PT-MA-RP-0010-OPS-GMA

by  
Martin Hechler, Arturo Yáñez

January 19, 2006



*ESOC European Space Operations Centre*

## Abstract

This document records, summarises or consolidates the mission analysis work performed for the Herschel/Planck mission. It is regularly updated and maintained to reflect the most recent knowledge on the spacecraft design, and to refine the mission analysis to the level required at launch.

The Herschel/Planck mission has been designed such that ARIANE5E/CA, with an optimum ascent trajectory, will inject the two spacecraft together onto the stable manifold of a large amplitude Lissajous orbit around  $L_2$ . Herschel will remain on this orbit. For Planck an optimum transfer strategy from there to an orbit with a smaller maximum sun-spacecraft-Earth angle of  $15^\circ$  has been constructed. A deviation from the Herschel orbit will be generated together with the first stochastic orbit correction manoeuvre 2 days from launch and one or two insertion manoeuvres will inject to the Planck orbit. The optimisation includes the choice of the in plane and out of plane amplitudes of that target Lissajous orbits as function of the launch time. The optimum manoeuvre strategies and the presented launch window guarantee a mission without eclipse for both spacecraft. The launch window from August 2007 to end 2008 is presented.

Estimates of the required propellant allocations for the Planck orbit insertion manoeuvre and all stochastic orbit corrections during the transfer and finally for the maintenance of the operational orbits are given, and the reachable orbit determination accuracies are derived.

## Change Record

Date	Issue no.	Rev. no.	Pages aff.	Description
1999/12/15	0	0	all	Draft Issue
2000/05/05	1	0		Implementing comments by project team and project scientists
2000/09/30	1	1		Draft development version
2001/07/30	1	2		Refinement and extension of scenario 2. Update of launcher dispersion and resulting updates of propellant budget
2002/06/25	2	0	all	Correction of numerical values of escape direction in section 2.3 Additional parameters in section 3.2 (Doppler, Doppler rate). Refinement of A5E/SV launch window in section 3.3. Consolidated launch scenario for A5E/CA (sub-optimum ascent) in section 3.4. Herschel orbit amplitude and launch clock angle condition in sections 3.3 and 3.4. Update of section 4.3 (navigation during transfer). Update of section 4.4 (orbit determination in Lissajous orbit). Implementation of comments from flight dynamics. Update of propellant budget and conclusions
2003/09/01	2	1		Update of launcher scenario, sub-optimum A5E/CA case with 7.5° line of apsides rotation has a major impact mainly on chapters 3, major changes in propellant budget and time until Planck operational orbit is reached (two manoeuvre strategies for A5E/CA case). All figures have been unified to the definition of the rotating frame with the x-axis from sun to Earth.
2004/06/14	2	2		Chapter 3: Update of launcher scenario, optimum A5E/CA case, change of spacecraft design to allow sun aspect angle at fairing jettison down to 20°. Update of launcher dispersion (transfer propellant estimate) not yet implemented. Update of orbit determination study (0.1 mm/s Doppler). Refinement of orbit maintenance study. Update of propellant budget and conclusions.
2004/07/16	2	3		Chapter 3: New reference case on 2007/11/15. Chapter 4: Update of orbit determination study (range bias estimation every day). Update of launcher dispersion and estimate of transfer correction manoeuvres. Chapter 5: Update of propellant budget (50 m/s for first correction).

2005/01/07	3	0		<p>Section 3.6, Earth aspect angle at insertion manoeuvre  Figure 3.4, amplification factor for perigee velocity variation  Section 3.8.4, update of estimate for day 2 correction, and Moon aspect angle from day 1 to day 3  Section 3.8.5, Eclipses and occultations by the moon  Section 4.5, effect of wheel offloading and helium venting on Herschel orbit  Section 4.4.2, update of predictability, including helium venting  Update of <math>\Delta V</math> budget</p>
2006/01/19	3	1		<p>Section 2.5 removed.</p> <p>All chapter 3 updated for new optimum Planck transfer strategy with deviation from stable manifold. Launch window calculations extended to 2008.</p> <p>Update of launcher dispersion in section 4.1 and update of transfer propellant estimates.</p> <p>Update of <math>\Delta V</math> budget in section 5.1 (one flight program on ARIANE + new transfer optimisation).</p>

## Document Approval

		Signature	Date
<b>Prepared by:</b>	M. Hechler, A. Yáñez - OPS/GA		
<b>Approved by:</b>	S. J. Dodsworth - OPS/OF		
<b>Authorised by:</b>	A. Elfving - SCI/PL		

*Electronic version not signed.*

## Distribution

Recipient	Organisation	Copies
all MAS staff	OPS/GA	
S.J. Dodsworth	OPS/O	
Micha Schmidt	OPS/O	
C.G. Watson	OPS/O	
Catherine Watson	OPS/O	
A. Head	OPS/O	
G. Gienger	OPS/GF	
J. Schoenmaekers	OPS/GF	
R. Cramm	OPS/GF	
F. Dreger	OPS/GF	
T. Morley	OPS/GF	
U. Feucht	OPS/GF	
A. Elfving	ESTEC	
P. Estaria	ESTEC	
T. Passvogel	ESTEC	

# Contents

<b>1</b>	<b>Introduction</b>	<b>1</b>
1.1	Purpose of Document . . . . .	1
1.2	Document Status . . . . .	1
1.3	Background . . . . .	2
<b>2</b>	<b>Theory of Lissajous Orbits Around <math>L_2</math></b>	<b>4</b>
2.1	Basic Dynamic Properties . . . . .	4
2.2	General Solution of the Linearised Differential Equations . . . . .	4
2.3	Escape Direction in the Linear Problem . . . . .	7
2.4	Numerical Construction of Lissajous Orbits . . . . .	7
<b>3</b>	<b>Transfer Optimisation, Launch Window and Reference Orbit</b>	<b>9</b>
3.1	Transfer Optimisation . . . . .	9
3.1.1	Basic Transfer Optimisation Assumptions and Previous Calculations . . . . .	9
3.1.2	Optimum Orbit Insertion for Planck . . . . .	11
3.1.3	ARIANE Performance and Launch Conditions . . . . .	12
3.1.4	Assumptions on Spacecraft and Target Orbit . . . . .	13
3.1.5	Planck Insertion Manoeuvre Propellant Allocation Update . . . . .	14
3.2	The Herschel/Planck Launch Window, Winter 2007/2008 . . . . .	16
3.2.1	Reference Launch Window Definition . . . . .	16
3.2.2	Reference Delivery Conditions by ARIANE for one Flight Program . . . . .	17
3.2.3	Moon Aspect Angles During Early Transfer . . . . .	19
3.2.4	Option with Multiple ARIANE Flight Programs . . . . .	21
3.3	The Herschel/Planck Launch Window 2008 . . . . .	21
3.3.1	Extension of Launch Window into Summer 2008 . . . . .	21
3.3.2	Launch Window, Second Half of 2008 . . . . .	24
3.4	Orbit Parameters over Launch Window, Winter 2007/2008 . . . . .	26
3.4.1	Planck Orbit Parameters . . . . .	26
3.4.2	Herschel Orbit Parameters over Launch Window . . . . .	33
3.4.3	Orbit Shapes over Launch Window, Winter 2007/2008 . . . . .	37
3.5	Reference Orbits for Herschel and Planck . . . . .	40
3.5.1	Planck Reference Orbit (Launch on 2007/11/15) . . . . .	40
3.5.2	Herschel Reference Orbit (Launch on 2007/11/15) . . . . .	45
3.5.3	Ground Station Coverage at Begin of Mission . . . . .	48
3.5.4	Ground Station Coverage in Operational Orbit . . . . .	56
3.6	Eclipses and Occultations by the Moon . . . . .	61
3.6.1	Duration and Depth of Eclipses by the Moon . . . . .	61
3.6.2	Avoidance of Eclipses by the Moon by Manoeuvres . . . . .	67
3.6.3	Eclipses by the Moon on Herschel . . . . .	70
3.6.4	Conclusions on Eclipses by the Moon . . . . .	70
3.6.5	Occultations by the Moon . . . . .	71

<b>4</b>	<b>Navigation and Orbit Maintenance</b>	<b>72</b>
4.1	Assumptions . . . . .	72
4.1.1	Tracking . . . . .	72
4.1.2	Noise . . . . .	72
4.1.3	Manoeuvre Execution . . . . .	73
4.1.4	Launcher Dispersion . . . . .	73
4.2	Navigation During Transfer . . . . .	74
4.2.1	First Orbit Correction on Day 2 . . . . .	74
4.2.2	Later Stochastic Transfer Orbit Correction Manoeuvres . . . . .	76
4.3	Orbit Determination in the Operational Lissajous Orbits . . . . .	77
4.3.1	Reference Operational Orbit . . . . .	77
4.3.2	Knowledge of Operational Orbit . . . . .	79
4.4	Orbit Maintenance . . . . .	83
4.4.1	Choice of Orbit Control Method . . . . .	83
4.4.2	Orbit Predictability . . . . .	85
4.4.3	Influence of Noise . . . . .	87
4.4.4	Time between Manoeuvres . . . . .	87
4.5	Orbit Maintenance with Wheel Off-loading and Helium Venting for Herschel . . . . .	90
4.5.1	Wheel off-loadings . . . . .	90
4.5.2	Effect of the Helium exhaust flow . . . . .	93
4.5.3	Treatment of the orbit perturbations . . . . .	93
4.5.4	Perturbing Forces . . . . .	93
4.5.5	Simulation results . . . . .	94
4.5.6	Helium venting during LEOP . . . . .	94
4.5.7	Required Increase of Maintenance $\Delta V$ . . . . .	95
4.6	Effect of Spin Axis Slew Manoeuvres for Planck . . . . .	95
<b>5</b>	<b>Conclusions</b>	<b>97</b>
5.1	$\Delta V$ Budget . . . . .	97
5.2	Summary of Results . . . . .	98
5.3	Open Issues . . . . .	99

## List of Tables

3.1	Reference launch orbit conditions . . . . .	12
3.2	Launcher axes orientation in launch pad system (case 1) . . . . .	12
3.3	Planck thruster mounting ad efficiencies . . . . .	14
3.4	Launch Window (45 minutes per day, no eclipses by Earth) . . . . .	17
3.5	Reference apogee radius for 1 flight program . . . . .	18
3.6	Reference apogee radii for 4 flight programs . . . . .	21
3.7	Transfer orbital parameters (reference case) . . . . .	42
3.8	Ground station coverage during first week in orbit (5° minimum elevation) . . . . .	48
3.9	Ground station coverage during first week in orbit (10° minimum elevation) . . . . .	49
3.10	3 $\sigma$ dispersion at tracking acquisition . . . . .	51
3.11	Doppler and Doppler rate from after 50 days . . . . .	56
3.12	Eclipses without and with 5 m/s z-manoevre on day 140 (Sept 9 launch) . . . . .	70
4.1	A5E/CA transfer orbit with dispersions . . . . .	73
4.2	Correlation factors of dispersion in orbital elements . . . . .	73
4.3	Launcher dispersion in local frame at perigee . . . . .	74
4.4	Correction $\Delta V$ as function of the execution time . . . . .	75
4.5	Launch date dependence of first orbit corrections . . . . .	75
4.6	Transfer Orbit Corrections . . . . .	76
4.7	Orbit Determination Accuracy . . . . .	79
4.8	Station keeping $\Delta V$ for 2 years (maximum of 20 simulations) . . . . .	83
4.9	$E_T$ Matrix for Herschel . . . . .	91
4.10	$E_F$ Matrix for Herschel . . . . .	92
4.11	$\Delta V$ budget for orbit maintenance, m/s per year . . . . .	94
4.12	Linear momentum per day (kg m/s) of slew manoeuvres . . . . .	95
4.13	Acceleration by slew manoeuvres ( $km/s^2$ ) . . . . .	95
5.1	$\Delta V$ budget for Herschel and Planck (A5E/SV - 15° Orbit) . . . . .	97

## List of Figures

1.1	Geometry of libration points in sun-Earth system . . . . .	2
2.1	Typical Lissajous orbit around $L_2$ . . . . .	6
2.2	Universal escape and non-escape directions of linear problem . . . . .	8
3.1	Launch window 2007 . . . . .	10
3.2	Launch window 2008 . . . . .	10
3.3	Equivalent $\Delta V$ for Planck transfer (LW opening) . . . . .	15
3.4	Equivalent $\Delta V$ for Planck transfer (LW closing) . . . . .	15
3.5	Equivalent $\Delta V$ for optimum Planck transfer (LW opening and closing) . . . . .	16
3.6	Deviation required Planck perigee velocity from that of Herschel . . . . .	17
3.7	Perigee velocity relative to escape velocity (LW opening and closing) . . . . .	18
3.8	Amplification factor for correction of variation of perigee velocity (per m/s) . . . . .	19
3.9	Sun-spacecraft-moon angle during transfer (30 days from 2007/8/1) . . . . .	20
3.10	Moon aspect angle around first orbit correction - $95^\circ$ . . . . .	20
3.11	Star mapper blinding at first orbit correction (spring 2008) . . . . .	22
3.12	Perigee velocity variation (spring 2008) . . . . .	23
3.13	Perigee velocity variation (spring 2008) . . . . .	23
3.14	Equivalent $\Delta V$ (LW opening and closing, end 2008) . . . . .	24
3.15	Perigee velocity (LW opening and closing, end 2008) . . . . .	25
3.16	Moon blinding (LW opening and closing, end 2008) . . . . .	25
3.17	Launch hour . . . . .	26
3.18	Sun aspect angle of launcher axis at event FJ . . . . .	27
3.19	Sun aspect angle of launcher axis at event H3 . . . . .	27
3.20	Size of orbit insertion manoeuvre for Planck . . . . .	28
3.21	Time to orbit insertion manoeuvre for Planck . . . . .	28
3.22	Size of out of plane manoeuvre for Planck . . . . .	29
3.23	Time of out of plane manoeuvre for Planck . . . . .	29
3.24	Maximum declination for Planck . . . . .	30
3.25	Minimum declination for Planck . . . . .	30
3.26	Y-amplitude for Planck . . . . .	31
3.27	Z-amplitude for Planck . . . . .	31
3.28	Sun aspect angle of -velocity on day 2 . . . . .	32
3.29	Maximum sun-spacecraft-Earth angle for Herschel . . . . .	33
3.30	Declination versus visibility duration ( $5^\circ$ minimum elevation) . . . . .	34
3.31	Declination versus visibility duration ( $10^\circ$ minimum elevation) . . . . .	34
3.32	Maximum declination for Herschel . . . . .	35
3.33	Minimum declination for Herschel . . . . .	35

3.34	Y-amplitude for Herschel . . . . .	36
3.35	Z-amplitude for Herschel . . . . .	36
3.36	Variation of orbit shape for Herschel (right) and Planck (left) August-September 2007 . . .	37
3.37	Variation of orbit shape for Herschel (right) and Planck (left) October-December 2007 . . .	38
3.38	Variation of orbit shape for Herschel (right) and Planck (left) January-March 2008 . . . . .	39
3.39	Transfer and Lissajous Orbit for PLANCK, 2007/11/15 launch . . . . .	40
3.40	Transfer and Lissajous Orbit for PLANCK (3D), 2007/11/15 launch . . . . .	41
3.41	Transfer and Lissajous Orbit for PLANCK, 2007/11/15 launch (inertial) . . . . .	43
3.42	Transfer and Lissajous Orbit for PLANCK, 2007/11/15 launch (parameters) . . . . .	44
3.43	Transfer and Lissajous Orbit for Herschel, 2007/11/15 launch (inertial) . . . . .	45
3.44	Transfer and Lissajous Orbit for HERSCHEL, 2007/11/15 launch . . . . .	46
3.45	Transfer and Lissajous Orbit for Herschel, 2007/11/15 launch (parameters) . . . . .	47
3.46	Ground track and altitude over first day of mission (A5E/CA-optimum) . . . . .	50
3.47	First tracking path from New Norcia . . . . .	51
3.48	Dispersion at tracking acquisition from New Norcia . . . . .	52
3.49	Long track and cross track errors as function of time . . . . .	52
3.50	Slant range from ground stations over first 3 days . . . . .	53
3.51	Elevation from ground stations over first 3 days . . . . .	53
3.52	Azimuth (North to East) from ground stations over first 3 days . . . . .	54
3.53	Doppler from ground stations over first 3 days . . . . .	54
3.54	Doppler rate from ground stations over first 3 days . . . . .	54
3.55	Doppler rate over first 8 hours . . . . .	55
3.56	Station-spacecraft-sun angle (deg) over first 8 hours . . . . .	55
3.57	Ground station coverage from New Norcia, 2007/11/15 launch . . . . .	57
3.58	Ground station coverage from Cebreros, 2007/11/15 launch . . . . .	58
3.59	Ground station coverage from New Norcia, 2007/10/17 launch, at closing of window . . . . .	59
3.60	Ground station coverage of Herschel jointly with Rosetta, Venus and Mars . . . . .	60
3.61	Duration of eclipses by the moon at opening of launch window in second half of 2007 . . . . .	62
3.62	Duration of eclipses by the moon at closing of launch window in second half of 2007 . . . . .	62
3.63	Depth of eclipses by the moon at opening of launch window in second half of 2007 . . . . .	63
3.64	Depth of eclipses by the moon at closing of launch window in second half of 2007 . . . . .	63
3.65	Power-normalised depth of eclipses by the moon at opening of launch window 2007 . . . . .	64
3.66	Power-normalised depth of eclipses by the moon at closing of launch window 2007 . . . . .	64
3.67	Normalised depth of eclipses versus duration (opening of window) . . . . .	65
3.68	Normalised depth of eclipses versus duration (closing of window) . . . . .	65
3.69	Duration times depth of eclipses by moon (opening of window) . . . . .	66
3.70	Duration times depth of eclipses by moon (closing of window) . . . . .	66
3.71	Depth of eclipses by the moon for eclipses on 2007/9/7, closing of window . . . . .	67

3.72	Depth of eclipses by the moon for eclipses on 2007/9/9, closing of window . . . . .	67
3.73	September 7 orbit at closing of window . . . . .	68
3.74	September 9 orbit at closing of window . . . . .	68
3.75	Normalised eclipse depth as function of time of 5 m/s z-manoeuve . . . . .	69
3.76	Occultations by the moon . . . . .	71
4.1	Launch Dispersion $\Delta V$ at day 2 (99-percentiles) over the launch window (old dispersion) .	76
4.2	Possible time dependence of second orbit correction manoeuvre . . . . .	77
4.3	Fit of Planck reference orbit from insertion manoeuvre . . . . .	78
4.4	Fit of Herschel reference orbit from day 20 . . . . .	78
4.5	Position determination accuracy for Herschel. Doppler and 1 point Range . . . . .	81
4.6	Position determination accuracy for Planck. Doppler and 1 point Range . . . . .	81
4.7	Velocity determination accuracy for Herschel. Doppler and 1 point Range . . . . .	82
4.8	Velocity determination accuracy for Planck. Doppler and 1 point Range . . . . .	82
4.9	Accumulated and single $\Delta V$ 's over 2 years with method 5 (Herschel) . . . . .	84
4.10	Orbit predictability for prescribed reference orbit (Herschel) . . . . .	85
4.11	Orbit predictability for free non-escape control (Planck) . . . . .	86
4.12	Orbit predictability for free non-escape control (Herschel) . . . . .	86
4.13	Double radiation pressure noise (Herschel) . . . . .	87
4.14	Double radiation pressure noise (Planck) . . . . .	88
4.15	Double coordinate acceleration noise . . . . .	88
4.16	Smaller manoeuvre execution error . . . . .	89
4.17	Time between manoeuvres (Herschel) . . . . .	89
4.18	Time between manoeuvres (Herschel with helium venting) . . . . .	90
4.19	Accelerations by radiation pressure and slews . . . . .	96
4.20	Orbit with non-gravitational perturbations . . . . .	96

# 1 Introduction

## 1.1 Purpose of Document

This Herschel/Planck Consolidated Report on Mission Analysis (CReMA) will compile or summarise all mission analysis results for Herschel/Planck which have been produced before the current date of issue and are still applicable at that date.

So in particular it will

- record the dynamic properties of the two different Lissajous orbits around  $L_2$  used for Herschel and Planck including the orbit maintenance and navigation issues,
- describe the transfer strategy for the chosen carrier option (Herschel and Planck on the same ARIANE 5 launcher) and the resulting launch window conditions,
- compile the  $\Delta V$  budget.

The **purpose of this document** is to provide a controlled reference to the spacecraft contractor and to ESA staff which collects all relevant information from Mission Analysis.

## 1.2 Document Status

The MAS working papers no. 393, 398, 402 and 412, [5], [6], [7], [8], give a full account of the mission analysis work performed for Herschel and Planck before phase B. Working paper 393 comprises all aspects of mission analysis from orbit selection to navigation at pre phase A level. The other working papers refine particular aspects, mainly related to the use of the linear theory for the construction of Lissajous orbits, transfers to those, and eclipse avoidance manoeuvres. An update of the navigation and orbit maintenance analysis had been done as part of a study contract [9]. CReMA issue 1.0 (5/2000) was based on the above references alone. It was part of the ITT for the industrial design and development contract for First/Planck, provided to the spacecraft contractor as an applicable document to the system specification.

Issue 1.2 incorporated the mission analysis work done from end 2000 to August 2001. The new parts covered the update of the propellant estimate for the first orbit correction manoeuvre based on an updated launcher dispersion matrix received from Arianespace. In addition the mission scenario with a parking orbit before the transfer has been studied in detail. Whereas this scenario in issue 1.0 was introduced for the case of very large launcher dispersion (which is now known to be rather moderate) in issue 1.2 it has been extended mainly to move the launch hour away from local midday and thus to satisfy for the Herschel telescope a sun aspect angle condition during the ascent trajectory. Issue 1.2 reflected the status of the mission analysis work at that time and was input to the System Requirements Review in August 2001.

The latter scenario with a parking orbit had been overcome by introducing a sub-optimum ascent trajectory for ARIANE5E/CA. With this new concept a common spacecraft design for the baseline ARIANE5E/SV and the backup ARIANE5E/CA launch was possible. This had been incorporated in issue 2.0. Issue 2.0 also updated the navigation analysis for the transfer and in the Lissajous orbits. Issue 2.0 has been prepared as input to the Preliminary Design Review in July 2002.

Issue 2.1 refined the A5E/CA launch scenario (sub-optimum ascent) which had become the baseline at that time. The A5E/SV case was not further possible, so the corresponding results have been removed.

Issue 2.2 completely updated the launch window following a change in the launch scenario baseline and a resulting spacecraft redesign to satisfy the sun aspect angle condition at fairing separation for the optimum ARIANE ascent. The discussions on previous launch scenarios have been removed from the CReMA, but have been kept in a working paper [13]. The other major update was on the orbit control in the operational orbit detailed in [14]. The launcher dispersion had not yet been updated in issue 2.2. Also the update of the reference orbit had been postponed at that stage.

Issue 2.3 further refined the launch window and updated all reference orbit data for a launch on 2007/11/15. The estimate for the first orbit correction manoeuvre has been updated using new input for the launcher dispersion.

Issue 3.0 describes a the full mission baseline after confirmation of the launcher dispersion by Arianespace. In addition the effects of the Helium venting on Herschel have been included. This led to an increase in the  $\Delta V$  budget.

Issue 3.1 completely updates the transfer strategy following a better solution found by ESOC Flight Dynamics. As a consequence of this the launch window, the reference orbit description and the transfer navigation results have also been updated. Launch window calculations have been extended into 2008.

### 1.3 Background

Orbits around the co-linear libration points in the Earth-sun system ( $L_1$  about  $1.5 \times 10^6$  km from the Earth towards the sun and  $L_2$  at about the same distance away from the sun) have been used for space missions since 1978, when ISEE-3 was launched into a Halo orbit around  $L_1$ . SOHO is still in such an orbit around  $L_1$ . Ideas for such missions (in the Earth-moon system) reach back to the early 60's (Giuseppe Colombo, Bob Farquhar [3]).

The orbits around  $L_2$  in the Earth-sun system have become of particular interest for astronomy missions, e.g. the New Generation Space Telescope, because they allow uninterrupted observation activities as Earth and sun remain more or less close together seen from the spacecraft (see figure 1.1), and they have a very stable thermal and radiation environment. Major drawbacks of these orbits are the large communications distance, the long transfer duration, and the necessity of orbit maintenance maneuvers about once per month to counteract the instability. Nevertheless, as a result of trade-off studies performed in 1997/1998, Lissajous orbits around  $L_2$  have been selected for the ESA Astronomy missions Herschel and Planck.

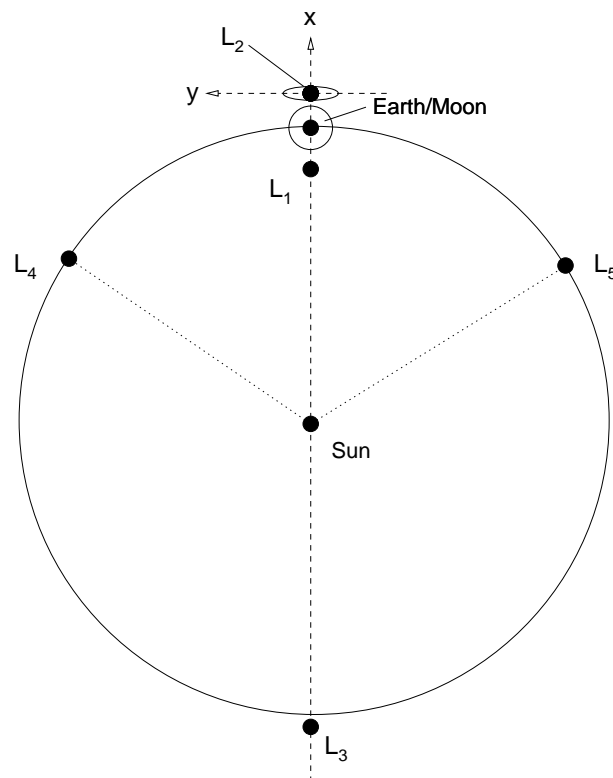


Figure 1.1: Geometry of libration points in sun-Earth system

The Herschel/Planck project is the 4th cornerstone project in the ESA Science program. It consists of two missions. Herschel is dedicated to far infrared Astronomy. Planck (renamed from COBRAS/SAMBA which was originally selected as Medium Size Mission M3) is to map the microwave background over the whole sky. The two mission have been combined for a launch in 2007. Several options have been studied

for this combined mission. First in the so-called "Merger" option both scientific payloads were planned to be integrated into one spacecraft and placed onto a small size Lissajous orbit around  $L_2$ . Another option "Planck alone" was assumed to use a Soyuz launch and lunar fly-bys for Planck.

In the finally adopted option, called the "Carrier" in the ITT, which then evolved to a double launch scenario using ARIANE provided interface equipment (e.g. SYLDA), the two spacecraft (Herschel and Planck) will be launched by the same ARIANE 5 rocket, but will separate immediately after launch, and then transfer to different orbits around  $L_2$  as explained later.

## 2 Theory of Lissajous Orbits Around $L_2$

### 2.1 Basic Dynamic Properties

Instability is a basic dynamic property of the co-linear libration points. This means a spacecraft placed in those points which theoretically are at gravitational equilibrium in the system rotating with the Earth around the sun, will move away from those points because small perturbations of the orbit cannot be avoided, and each small deviation will amplify as explained below. This property is inherited by the family of orbits which exist 'around the libration points'.

Placing a spacecraft into the libration point  $L_2$  itself does not appear desirable. The spacecraft would be permanently in the Earth half shadow, and the  $\Delta V$  to stop the spacecraft at  $L_2$  from the transfer orbit would be about 500 m/s to 600 m/s for ARIANE perigee conditions (cases which allow to use a lunar gravity assists may make this easier). But there is a family of 'quasi periodic orbits' around  $L_2$  which appear well suited for space missions. Some properties of these orbits will be discussed in the following, starting from the linear approximation, and then extending to the construction of transfer and maintenance strategies in the exact problem.

### 2.2 General Solution of the Linearised Differential Equations

We denote the ecliptic plane as the  $xy$ -plane with the  $x$ -axis from the sun to the Earth/moon baricentre in the rotating frame, and  $z$  out of the ecliptic. We chose the coordinates centred at the Libration point  $L_2$ . As usual, the coordinates are normalised by choice of the distance unit as the sun-Earth distance (1 AU = 1.4959610<sup>8</sup> km) and the corresponding time unit is set as  $\frac{1 \text{ year}}{2\pi}$  (with sidereal years).

Using the linear approximation for the circular restricted three-body problem, the differential equations of the relative motion then can be written as

$$\left. \begin{aligned} \ddot{x} - 2\dot{y} - (1 + 2K)x &= 0 \\ \ddot{y} + 2\dot{x} - (1 - K)y &= 0 \\ \ddot{z} + Kz &= 0 \end{aligned} \right\} \quad (2.1)$$

$K$  is a constant depending on the masses only

$$K = \frac{\mu}{x_L^3} + \frac{1 - \mu}{(1 + x_L)^3} \quad (2.2)$$

with

$$\mu = \frac{m_2}{m_1 + m_2} \quad (m_1 = \text{mass of sun}, m_2 = \text{mass of Earth} + \text{moon}).$$

$x_L$  is one of the three real roots (for each collinear libration point one) of the quintic equation

$$x_L^5 + (3 - \mu)x_L^4 + (3 - 2\mu)x_L^3 - \mu x_L^2 - 2\mu x_L - \mu = 0. \quad (2.3)$$

For  $L_2$  in the sun - Earth/moon system

$$x_L = 1.00782405 \cdot 10^{-2} = 1507683 \text{ km from Earth}, \quad (2.4)$$

$$K = 3.9405221845259 \quad (2.5)$$

The general solution of 2.1, characterised by a harmonic motion in the  $xy$ -plane and a uncoupled oscillation in  $z$  with a different period, can be written as

$$x = A_1 e^{\lambda_{xy}t} + A_2 e^{-\lambda_{xy}t} + A_3 \cos \omega_{xy}t + A_4 \sin \omega_{xy}t \quad (2.6)$$

$$y = c_1 A_1 e^{\lambda_{xy}t} - c_1 A_2 e^{-\lambda_{xy}t} + c_2 A_4 \cos \omega_{xy}t - c_2 A_3 \sin \omega_{xy}t \quad (2.7)$$

$$z = A_z \cos(\omega_z t + \phi_z), \quad (2.8)$$

with

$$\omega_{xy} = \frac{1}{\sqrt{2}}(-K + 2 + \sqrt{9K^2 - 8K})^{\frac{1}{2}} = \frac{2\pi}{177.566 \text{ days}} \quad (2.9)$$

$$\lambda_{xy} = \frac{1}{\sqrt{2}}(K - 2 + \sqrt{9K^2 - 8K})^{\frac{1}{2}} = 0.0427355 \text{ per day} \quad (2.10)$$

$$c_1 = \frac{\lambda_{xy}^2 - 1 - 2K}{2\lambda_{xy}} = -0.545263 \quad (2.11)$$

$$c_2 = \frac{\omega_{xy}^2 + 1 + 2K}{2\omega_{xy}} = 3.1872293 \quad (2.12)$$

$$\omega_z = \sqrt{K} = \frac{2\pi}{184.0 \text{ days}} \quad (2.13)$$

The coefficients  $A_1, A_2, A_3, A_4$  can be written as linear functions of the initial conditions

$$\begin{pmatrix} A_1 \\ A_2 \\ A_3 \\ A_4 \end{pmatrix} = \begin{pmatrix} \frac{c_2\omega_{xy}}{2d_1} & \frac{\omega_{xy}}{2d_2} & -\frac{c_2}{2d_2} & \frac{1}{2d_1} \\ \frac{c_2\omega_{xy}}{2d_1} & -\frac{\omega_{xy}}{2d_2} & \frac{c_2}{2d_2} & \frac{1}{2d_1} \\ \frac{c_1\lambda_{xy}}{d_1} & 0 & 0 & -\frac{1}{d_1} \\ 0 & -\frac{\lambda_{xy}}{d_2} & \frac{c_1}{d_2} & 0 \end{pmatrix} \begin{pmatrix} x_0 \\ y_0 \\ \dot{x}_0 \\ \dot{y}_0 \end{pmatrix} \quad (2.14)$$

with

$$d_1 = c_1\lambda_{xy} + c_2\omega_{xy}$$

$$d_2 = c_1\omega_{xy} - c_2\lambda_{xy}$$

The initial values can now be chosen such that  $A_1 = A_2 = 0$  and only the periodic in plane motion remains. Together with the oscillation in  $z$  at a different period, this represents the Lissajous orbits in the linearised restricted circular three-body problem which evolve according to

$$x = A_x \cos(\omega_{xy}t + \phi_{xy}) \quad (2.15)$$

$$y = -A_y \sin(\omega_{xy}t + \phi_{xy}) \quad (2.16)$$

$$z = A_z \cos(\omega_z t + \phi_z). \quad (2.17)$$

with

$$A_y = c_2 A_x.$$

Figure 2.1 shows the geometry of such a typical orbit ( $A_z = A_y = 100000$  km) using this analytic propagation. The initial  $z$ -phase  $\phi_z$  for the shown orbit has been chosen as one of the two solutions (near  $90^\circ$  or near  $270^\circ$ ) which maximise the time without eclipse.

A numerical propagation will always deviate from this oscillation. When setting the time  $t$  at epoch to zero, the equations

$$x = A_1 e^{\lambda_{xy}t} + A_2 e^{-\lambda_{xy}t} + A_x \cos(\omega_{xy}t + \phi_{xy}) \quad (2.18)$$

$$y = c_1 A_1 e^{\lambda_{xy}t} - c_1 A_2 e^{-\lambda_{xy}t} - A_y \sin(\omega_{xy}t + \phi_{xy}) \quad (2.19)$$

$$z = A_z \cos(\omega_z t + \phi_z) \quad (2.20)$$

$$\dot{x} = A_1 \lambda_{xy} e^{\lambda_{xy}t} - A_2 \lambda_{xy} e^{-\lambda_{xy}t} - A_x \omega_{xy} \sin(\omega_{xy}t + \phi_{xy}) \quad (2.21)$$

$$\dot{y} = c_1 A_1 \lambda_{xy} e^{\lambda_{xy}t} + c_1 A_2 \lambda_{xy} e^{-\lambda_{xy}t} - A_y \omega_{xy} \cos(\omega_{xy}t + \phi_{xy}) \quad (2.22)$$

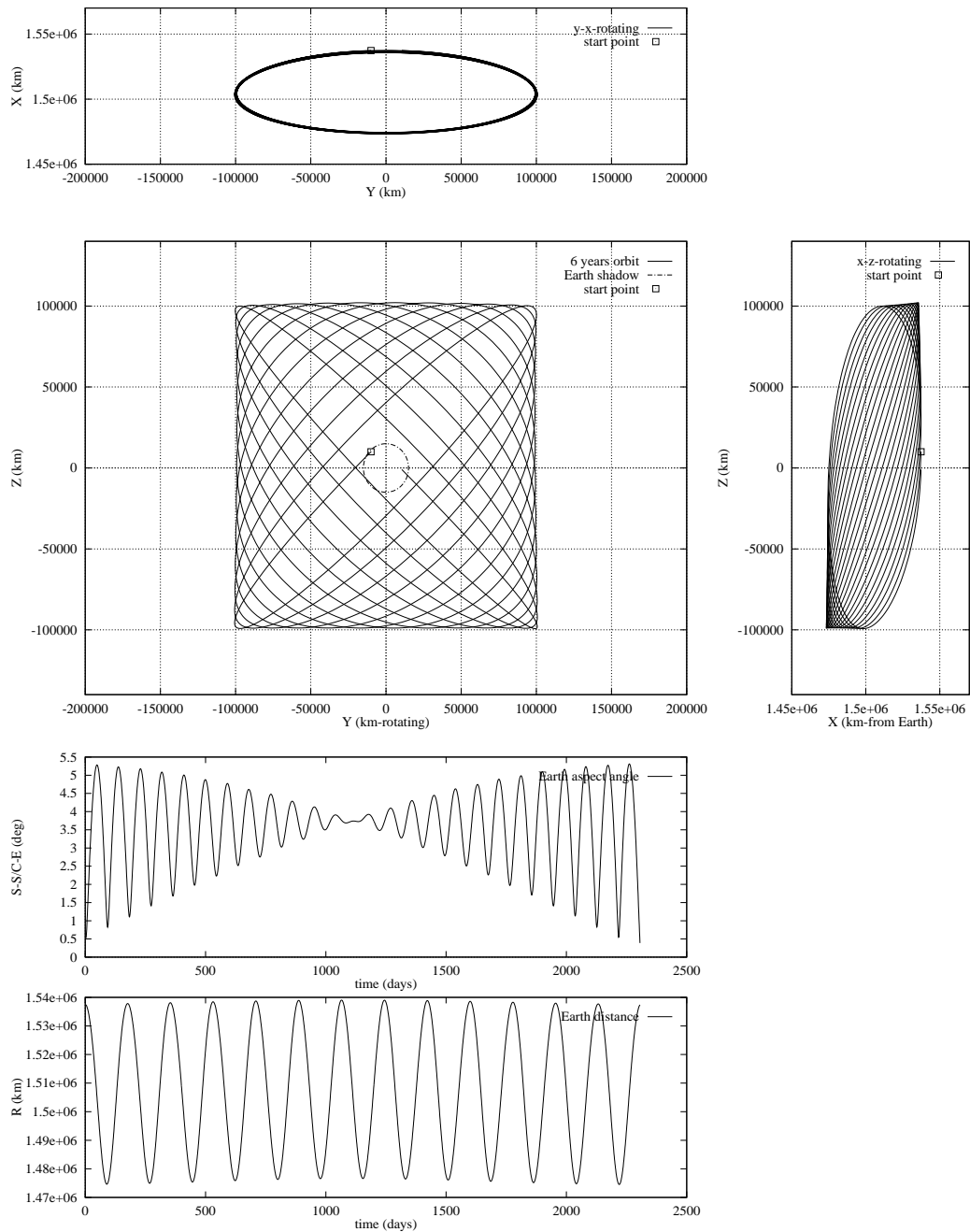
$$\dot{z} = -A_z \omega_z \sin(\omega_z t + \phi_z) \quad (2.23)$$

define a one-to-one relation between a set of "osculating Lissajous elements"

$$(A_1, A_2, A_y, A_z, \phi_{xy}, \phi_z)$$

and the state vector.

Figure 2.1: Typical Lissajous orbit around  $L_2$  (restricted-circular, Sun on  $-x$ )



### 2.3 Escape Direction in the Linear Problem

Assume a manoeuvre

$$(\Delta\dot{x}_0, \Delta\dot{y}_0, 0)$$

in the  $x, y$ -plane is executed at a point

$$(x_0, y_0, z_0, \dot{x}_0, \dot{y}_0, \dot{z}_0)$$

on a Lissajous orbit. The two coefficients  $(A_1, A_2)$  after the manoeuvre then can be written as

$$\begin{pmatrix} A_1 \\ A_2 \end{pmatrix} = \begin{pmatrix} \frac{c_2\omega_{xy}}{2d_1} & \frac{\omega_{xy}}{2d_2} & -\frac{c_2}{2d_2} & \frac{1}{2d_1} \\ \frac{c_2\omega_{xy}}{2d_1} & -\frac{\omega_{xy}}{2d_2} & \frac{c_2}{2d_2} & \frac{1}{2d_1} \end{pmatrix} \begin{pmatrix} x_0 \\ y_0 \\ \dot{x}_0 + \Delta\dot{x}_0 \\ \dot{y}_0 + \Delta\dot{y}_0 \end{pmatrix} \quad (2.24)$$

From equation 2.24 it can be seen that, starting from a state vector on a Lissajous orbit which satisfies  $A_1 = 0$ , any velocity increment  $\Delta\mathbf{V} = (\Delta\dot{x}_0, \Delta\dot{y}_0)$  in the  $xy$ -plane which satisfies

$$\mathbf{u}^T \Delta\mathbf{V} = 0 \quad (2.25)$$

with

$$\mathbf{u} = \left( -\frac{c_2}{d_2}, \frac{1}{d_1} \right) \quad (2.26)$$

will not lead to an escape from the family of orbits with periodic components only.  $A_1$  remains zero and the  $A_2$  component (related to the 'stable manifold') will exponentially decay. The periodic  $z$ -motion remains un-affected.

The vector  $\mathbf{u}$  defines the **escape direction**. It can be seen that  $\mathbf{u}$  does not depend on the point in the orbit, only on the constants in the equation of motion.

Therefore a simple but effective orbit generation and maintenance strategy can be implemented using this "universal" direction of the linear problem. In fact, repeated bisections in velocity increments along the escape direction are used as the basic construction element for the numerical generation of the Lissajous (or better non-escape) orbits in the full nonlinear problem with any type of perturbations.

The direction of the line in the  $xy$ -plane orthogonal to  $\mathbf{u}$

$$\mathbf{s} = \left( \frac{1}{d_1}, \frac{c_2}{d_2} \right) \quad (2.27)$$

defines the **non escape direction** which has been used to derive amplitude reduction and eclipse avoidance manoeuvres. These two "universal" directions have the following angles to the x-axis (sun to Earth):

$$\begin{aligned} \text{non-escape direction:} & \quad -61.4^\circ \\ \text{escape direction:} & \quad 28.6^\circ \end{aligned}$$

Figure 2.2 shows the escape direction  $\mathbf{u}$  and the non-escape direction  $\mathbf{s}$ .

### 2.4 Numerical Construction of Lissajous Orbits

Using the concept developed in the preceding section an algorithm to generate Lissajous orbits numerically in the exact problem has been derived as follows:

- Take an initial guess of a state vector on a Lissajous orbit around  $L_2$  for given amplitudes from the analytic theory according to [4].
- Correct the velocity along escape direction of the linear theory ( $\Delta\mathbf{V}$  along  $\mathbf{u}$ ) by a **bisection** algorithm as follows:

1. forward integration for e.g. 450 days and stop if
  - orbit escapes from Earth system (e.g.  $\geq 2 \times 10^6$  km ) or

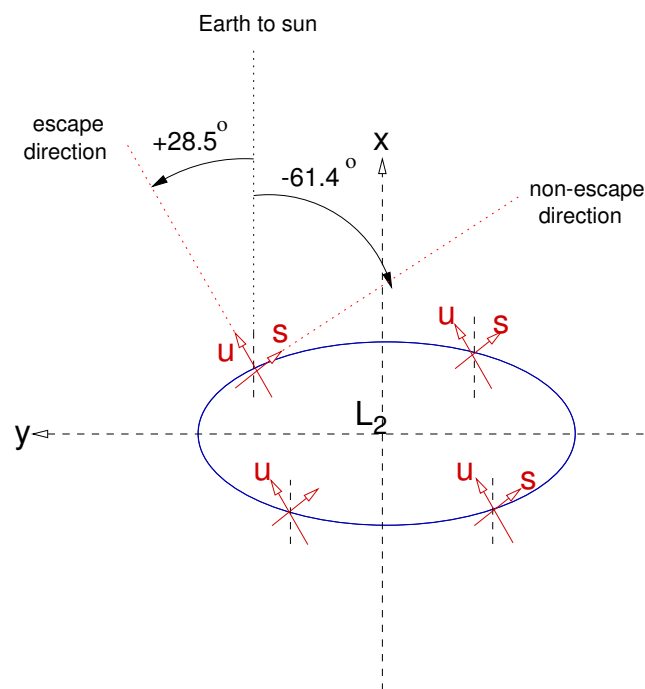


Figure 2.2: Universal escape and non-escape directions of linear problem

- orbit comes close to Earth (e.g.  $\leq 0.5 \times 10^6$  km )
  - 2. change initial velocity and repeat 1 (bisection depending on stop)
  - 3. if stop conditions not reached  $\Rightarrow$  **Non-escape orbit at  $L_2$  found.**
- Shift start point e.g. to next  $xy$ -plane crossing and repeat velocity correction.

All orbit calculations are done in the J2000 inertial frame using the JPL ephemeris file de405. Launch window calculations at this stage of the mission analysis use Earth, sun and moon only. Detailed orbit calculations and in particular the final launch window will use in addition the  $J_2$  of the Earth (in initial phase), radiation pressure and Mars, Venus, Jupiter, Saturn.

Using the described algorithm any kind of Lissajous orbits passing through an initial position, also in perturbed dynamic systems, can be easily generated. The orbit needs small correction manoeuvres e.g. every revolution (period of motion around  $L_2$  in  $xy$ -plane). But this is a necessity for the numerical generation of Lissajous orbits anyhow, because of the finite computer word length and the instability property.

The algorithm may be started not only from initial positions which lie on a Lissajous orbit, also arbitrary points in space can be used. They may lie on the stable manifold of a Lissajous orbit ( $A_1 = 0, A_2 \neq 0$ ). So the algorithm may find a non-escape orbit around  $L_2$  passing through this initial position. In fact there are Lissajous orbits with a combination of the amplitudes and the phase such that their stable manifold contains an orbit with a perigee altitude as that of a geostationary transfer orbit or another orbit which can be easily reached from an ARIANE launch. This is true even for a fixed launch time. this property has been used to construct the transfer for Herschel/Planck. The bisection then is done at the perigee in the direction of the velocity.

## 3 Transfer Optimisation, Launch Window and Reference Orbit

### 3.1 Transfer Optimisation

#### 3.1.1 Basic Transfer Optimisation Assumptions and Previous Calculations

A specific feature of an ARIANE launch is introduced by the launch site near the equator. The orbits around the libration points lie near the ecliptic plane. So orbits into which ARIANE can deliver large payloads may not always be well suited to start a transfer to the  $L_2$  region.

In previous work (1984) [2] a launch window was constructed by integrating backward from a given Halo orbit, optimising the injection point on the Halo for minimum injection  $\Delta V$ , and matching conditions at perigee which can be reached by ARIANE, accepting some mass loss away from the equator plane and the optimum line of apsides. The mass of the Herschel and Planck satellites in conjunction with the launcher performance data does not allow such a mass reduction at launch. Therefore rather than prescribing the target orbit, orbits around  $L_2$  were searched which can be reached from maximum mass ARIANE launch conditions [5] (1998).

This led to the family of large amplitudes Lissajous or Halo like ("Mean Halo") orbits, depending on the initial conditions (see Herschel figures 3.36 to 3.38), which is now the baseline for Herschel. Planck cannot accept the large size (maximum sun spacecraft Earth angle) of these orbits, because of its sky scanning strategy and the resulting constraint on the Earth to sun viewing angle arising from thermal and communications design. This led to the concepts of amplitude reduction manoeuvres and eclipse avoidance manoeuvres [6, 7].

So at the time of the ITT, mid 2000, the strategy selected to construct the transfer for the Herschel/Planck double launch case, independent on how the two spacecraft are mounted on ARIANE, was to inject at perigee (by the launcher upper stage) to the stable manifold of the large Lissajous (Mean Halo) orbit around  $L_2$  on which Herschel remains, without any further deterministic maneuvers. It was also assumed that Planck uses the same transfer orbit and performs one or two orbit manoeuvres along the non-escape direction in the  $xy$ -plane either separate or combined with a manoeuvre in the  $z$ -component, which changes the orbit to enter from the one stable manifold to another of a Lissajous orbit with the desired smaller amplitudes. This was the baseline strategy until CReMA issue 3.0.

The launch windows in 2007 and 2008 as derived with above amplitude reduction manoeuvre concept are shown in figure 3.1 and 3.2. The 2008 window is identical to the 2007 window except for the ripples caused by the moon.

From issue 3.1 of the CReMA, the amplitude reduction manoeuvre concept is replaced by an optimum transfer concept as explained in the following section 3.1.2. The optimisation is computationally heavy, therefore not well suited for the approach represented by the level lines figures 3.1 and 3.2. However a few ideas have been kept from the previous concept:

- The seasonal launch window, defined by the Planck propellant allocation and the eclipse conditions, has been kept unchanged. This implicitly will avoid eclipses in the transfer for Herschel, for Planck that has to be verified in case the transfer orbit deviates. Rather than extending the seasonal window using the gain in propellant on Planck, the propellant allocation has been reduced (see section 3.1.5).
- The exact opening hour of the launch window on each day will in general be determined by the sun aspect angle constraint at fairing separation. However for the time interval from 1 August 2007 to 27 August 2007 (dates before August 2007 are not further discussed) it has been taken near on a line the minimum insertion  $\Delta V$  (see figure 3.1). From 22 February 2008 to 27 February 2008 at the opening of the window as defined by the sun aspect angle condition at fairing separation, the Herschel orbit will go into an eclipse by the Earth towards the end of the Herschel mission (before 5 years). Therefore the opening has been delayed, in this case to be 45 minutes before the closing, then defined by the sun aspect angle condition at H3.

Figure 3.1: Launch window 2007

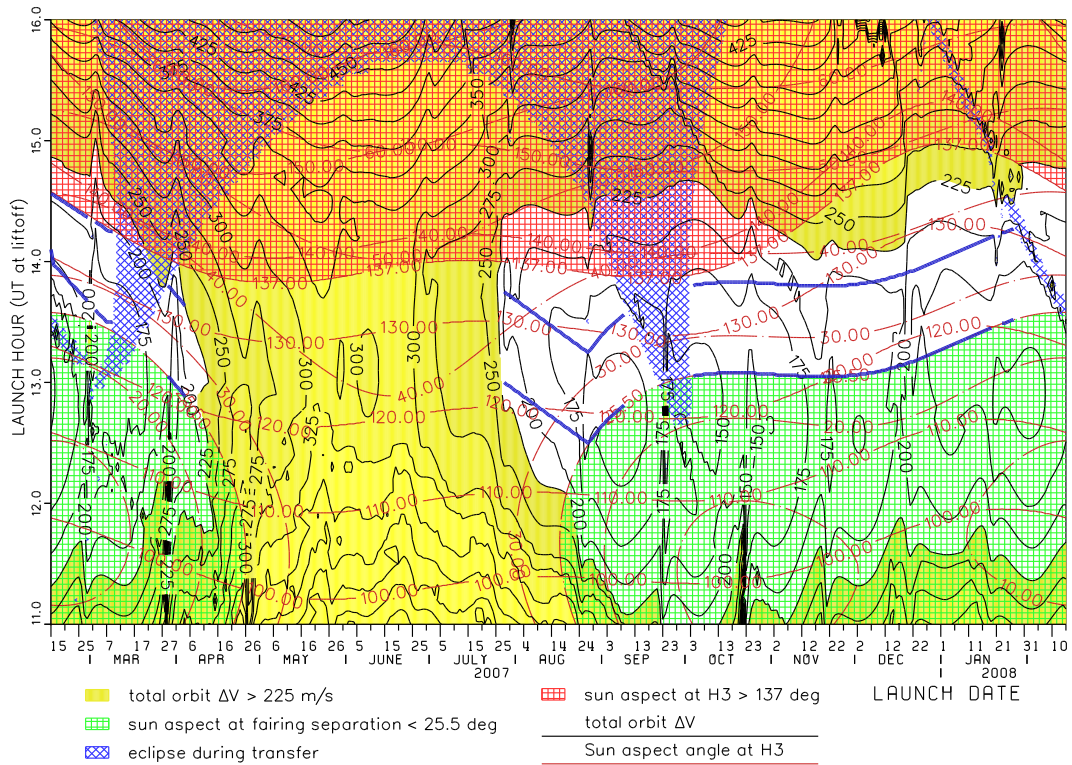
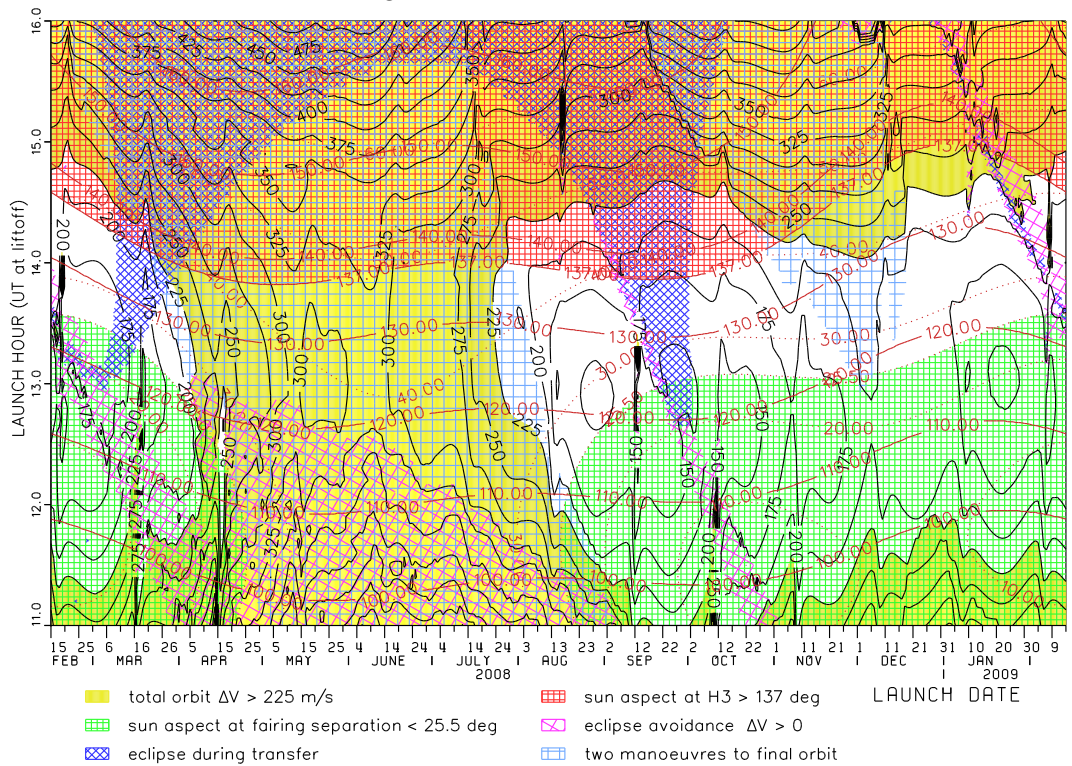


Figure 3.2: Launch window 2008



- The closing of the daily launch window has been taken 45 minutes after the opening, this will always be before the closing by the sun aspect angle condition at spacecraft separation (H3), or the limit by the Planck propellant budget. The idea of not fully extending to one of these two conditions is to possibly keep some propellant margin; the minimum will be near the opening, a launch at the opening of the window is most likely, and a 45 minutes daily slot was assumed to be necessary and sufficient for launch operations. Dates for which a 45 minutes interval cannot be obtained have been removed from the seasonal window.

### 3.1.2 Optimum Orbit Insertion for Planck

A basic concept of the previous approach using an amplitude reduction manoeuvre was that the Planck transfer orbit will not deviate from the Herschel stable manifold. It was verified that, with this assumption, the amplitude reduction insertion manoeuvre calculation derived from linear theory was close to the optimum. However the injection conditions by ARIANE in all cases will be different from that stable manifold. There will be the launcher dispersion, but also systematic deviations in the perigee velocity from that required have been introduced to keep the perigee velocity constant over time intervals with the objective to reduce the number of flight programs on ARIANE (the current concept is even to have only one flight program). Therefore within the first 2 days after launch a major orbit correction manoeuvre will have to be done in any case.

In [18] it was now shown that the size of the insertion manoeuvre (or a pair of manoeuvres) can be considerably reduced when deviating from that stable manifold transfer. The manoeuvre required on day 1 or 2 for this change of the transfer is an order of magnitude smaller than the allocation made for that early orbit correction. Assuming a free manoeuvre direction, it came out that the sun aspect angle of the optimum insertion manoeuvre is systematically different from that derived in the CReMA issue 3.0. [18] also treats the case assuming the thruster mounting as is on the Planck spacecraft. In addition, solving the correct optimisation problem, the initial conditions on the Lissajous orbit can be chosen such that the orbit remains free of eclipses by the Earth, and the sun-spacecraft-Earth condition is satisfied just for the required mission duration. Also with prescribed thruster mounting a slight reduction in the insertion  $\Delta V$  can be reached. This will be the new transfer optimisation baseline.

Following [18] the transfer optimisation has been re-done for the whole launch window. First the software used for [18] was implemented in the mission analysis environment, however not actually used. Rather new transfer optimisation code was developed based on the mission analysis software. In parallel an ongoing study contract with Deimos Space related to the subject (LODATO = Libration Orbit Design Tool) was redirected to cover the Planck transfer orbit optimisation. With all three approaches the same results were obtained. This section reports on the results obtained with the newly coded mission analysis software. This used prototype elements of a first delivery by the LODATO study developed for the Darwin rendezvous problem.

In addition to abandoning the unnecessary condition that the Planck transfer orbit is identical to that of Herschel, another constraint has been implemented in a more refined way:

- The sun-spacecraft-Earth angle on Planck has to remain below  $15^\circ$  for 2 years from the insertion manoeuvre. Different from the previous more conservative approach, the maxima of the sun aspect angle in the operational orbit are now explicitly included in the optimisation as constraints. This has also been done in [18] and leads to an additional improvement in the  $\Delta V$ . The duration over which these conditions are included has been taken as 1000 days from launch. This will cover with margin the transfer + 2.5 years in orbit.

Strategies with one or with two manoeuvres are studied. If there is a second manoeuvre it will be placed before the main orbit insertion which is after about 100 to 120 days from launch. In CReMA issue 3.0 such a manoeuvre was taken after the insertion, however it can be shown that there is always a possibility to place it earlier. The perigee velocity of the transfer orbit has been taken as an optimisation variable. The deviation from the reference velocity of Herschel has been included in the budget of the equivalent  $\Delta V$  with a penalty factor of 12, to cover an execution on day 2 and a worst case decomposition.

### 3.1.3 ARIANE Performance and Launch Conditions

At the Preliminary Mission Analysis Review on 2004/03/11 Arianespace presented an update the performance assumptions for the Herschel-Planck launch, based on a complete update of the launcher model following the design modifications made as a consequence of the V157 (failed launch) post flight analysis. The main result is a reduction of the payload performance to the  $L_2$  transfer

- from 7100 kg to 6279.9 kg.

In addition Arianespace announced that a range of  $\pm 5.5^\circ$  has to be allocated for the pitch guidance, which for the launch window means that the sun aspect angle constraint at fairing separation has to be changed accordingly.

The performance of ARIANE5E/CA as to be assumed for Herschel-Planck is given in [10], including trajectory printouts for different cases. As baseline the case with optimum performance (case 1 in [10]) has been selected.

It delivers the spacecraft to the conditions given in table 3.1.

Table 3.1: Reference launch orbit conditions

	<b>A5E/CA</b> optimum (case 1)
inclination $i$	14.0°
argument of perigee $\omega$	207.754°
ascending node $\Omega_K$ (relative Kourou at H0 - 3 sec)	-154.315°
perigee altitude $h_p$	319.68 km
time from lift off to S/C sep.	1540.000 sec
true anomaly at injection $f_{inj}$	34.642°
mass in orbit	<b>6272.9 kg</b>
impact longitude of EPC	4.203°
impact latitude of EPC	-8.432°

The launcher axis at fairing separation (FJ) and at shut down of ESC-A (H3) is given in the trajectory printout [10] in the launch pad system as shown in table 3.2.

Table 3.2: Launcher axes orientation in launch pad system (case 1)

	Fairing Sep. FJ	ESC Shutdown H3
time of event (from $H_0$ )	190.624 s	1540.000 s
launcher pitch angle ( $\psi$ )	60.919°	160.548°
launcher axis azimuth ( $A_Z$ )	-16.816°	-15.486°

The inertial launch pad reference system at  $H_0 - 3$  sec, with respect to which the launcher axis is given is defined by

$X_{PL}$  geodesic vertical at launch pad  
 $Y_{PL}$  east (azimuth  $A_Z = 0^\circ$ )  
 $Z_{PL}$  north completing triple

The pitch angle is measured from the vertical. The Azimuth is measured from east to north. The Earth flattening has been ignored in the calculations for the time being. The longitude of the meridian through the launch pad is  $\lambda_K = -52.805979^\circ$ . The coordinates of the launch pad in the inertial equatorial system with the x-axis through this "Kourou meridian" at  $H_0 - 3$  sec are

$$\begin{aligned} X_{EQ} &= 6351.649 \text{ km} \\ Y_{EQ} &= 0. \\ Z_{EQ} &= 578.6528 \text{ km} \end{aligned}$$

### 3.1.4 Assumptions on Spacecraft and Target Orbit

A major re-design on the spacecraft level was decided at the point after the PMAR to regain a launch window. The spacecraft now allows to accept

- sun aspect angles at fairing separation down to  $20^\circ + 5.50^\circ = 25.5^\circ$ ,
- sun aspect angles at ESC cut-off (H3) up to  $140^\circ - 3^\circ = 137^\circ$ .

At the same time it was decided to define the limitation of the launch window by a  $\Delta V$  allocation for deterministic manoeuvres on Planck of

- 215 m/s,

for a target orbit with a maximum sun-spacecraft-Earth angle of  $15^\circ$  over a 2 years mission, and to select as baseline the

- optimum ascent for ARIANE 5E/CA (table 3.1 with launcher axis as given in table 3.2)

The latter requirement is to be interpreted in the sense that the interface with Arianespace shall be as simple as possible, this means the launcher shall inject to not more than TBD different orbits in the Earth fixed frame for any launch date. This is to minimise the number of flight programs. the goal is to have only one target orbit condition, the number of flight programs to handle the roll angle history is TBD.

In addition

- there shall be no eclipse during transfer neither for Herschel nor for Planck,
- propellant for possibly required eclipse avoidance manoeuvres on Planck shall be allocated as part of the above deterministic  $\Delta V$ ,
- there shall be no eclipse in the nominal orbit for Herschel over 4.5 years from launch.

The Planck spin-axis is assumed to be directed toward the sun during all manoeuvres. Two optimisation cases are treated:

- The case of optimum manoeuvres without restriction in their direction, an equivalent  $\Delta V$  is then derived using the decomposition, canting and duty cycle losses of the actual thruster configuration of the Planck spacecraft.
- Each manoeuvre is modelled by 5 parameters, the sizes of the manoeuvres by axial, flat and upper thrusters, the size of a second manoeuvre with the upper thrusters ( $180^\circ$  off from the first in phase angle) in some cases, and the phase angle of the flat and upper thruster manoeuvres. The phase angle is counted from the ecliptic trace.

The assumptions made for the Planck thrusters are listed in table 3.3.

The thrust vector declination (opposite the thruster itself) is counted from the spin axis, so it is identical to the sun aspect angle. The equivalent  $\Delta V$  is given to represent the canting and duty cycle losses (1 rpm spin) as indicated by the above effective specific impulses. The total required propellant can then be calculated from this equivalent  $\Delta V$  using the actual specific impulse of one "ideal" thruster (current value is 215 s).

Table 3.3: Planck thruster mounting ad efficiencies

Thruster	Declination	Effective specific impulse
axial	180.000°	215.000 s
flat	128.412°	212.819 s
upper	49.825°	174.417 s

### 3.1.5 Planck Insertion Manoeuvre Propellant Allocation Update

Figure 3.3 and 3.4 compare the equivalent  $\Delta V$  (including geometric losses) for the optimum transfer (newly calculated) using the Planck thruster mounting information, with that given in CReMA Issue 3.0 figure 3.13 and 3.15 (pure  $\Delta V$ ) (denoted by CREMA in the figure) and adding decomposition and canting losses for the Planck thruster mounting (equivalent  $\Delta V$ ) to the pure  $\Delta V$  given in CReMA issue 3.0 (denoted by CREMA w. loss in the figure). In the  $\Delta V$  budget (215 m/s for insertion manoeuvre) of CReMA issue 3.0 the geometric losses were not accounted for, this was left to the spacecraft contractor. In fact Alcatel assumed 91% efficiency, so actually an allocation with losses of 236 m/s was made. According to figures 3.3 and 3.4 slightly over 240 m/s equivalent  $\Delta V$  was required with the previous strategy, so a few days would have been to be removed from the launch window. With the new optimum strategy the allocation with losses can be reduced to 215 m/s, for the same launch window.

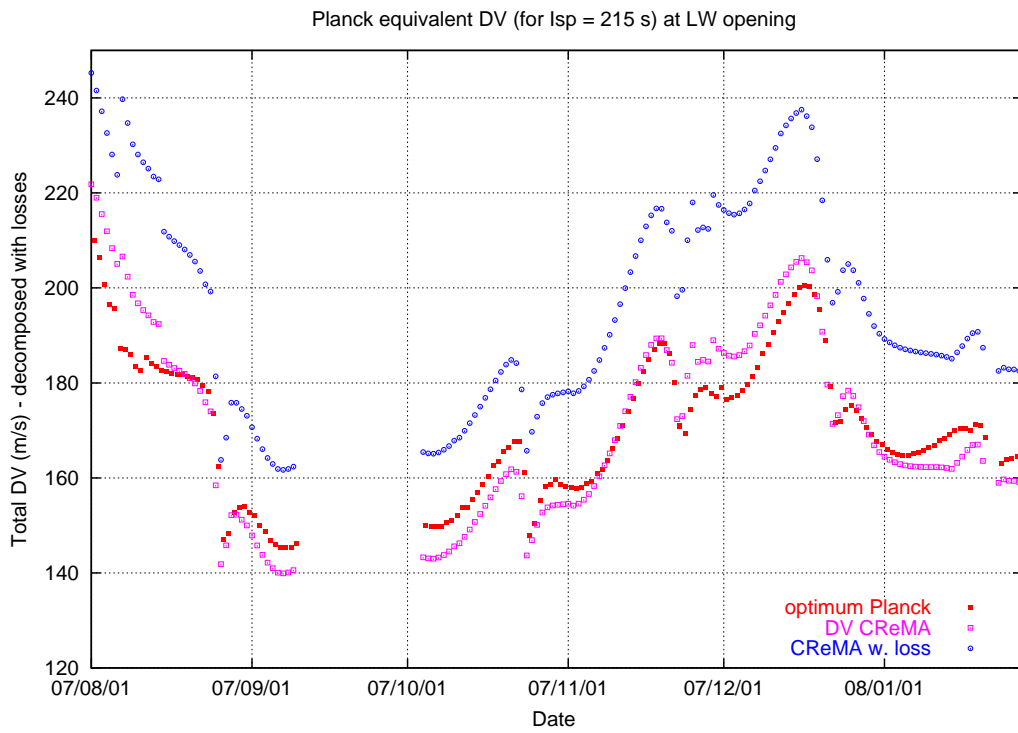


Figure 3.3: Equivalent  $\Delta V$  for Planck transfer (LW opening)

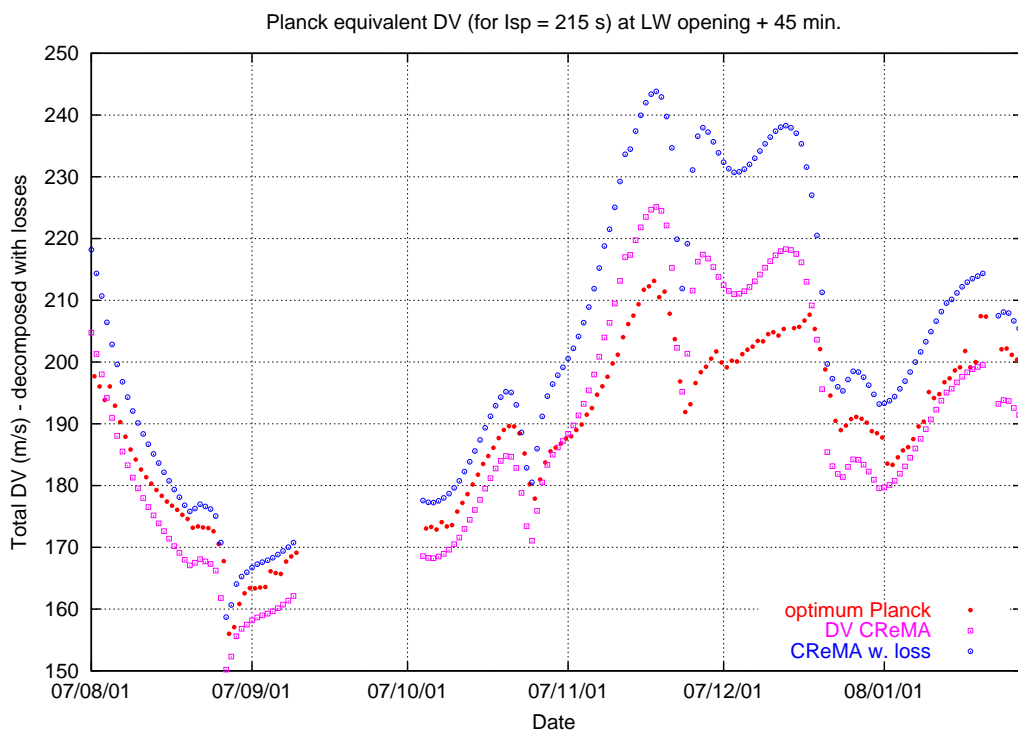


Figure 3.4: Equivalent  $\Delta V$  for Planck transfer (LW closing)

## 3.2 The Herschel/Planck Launch Window, Winter 2007/2008

### 3.2.1 Reference Launch Window Definition

Figure 3.5 shows the equivalent  $\Delta V$  for the newly optimised transfer at the opening and closing of the daily launch window (45 minutes per day) in from 1 August 2007 to 4 April 2008. The given  $\Delta V$  is the total deterministic  $\Delta V$  for Planck, this means orbit insertion using one or two manoeuvres plus an allocation for the correction of the perigee velocity by a manoeuvre on day 2. The figure also contains the corresponding  $\Delta V$  for a launch time (after the closing) at which the sun aspect angle constraint at H3 ( $137^\circ$ ) is satisfied. Figure 3.17 shows how much this would mean in duration, ignoring the  $\Delta V$  limit, but removing cases with an eclipse in the transfer. Figures 3.1 and 3.2 show the context, except that the  $\Delta V$  level lines are not for the optimum transfer (they have been done with the amplitude reduction method).

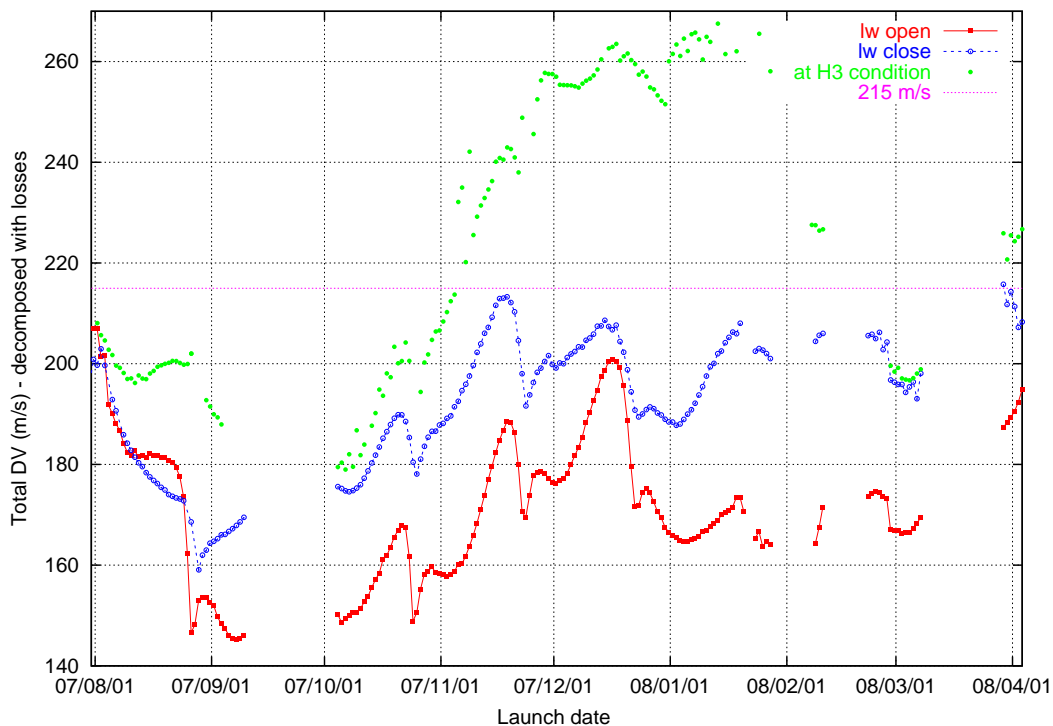


Figure 3.5: Equivalent  $\Delta V$  for optimum Planck transfer (LW opening and closing)

Remarks:

- All manoeuvres (except the small manoeuvre on day 2 to be combined with the other correction manoeuvres) come out to be done with the flat thrusters (sun aspect angle  $128^\circ$ ), the optimiser never comes to solution with decomposed manoeuvres, rather the execution times are shifted.
- All orbits are free of Earth eclipses from launch to the end of the Planck mission (1000 days). Eclipses by the moon will be discussed in section 3.6.

The deviation of the Planck perigee velocity from that of Herschel is shown in figure 3.6. An allocation for correcting this deviation with a penalty factor of 12 for a latest execution on day 2 and the possible need of decomposition has been made in the Planck deterministic propellant budget in figure 3.5. The maximum allocation is  $12 \times 0.25 \text{ m/s} = 3 \text{ m/s}$  for those launch dates with a large out of plane manoeuvre. It can be assumed that this correction will be combined with the first stochastic orbit correction.

The seasonal launch window in Winter 2007/2008 is given in table 3.4. As a launch before August 2007 now appears to be not likely, the first half of 2007 has been removed from the table and also from the figures. The dates from

The selection of the seasonal launch window includes:

Figure 3.6: Deviation required Planck perigee velocity from that of Herschel

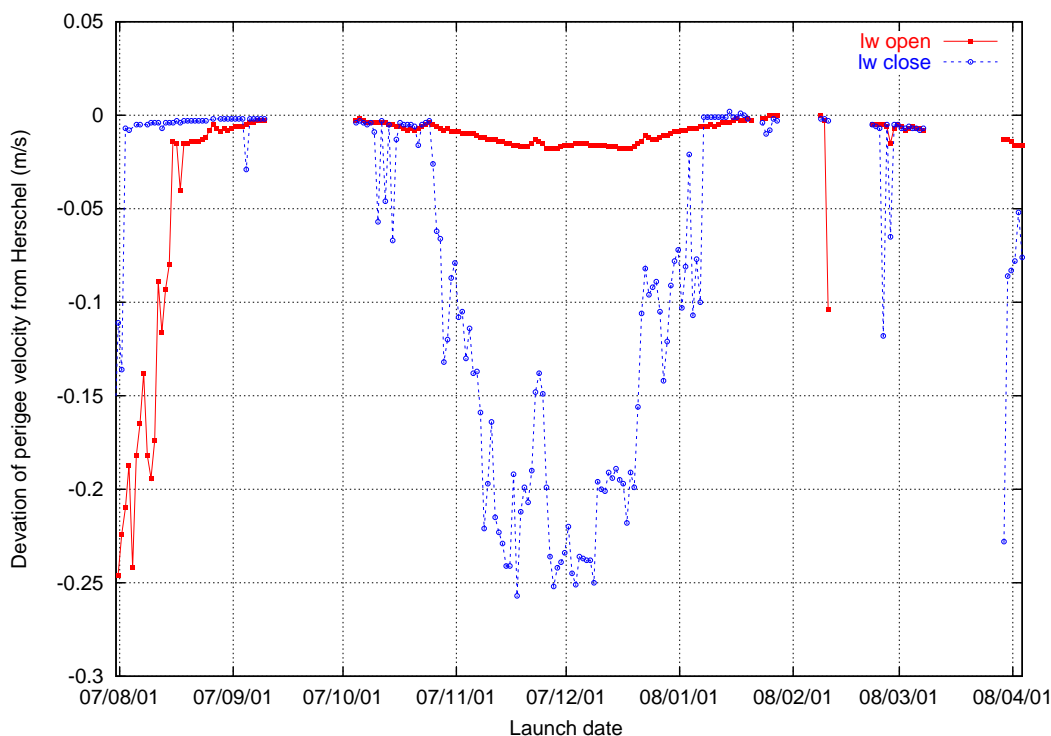


Table 3.4: Launch Window (45 minutes per day, no eclipses by Earth)

07/08/03 - 07/09/09
07/10/04 - 08/01/20
08/01/23 - 08/01/27
08/02/08 - 08/02/10
08/02/22 - 08/03/07
08/03/29 - 08/04/03

- A daily slot of at least 45 minutes.
- The avoidance of any eclipse during the transfer and in the operational orbit for both spacecraft. Note that with the new optimisation of the Planck insertion manoeuvre eclipses by the Earth are also implicitly avoided for Planck in the operational orbit, without any additional deterministic manoeuvre after the orbit insertion.
- A propellant limit on Planck of 215 m/s for the insertion manoeuvres including the geometric losses.

### 3.2.2 Reference Delivery Conditions by ARIANE for one Flight Program

It has been agreed to fix the delivery conditions by ARIANE such that only one flight program will be used. All orbital parameters except the apogee radius ( $\sim$  perigee velocity) have already been fixed. Figure 3.7 shows the perigee velocity variation from August 2007 to March 2008. This time interval has been taken as reference to select the nominal delivery conditions for ARIANE. Propellant is to be allocated on the spacecraft to correct the deviation of the required perigee velocity from that one delivered by ARIANE. Alternatives with more than one flight program to reduce the propellant allocation on the spacecraft are

discussed in section 3.2.4, and for a possible extension of the launch window into 2008 in section 3.3.1. In particular figure 3.12 shows the perigee velocity variation to July 2008.

The minimum and maximum perigee velocities (relative to the escape velocity) in the reference time interval are

- -32.77 m/s and -26.68 m/s respectively.

When fixing the delivery conditions as given in table 3.5 perigee velocity variations of  $\pm 3.1$  m/s have to be corrected by the spacecraft.

Table 3.5: Reference apogee radius for 1 flight program

perigee velocity (m/s)	relative escape velocity (m/s)	apogee radius (km)
10880.0	-29.735	1223699

This will be done by a manoeuvre on day 2. The amplification factor on day 2 according to figure 3.8 is 8.2. For one flight program therefore an allocation of 26 m/s has been made for a manoeuvre execution on day 2 (see propellant budget in table 5.1). It is assumed that decomposition losses for the possible manoeuvre directions according to figure 3.28 are covered on the spacecraft level. A minor gain might be achieved from combining the manoeuvre with the stochastic orbit correction.

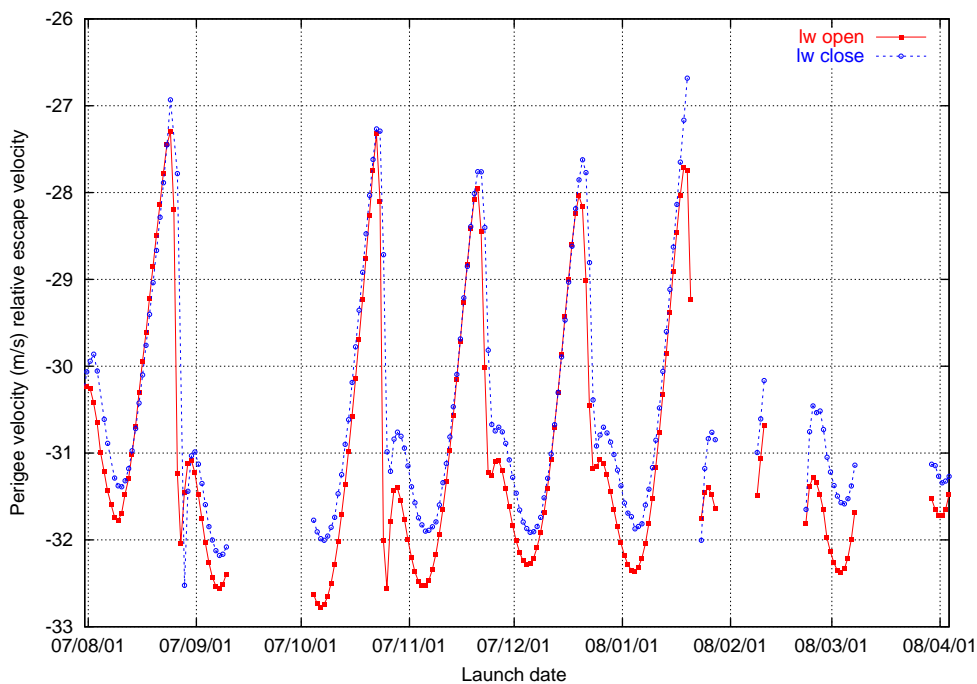


Figure 3.7: Perigee velocity relative to escape velocity (LW opening and closing)

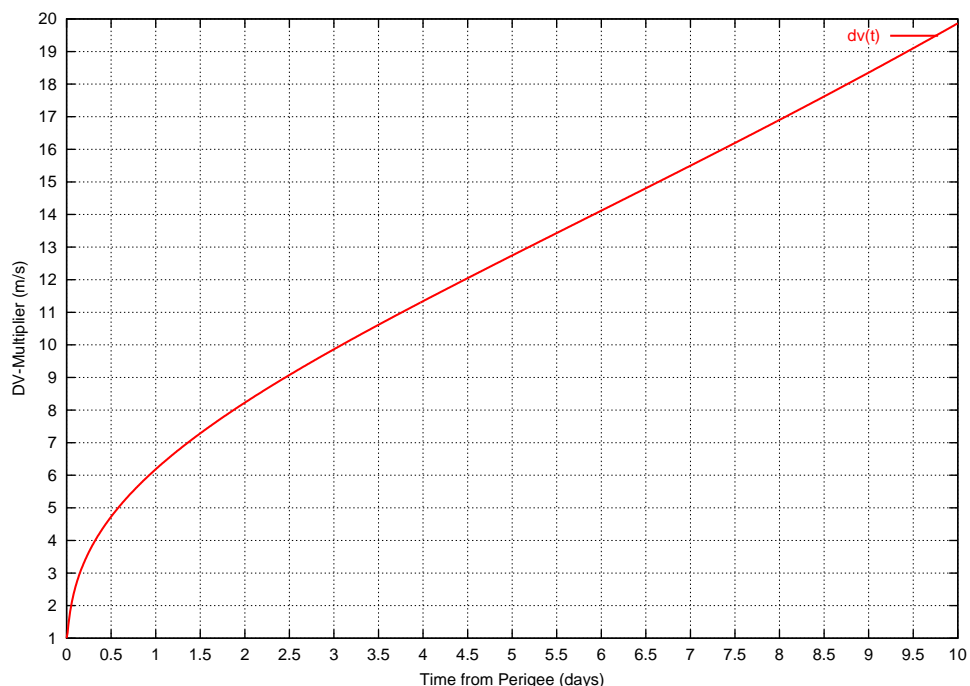


Figure 3.8: Amplification factor for correction of variation of perigee velocity (per m/s)

Remark:

- The perigee radius is 6697.845 km. The escape velocity is 10909.81 m/s.
- If perigee velocities outside the assumed band will appear in case the launch window slips further into 2008, it can be assumed that the very few days for which this may happen will be removed from the launch window.

### 3.2.3 Moon Aspect Angles During Early Transfer

The first orbit correction manoeuvre on Planck will be done with exact sun pointing of the (anti)spin axis. When executing this manoeuvre after 2 days, to compensate for the deterministic variations in the perigee velocity and to remove the launcher dispersion, the attitude control will use the star mappers. At that time the moon may be in the field of view of the star mapper and cause glares. Planck will be slowly spinning and sun pointing. There will be glares for moon-spacecraft-sun angles between  $75^\circ$  and  $115^\circ$ , so this range of sun-spacecraft-moon angles will not be allowed.

To visualise this problem the sun-spacecraft-moon angle (arc cosine) is shown in figure 3.9, over one month from 2007/8/1 at the opening of the daily launch window. The time is counted from spacecraft separation. It can be seen that for about 6-7 days per month the moon will blind the star mapper in the period around day 2, and that to remove the problem the manoeuvre would have to be moved to after day 3.

Figure 3.10 shows the minimum deviation of the Moon-spacecraft-sun angle from  $90^\circ$  from day 1.5 to day 2.5 over the full launch window. If this angle is above  $20^\circ$  the manoeuvre can be nominally executed. If not, it may have to be delayed and additional propellant then has to be allocated according to figure 3.8, or the corresponding days have to be removed from the launch window, which would lead to a loss of 1 week per month. The current propellant allocation by the spacecraft contractor accounts for a delay of the first orbit correction from day 2 to day 3.5 such that the launch window in 2007 remains un-affected. According to figure 3.8 this will require an increase of the propellant allocation for the manoeuvres by a factor  $0.5/8.2 = 1.28$ .

Figure 3.9: Sun-spacecraft-moon angle during transfer (30 days from 2007/8/1)

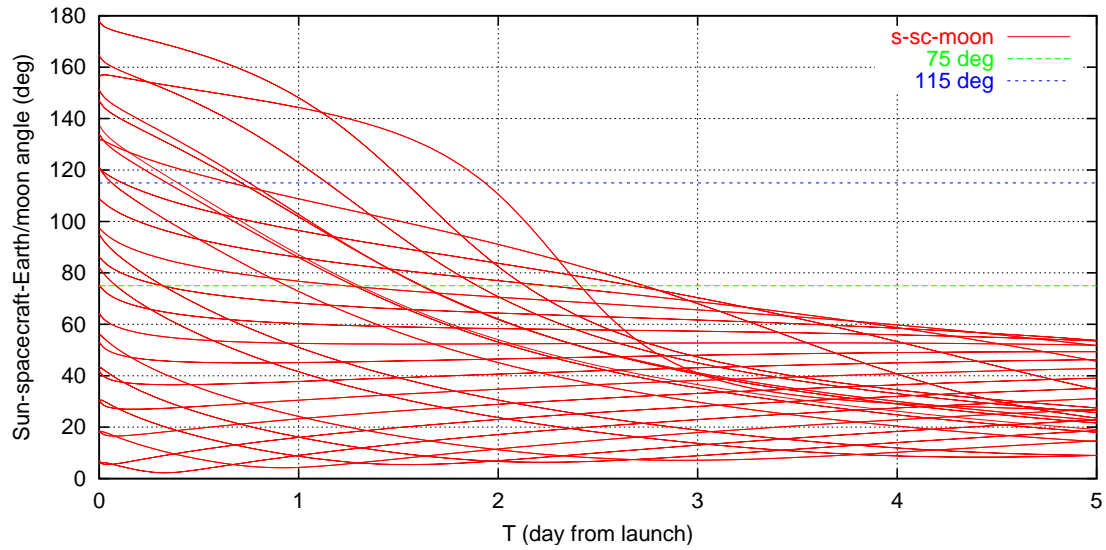
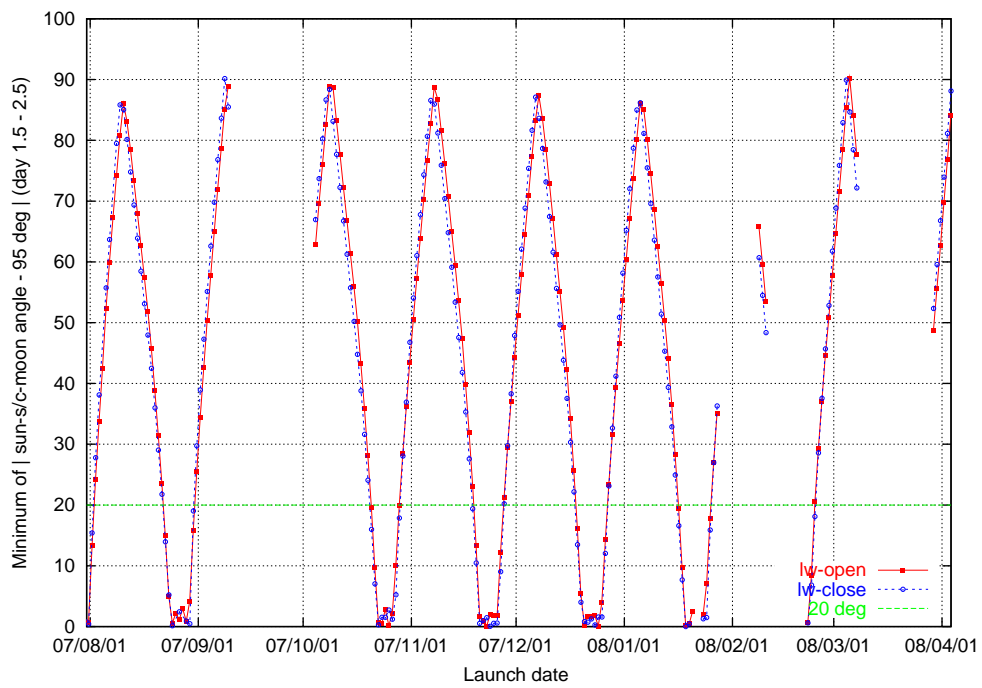


Figure 3.10: Moon aspect angle around first orbit correction - 95°



### 3.2.4 Option with Multiple ARIANE Flight Programs

If the allocation to compensate for the deterministic variation of the perigee velocity as shown in figure 3.7 by a manoeuvre on day 2 has to be reduced this will require that ARIANE delivers to different perigee velocities (=apogee radii) depending on the launch date, this means several flight programs have to be prepared. Assume 11 m/s on each of the two spacecraft are allocated for the correction manoeuvre to compensate the deviation from the required perigee velocity. From figure 3.8 showing the  $\Delta V$  to correct for the change in apocentre radius caused by 1 m/s deviation in perigee velocity (two-body problem approximation) as function of manoeuvre execution time, it can be seen that the amplification factor from perigee to day 2 is 8.2. So with an allocation of 11 m/s a perigee velocity variation of  $\pm 1.3$  m/s can be corrected. This means 4 flight programs would be necessary to cover the variation in perigee velocity (figure 3.7), assuming the correction cannot be done before day 2. It should be noted that this correction will only depend on the launch date, so it will be known before lift-off, in principle orbit determination will not be required before it, so it could even be done before day 2. However a concept of such a "blind manoeuvre" was not appreciated by ESOC, so it was decided to combine it with the first stochastic correction manoeuvre on day 2.

Those 4 perigee velocities have been chosen for the full year of 2007 (see CReMA issue 3.0) at the values given in table 3.6. The resulting apogee radii are also given in table 3.6. By removing some launch dates from the launch window a strategy with e.g. 3 flight programs and less than 10 m/s allocation for the corresponding orbit correction would be possible (compare section 3.3.1).

Table 3.6: Reference apogee radii for 4 flight programs

perigee velocity (m/s)	relative escape velocity (m/s)	apogee radius (km)
10876.0	-33.8	1075914
10878.6	-31.2	1165990
10881.2	-28.6	1272444
10883.8	-26.0	1400188

When prescribing the osculating orbital elements at spacecraft separation for the flight programs on ARIANE, the reference values in apogee radius should be chosen equidistant in perigee velocity.

## 3.3 The Herschel/Planck Launch Window 2008

### 3.3.1 Extension of Launch Window into Summer 2008

With the conditions as assumed:

- 215 m/s on Planck,
- one flight program on ARIANE (26 m/s on day 2),
- possible increase of day 2 manoeuvres (45 m/s + 26 m/s) by a factor 1.28 for a delay to day 3.5 to avoid glares by the Moon in the Planck star mapper,

the launch window will close on 2008/4/3 and re-open not before 2008/7/28.

To regain parts of the launch window from April 2008 to August 2008, these conditions could be relieved, this means a strategy with more than one flight program on ARIANE could be applied to reduce the allocation for the perigee velocity variation manoeuvre.

From figure 3.2 it can be seen that the minimum  $\Delta v$  through the saddle point in spring 2008 will be near a line of constant launch hour = 13:00. As a first approximation a daily launch hour window from 13:00 to 13:45 has therefore been assumed. Figure 3.11 gives the seasonal windows in which the moon blinds the star mapper, when then sun-spacecraft moon angle is less than  $20^\circ$  from  $95^\circ$ . If these windows are removed the propellant for the first orbit correction can be allocated without the penalty factor 1.28.

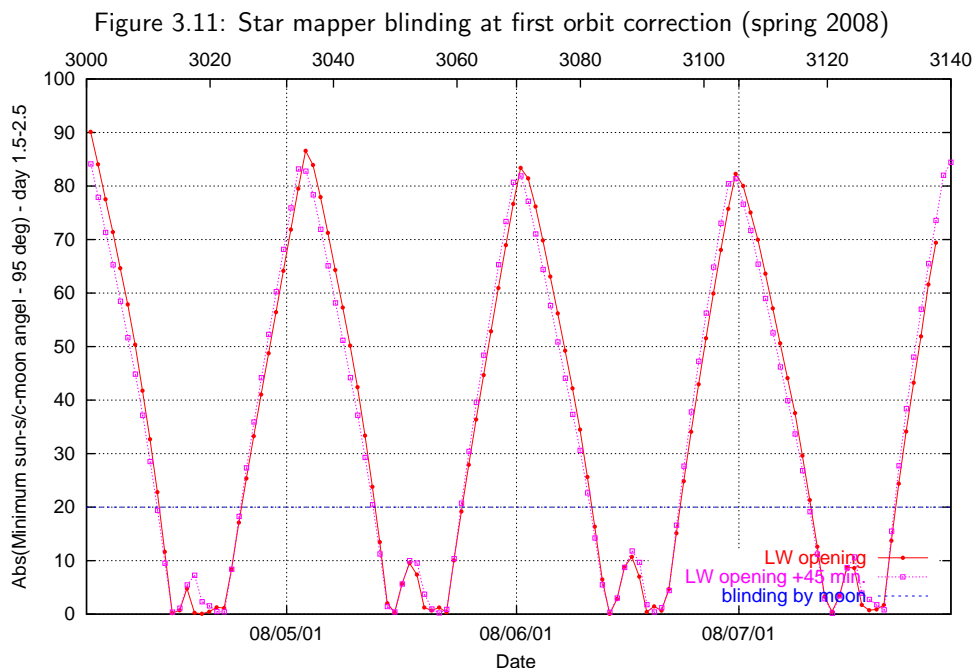


Figure 3.12 shows the perigee velocity variation over the same time interval, indicating a reduced band of admitted values to allow a strategy with 1 flight program and an allocation of 10.6 m/s ( $=8.2*1.3$ ) to cover  $\pm 1.3$  m/s. Outside that band it is assumed that the launch window is closed (no flight program).

Finally figure 3.13 shows the Planck insertion manoeuvre  $\Delta V$  from April to July 2008, also indication the intervals which have to be removed to avoid star mapper moon blinding and for the 10.6 m/s strategy with 1 flight program. It should be noted that the reference value for the flight program has to be selected differently (at -29.3 m/s) from that discussed in section 3.2.2.

In the open intervals the  $\Delta V$  required for the first orbit correction on Planck is  $45 \text{ m/s} + 11 \text{ m/s} = 56 \text{ m/s}$ . This compares to  $1.28*(45 \text{ m/s} + 26 \text{ m/s}) = 91 \text{ m/s}$ . So in these intervals the allocation for the insertion manoeuvre could be increased by  $91 \text{ m/s} - 56 \text{ m/s} = 35 \text{ m/s}$ . In addition the new transfer optimisation has saved at least 21 m/s (91% manoeuvre efficiency used before, now the 215 m/s allocation contains the geometric losses). this means a total of 271 m/s ( $=215+35+21$ ) would be available in these intervals, not taking into account the possibility of a higher filling of the Planck tank. So there is a possibility to open up to 2 week windows around begin of May 2008 and begin of July 2008.

Figure 3.12: Perigee velocity variation (spring 2008)

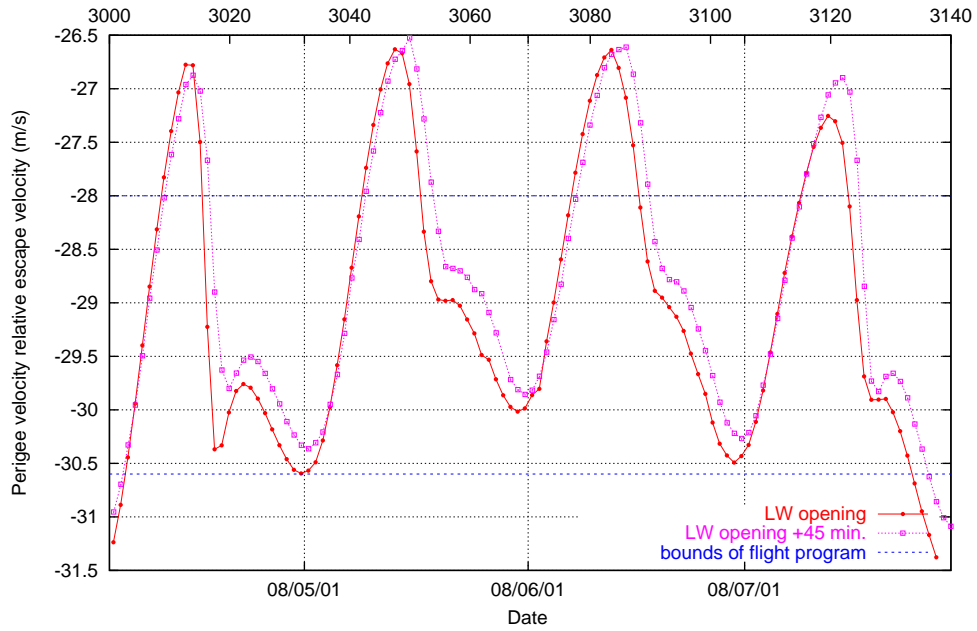
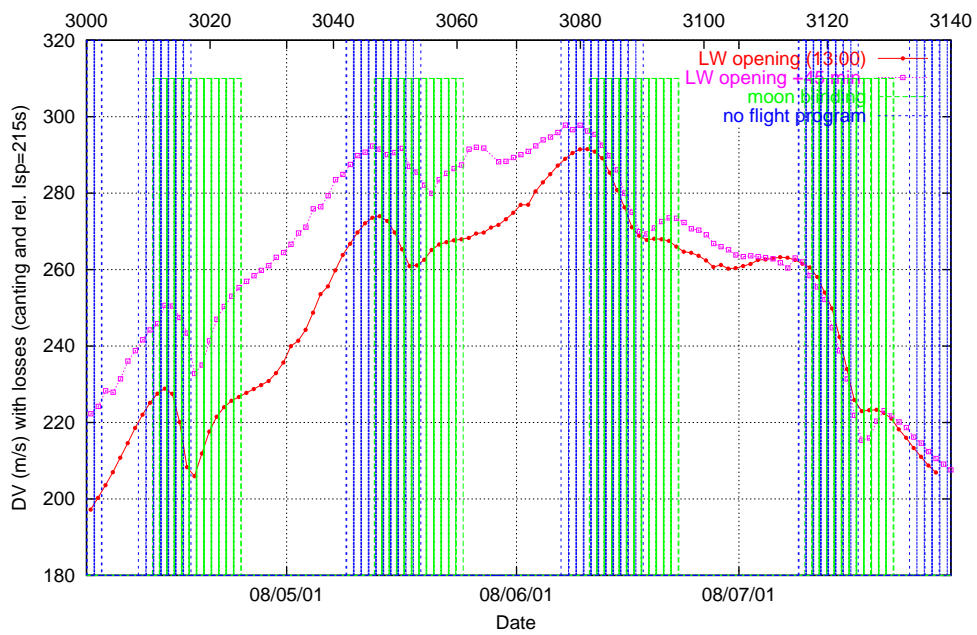


Figure 3.13: Perigee velocity variation (spring 2008)



### 3.3.2 Launch Window, Second Half of 2008

The launch window in the second half of 2008 repeats almost exactly as the launch window in the second half of 2007. The only differences come from the different phasing of the moon relative to the launch times. This may lead to different extrema in the required perigee velocity, and different time intervals with moon blinding of the star-mapper on day 2.

Figure 3.14 shows the deterministic  $\Delta V$  required on Planck. The time intervals requiring a 2 manoeuvre strategy are as in 2007. Figure 3.15 shows the required perigee velocity. It can be seen that for the one flight program strategy (perigee velocities from  $-32.77$  m/s to  $-26.68$  m/s) two days (October 13 and 14) have to be removed from the launch window (or the opening must be delayed).

Figure 3.16 shows the time intervals for which the moon may blind the star mapper around the orbit correction on day 2 (those intervals when the shown angle is below  $20^\circ$ ), such that this manoeuvre has to be delayed.

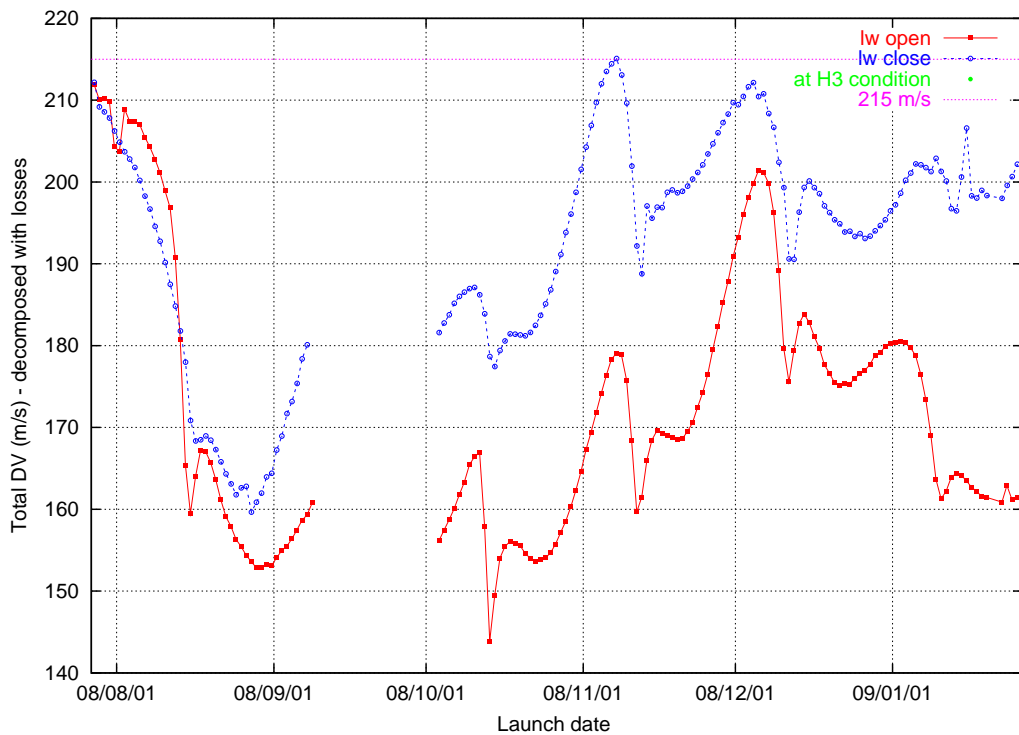


Figure 3.14: Equivalent  $\Delta V$  (LW opening and closing, end 2008)

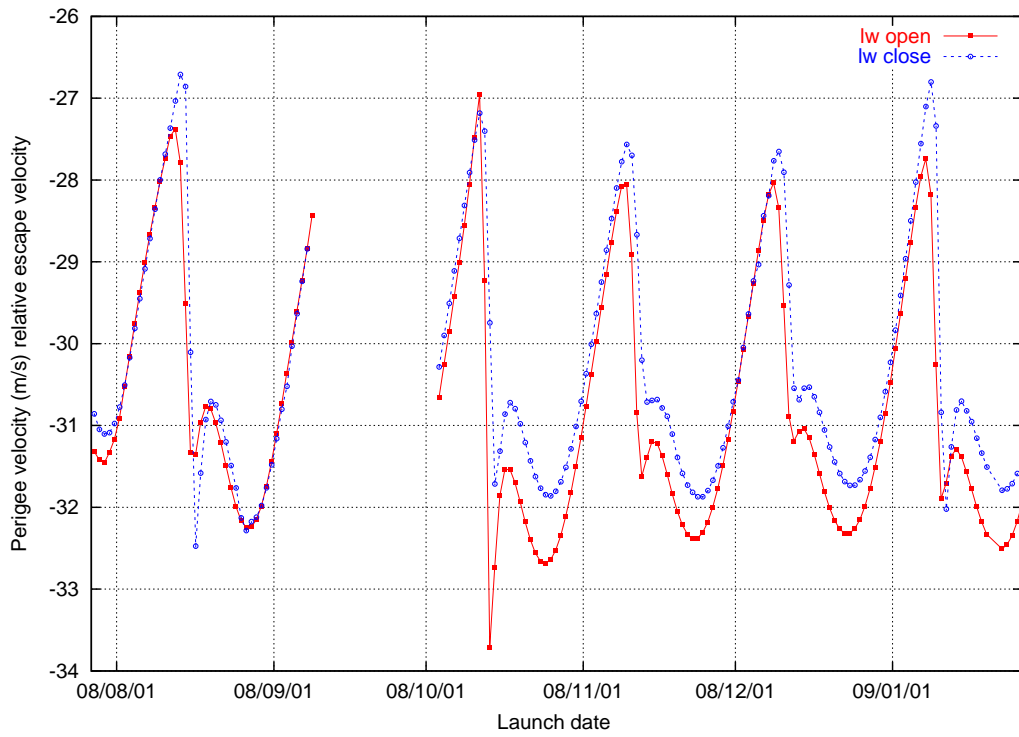


Figure 3.15: Perigee velocity (LW opening and closing, end 2008)

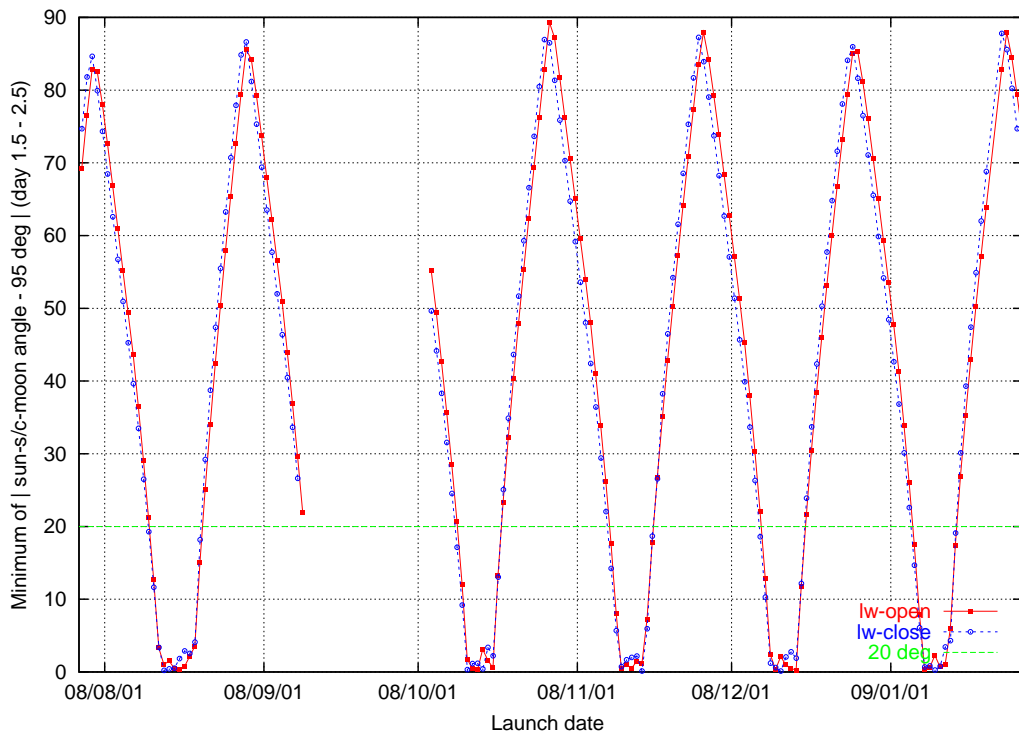
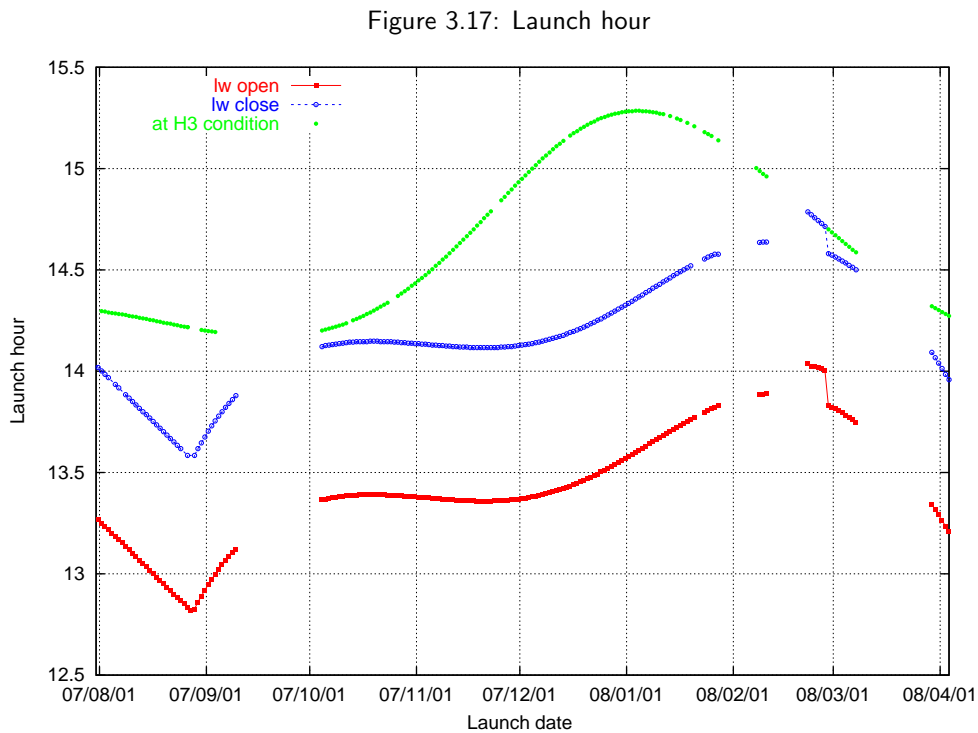


Figure 3.16: Moon blinding (LW opening and closing, end 2008)

### 3.4 Orbit Parameters over Launch Window, Winter 2007/2008

#### 3.4.1 Planck Orbit Parameters

Figure 3.17 gives the launch hour at the opening and closing of the daily slot for the launch window in winter 2007/2008. The figure also contains the time at which the sun aspect angle condition at H3 closes the launch window independent of the  $\Delta V$  (see figure 3.5).



A variety of orbit parameters has been evaluated at the opening and closing of a 45 minutes per day launch window. Figure 3.18 and 3.19 show the sun aspect angle of the launcher axis at fairing jettisoning (FJ) and at burnout of the upper stage (H3).

Figure 3.20 shows the size of the orbit insertion manoeuvre. Figure 3.21 shows the time from launch to the insertion manoeuvre. The insertion manoeuvres on Planck will use the flat thrusters only. There will be no major manoeuvre after this time. For some periods in the launch window (2007/8/1-8/22, 2007/11/6-12/29) the sun-spacecraft-Earth angle will be slightly above  $15^\circ$  at the time of the insertion manoeuvre. This condition will only be satisfied about a day later.

Figure 3.23 shows the time from launch to the out of plane manoeuvre, which will always be done before the main insertion manoeuvre. Figure 3.22 shows the size of the out of plane manoeuvre on Planck. The out of plane manoeuvre will use the flat thrusters only. The curves show that the optimisation of the distribution of  $\Delta V$  between the two manoeuvres needs refinement.

Figures 3.24 and 3.25 show the maximum and minimum declination over the Planck mission duration, from which the visibility from a ground station can be concluded using figure 3.30 and figure 3.26; and 3.27 give the orbit amplitudes.

Figure 3.18: Sun aspect angle of launcher axis at event FJ

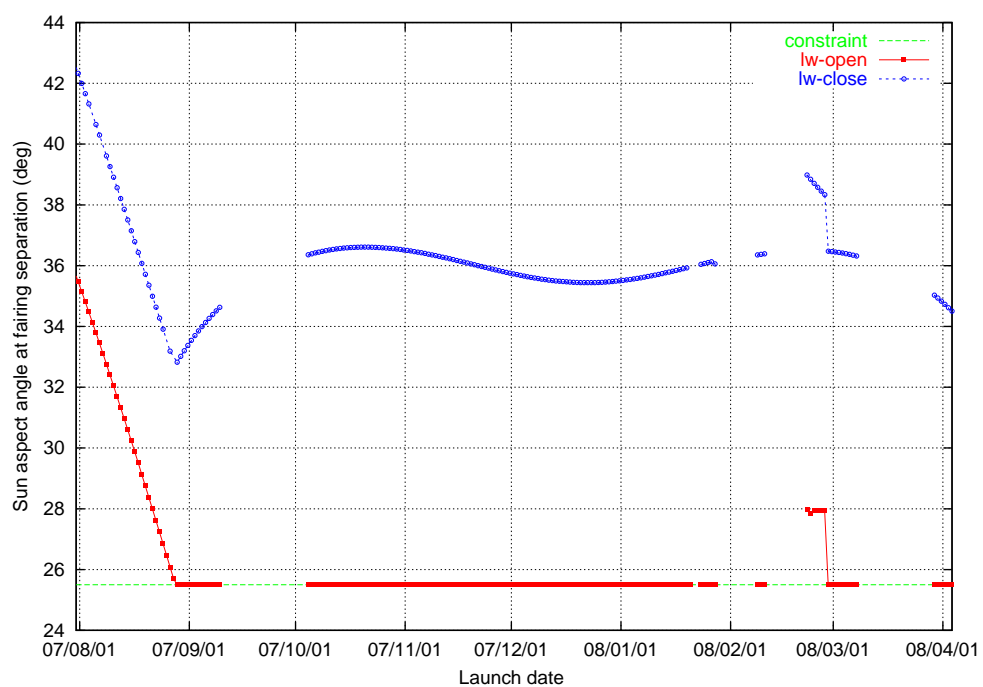


Figure 3.19: Sun aspect angle of launcher axis at event H3

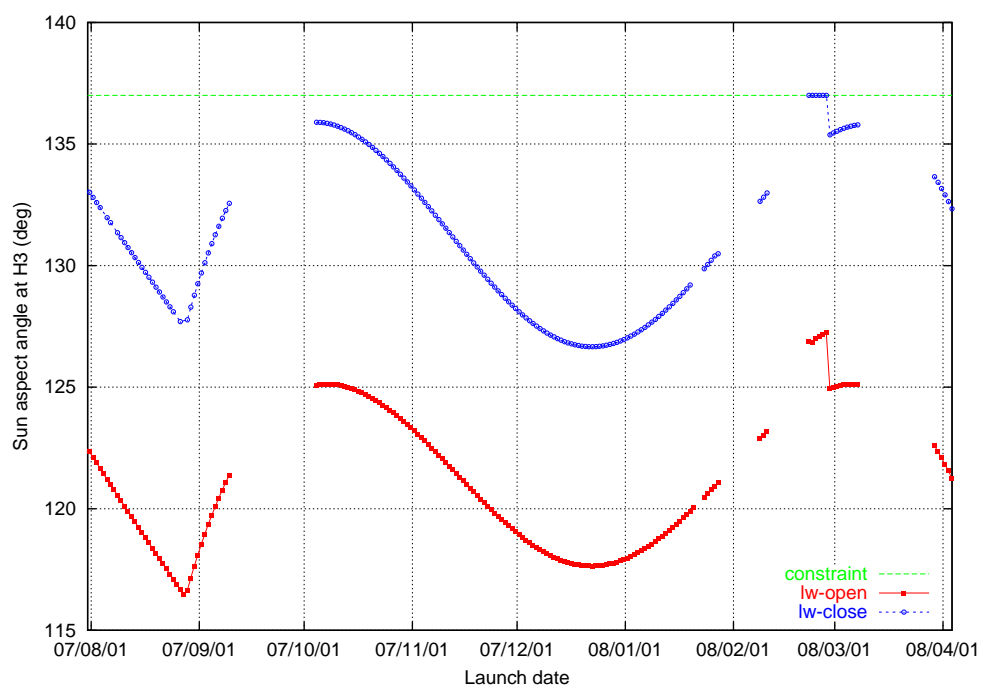


Figure 3.20: Size of orbit insertion manoeuvre for Planck

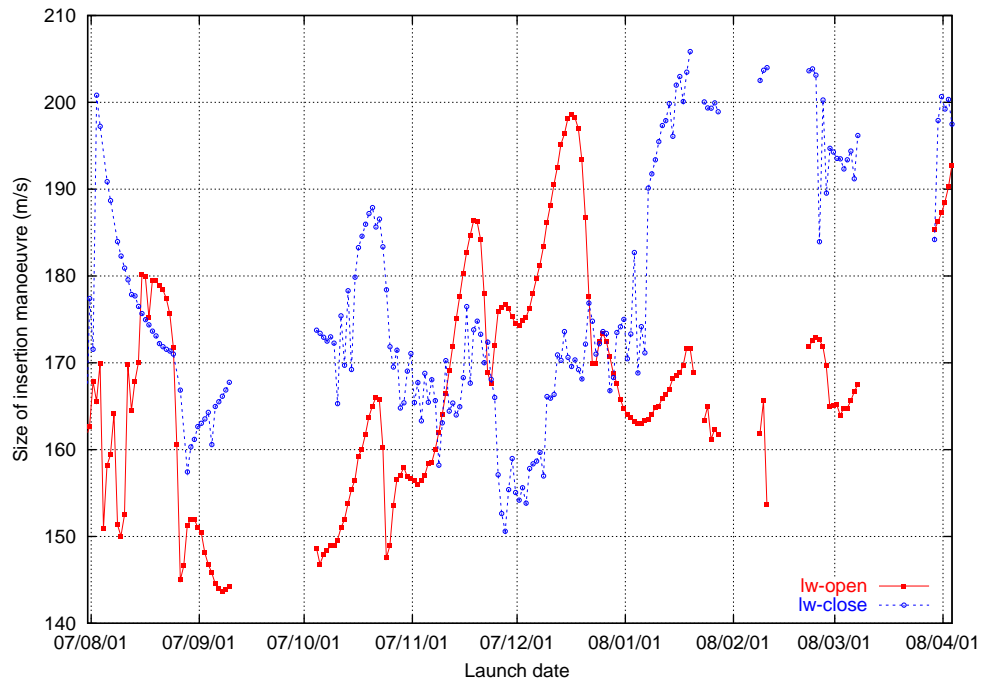


Figure 3.21: Time to orbit insertion manoeuvre for Planck

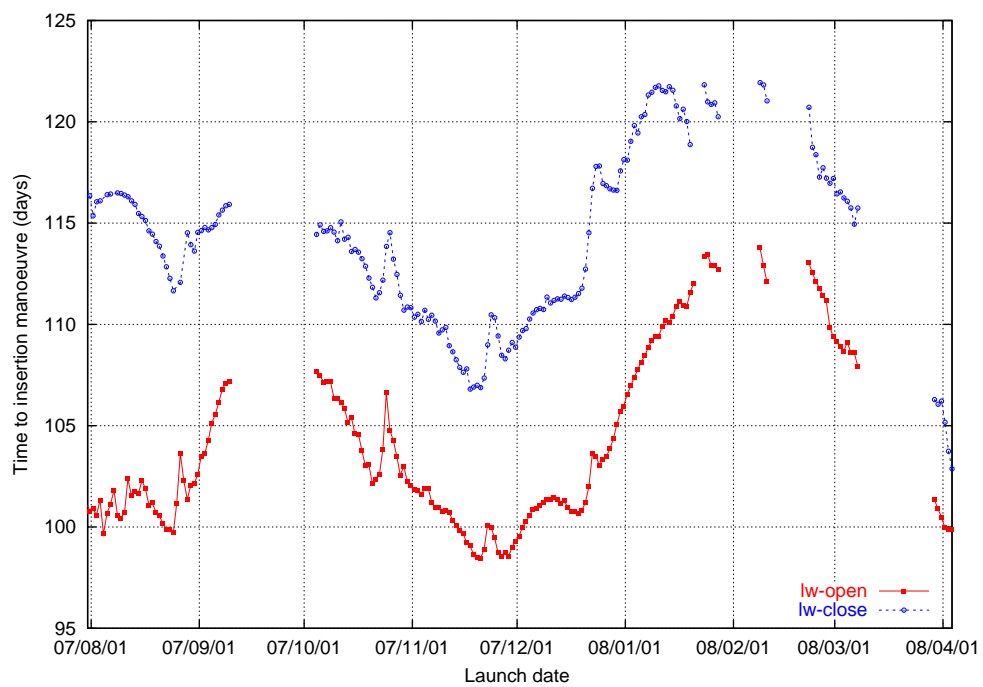


Figure 3.22: Size of out of plane manoeuvre for Planck

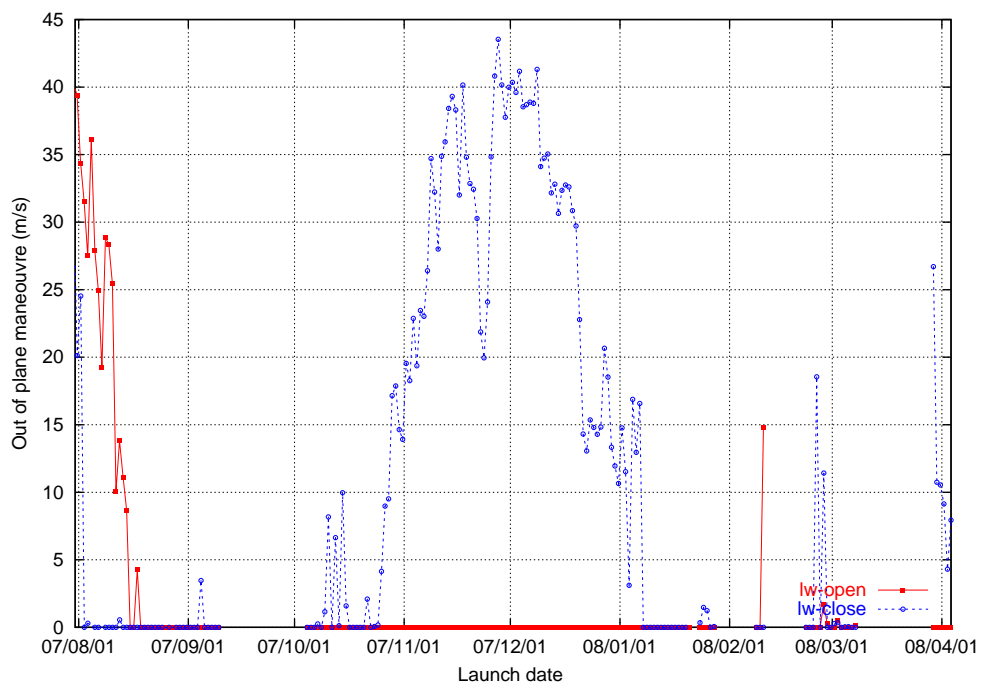


Figure 3.23: Time of out of plane manoeuvre for Planck

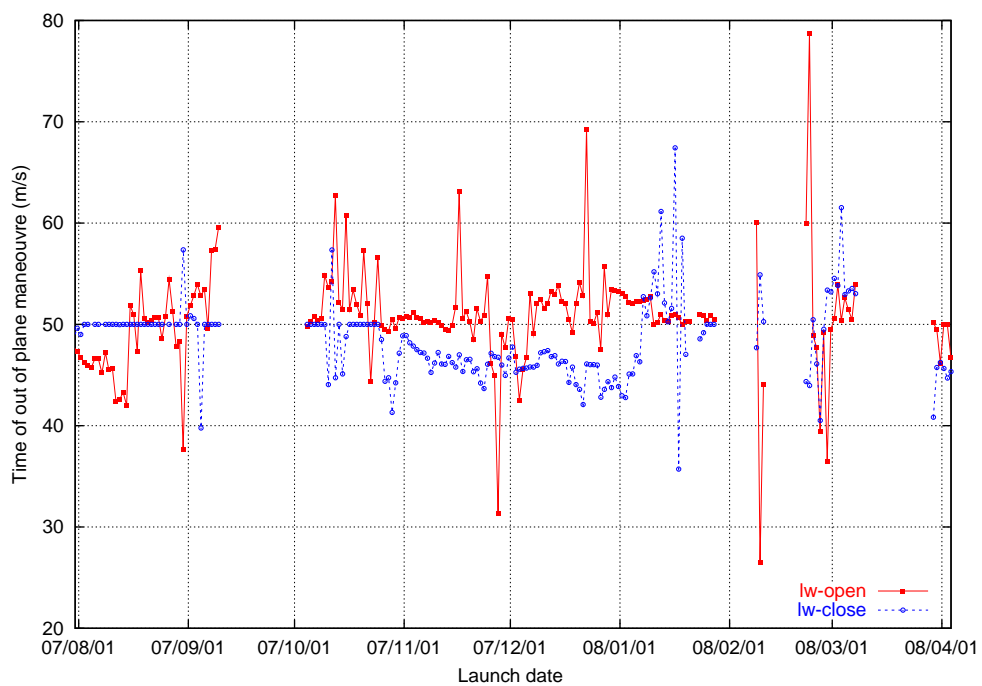


Figure 3.24: Maximum declination for Planck

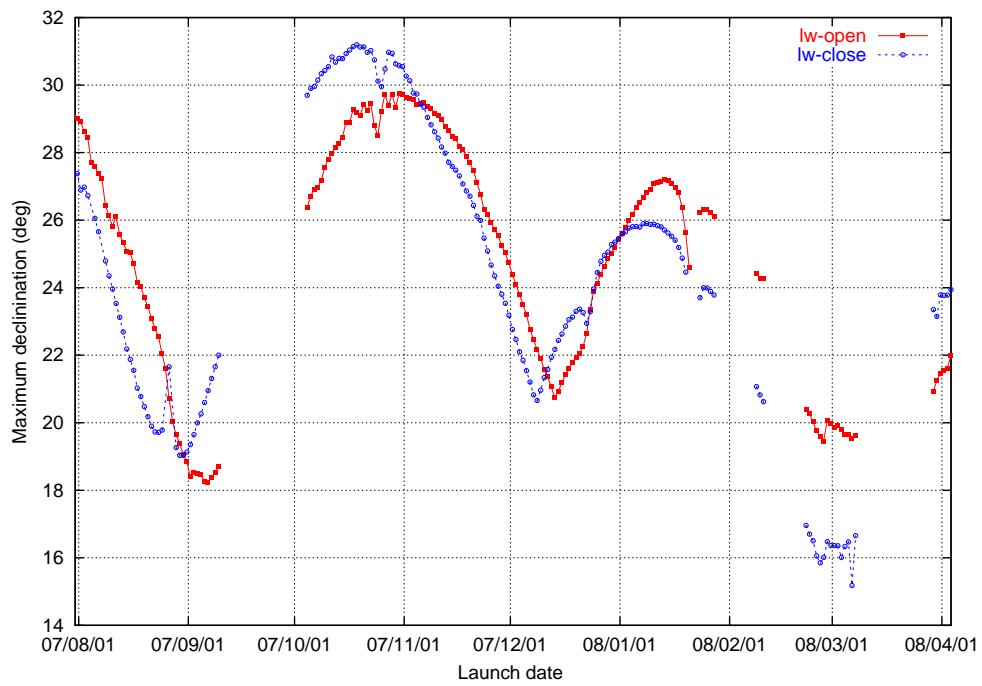


Figure 3.25: Minimum declination for Planck

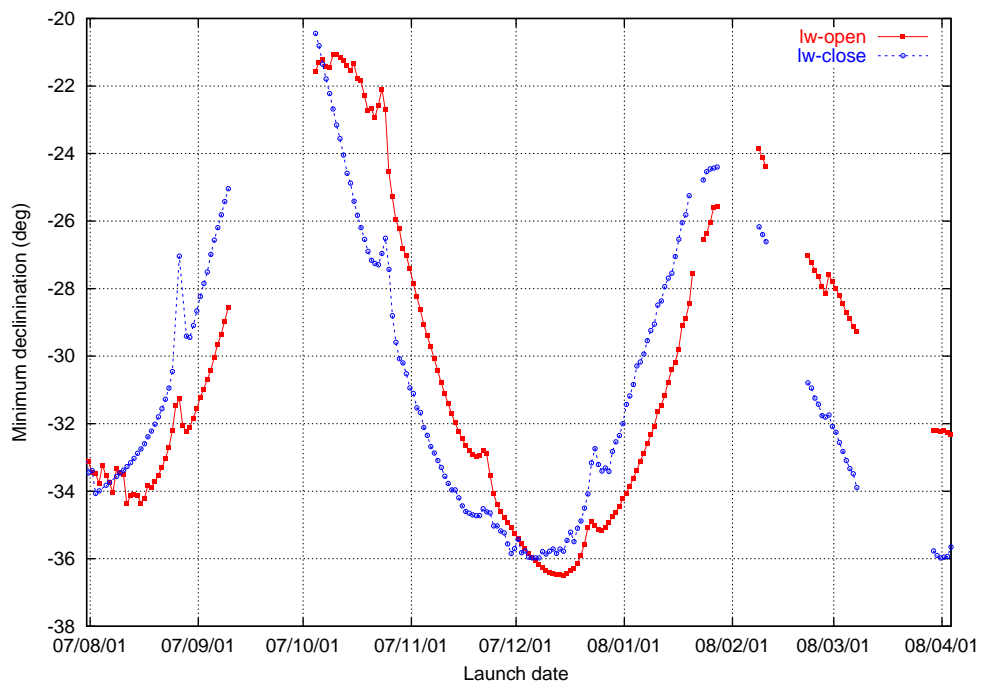


Figure 3.26: Y-amplitude for Planck

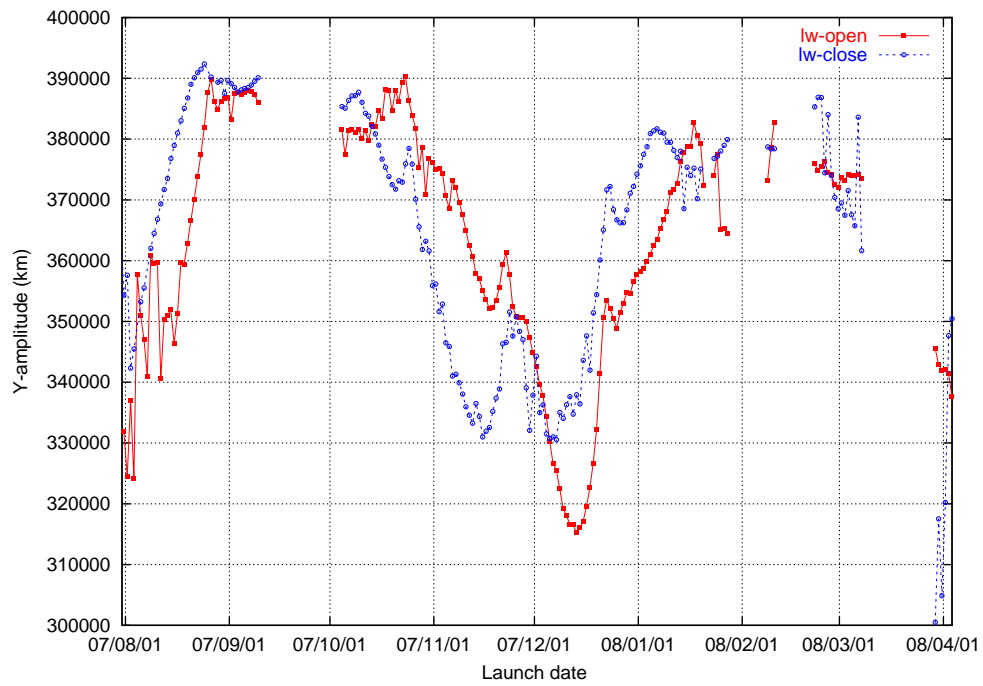


Figure 3.27: Z-amplitude for Planck

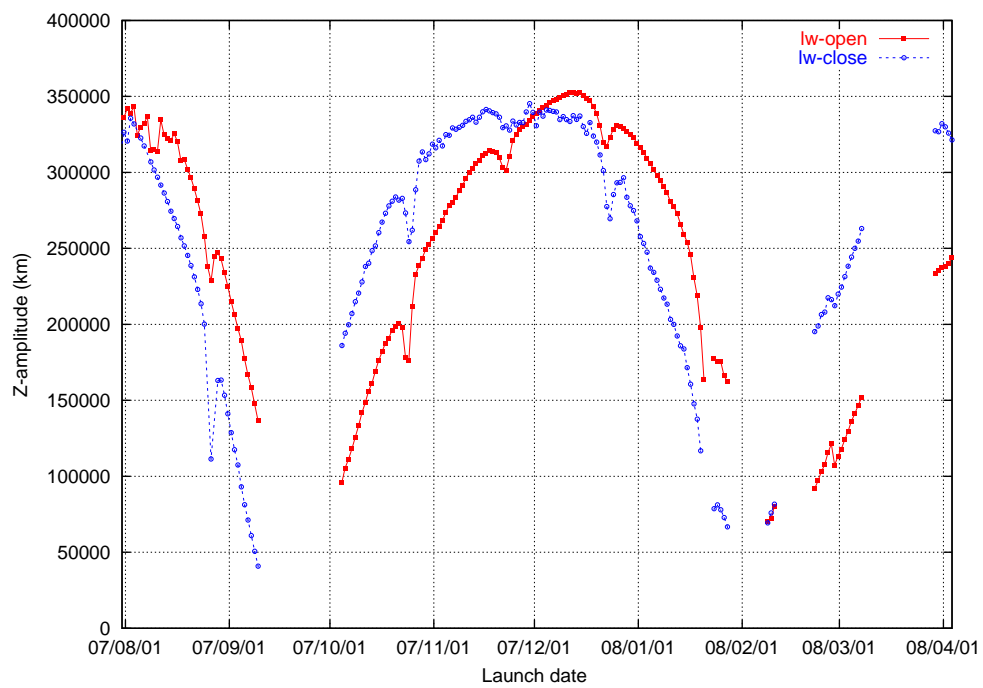
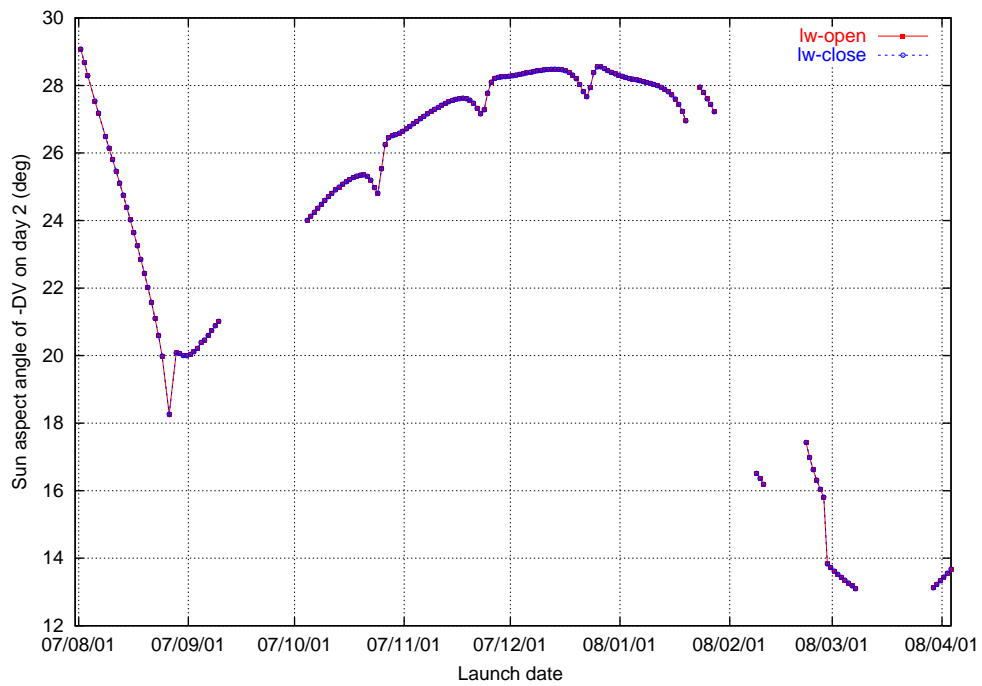


Figure 3.28 shows the sun aspect angle of a vector opposite to the spacecraft velocity on day 2 from launch. The optimum direction of the deterministic perigee velocity correction manoeuvre can be assumed to be close to the velocity or opposite, so the manoeuvre will have a sun aspect angle as shown in figure 3.28 or  $180^\circ$  minus that angle, depending on how the ARIANE flight programs are selected and then depending on the launch date. It can also be assumed that for large launcher dispersions the first stochastic orbit correction manoeuvre on day 2 will be closely aligned to the line defined by the angle shown in figure 3.28. The second Eigenvalue of the covariance matrix on day 2 is much smaller than the first ("cigar shape"), so if the manoeuvre is not aligned to that line it will be much smaller.

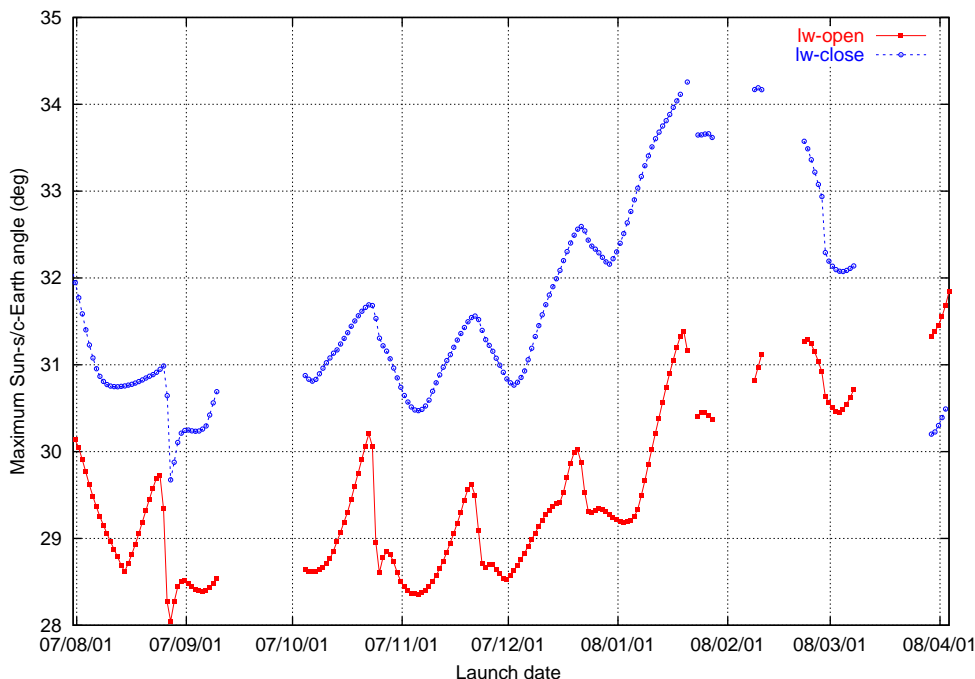
Figure 3.28: Sun aspect angle of -velocity on day 2



### 3.4.2 Herschel Orbit Parameters over Launch Window

Figure 3.29 shows the maximum sun-spacecraft-Earth angle at opening and closing of the daily slot of the days in the launch window, as reached by Herschel in its 4.5 years extended mission.

Figure 3.29: Maximum sun-spacecraft-Earth angle for Herschel



An important parameter for Herschel is the maximum declination reached over the mission. In the previous launch window (before PMAR) values could be reached for some launch dates which led to zero coverage from New Norcia according to figure 3.31. It has now been assumed that the elevation from the ground station at which telemetry can be received and commands can be sent can go down to 5°, as permitted for non-deep-space missions. The now relevant coverage duration as function of elevation is given in figure 3.30. In the orbit determination study the performance of the tracking at elevations below 15° has been assumed to be 10 times worse. In general low elevation tracking data will be disregarded.

Figure 3.33 and 3.32 give the minimum and maximum declination reached over 5 years for Herschel. The worst case is for a launch in October, the maximum then is +41°, which means 6.5 hours visibility from New Norcia (4.6 hours above 10° elevation). Ground station coverage in the operational orbits will be further discussed in section 3.5.4.

Figure 3.30: Declination versus visibility duration (5° minimum elevation)

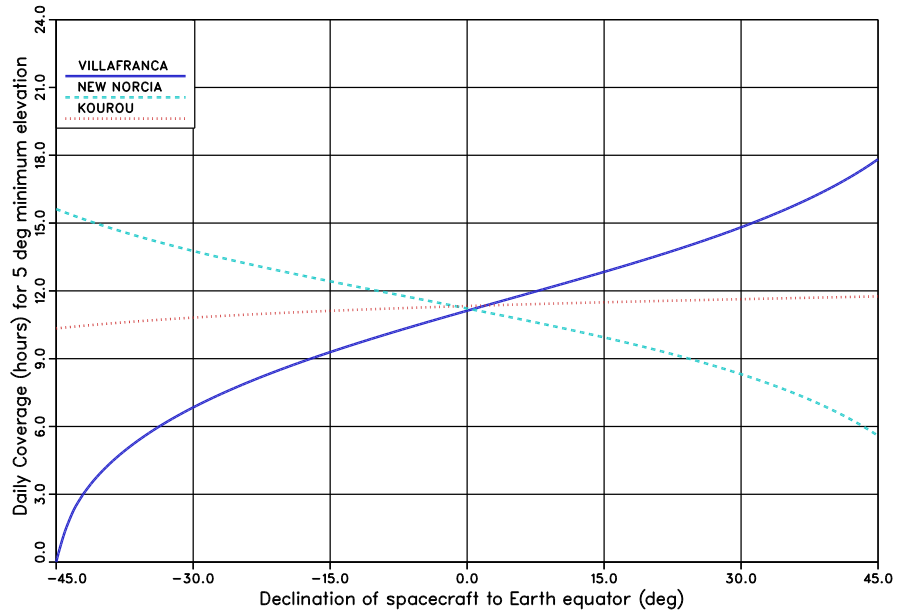


Figure 3.31: Declination versus visibility duration (10° minimum elevation)

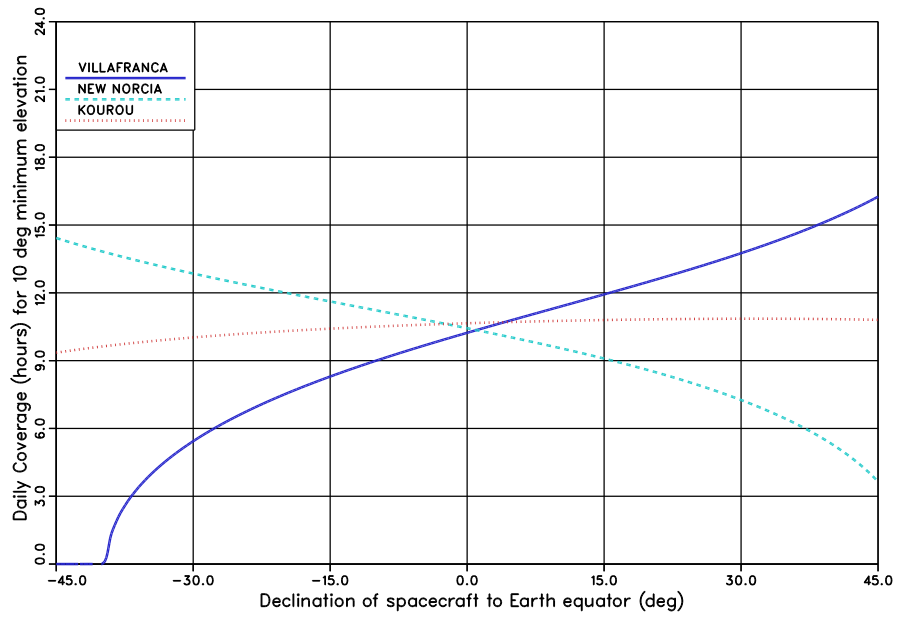


Figure 3.32: Maximum declination for Herschel

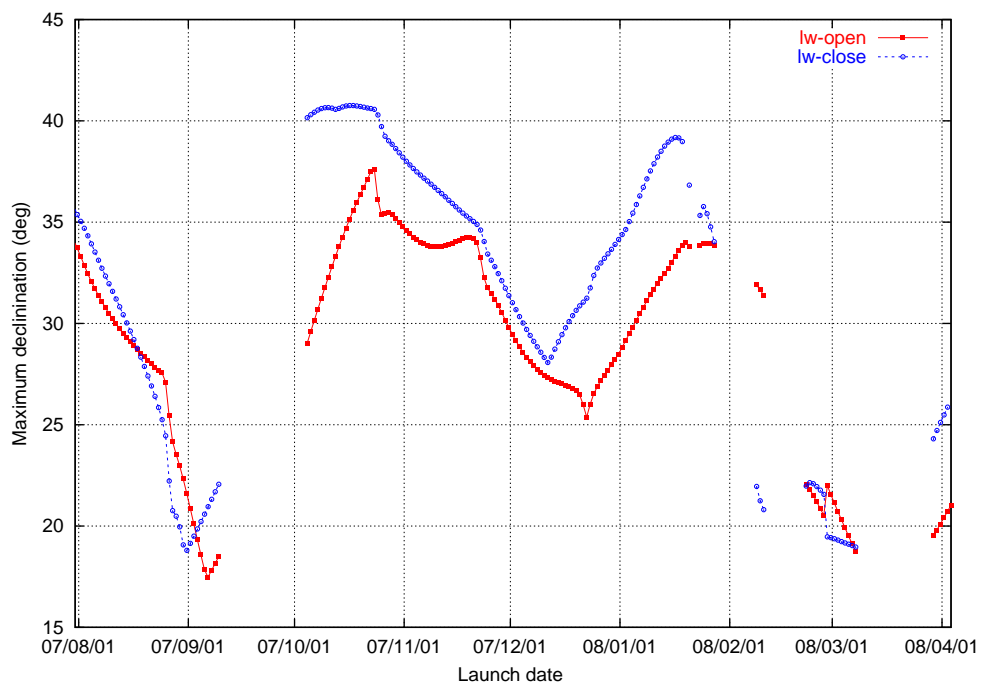


Figure 3.33: Minimum declination for Herschel

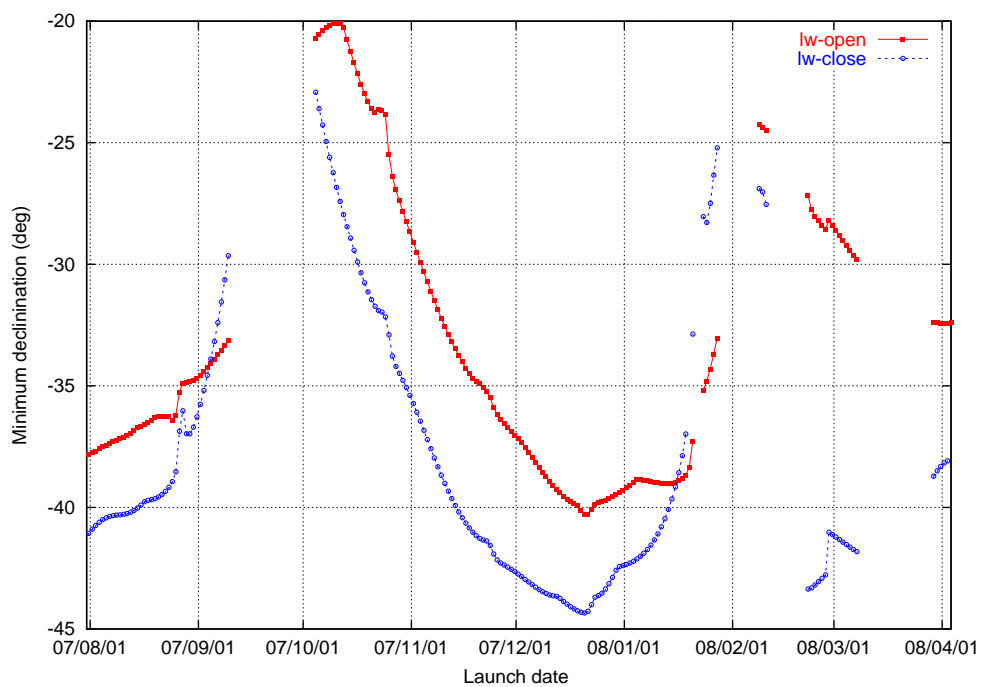


Figure 3.34: Y-amplitude for Herschel

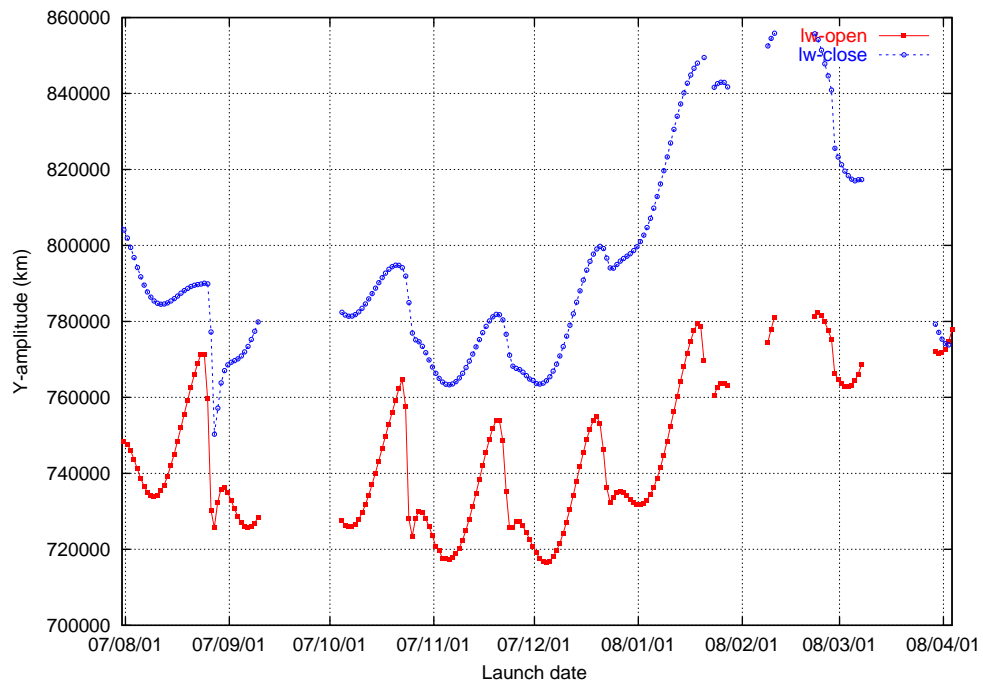
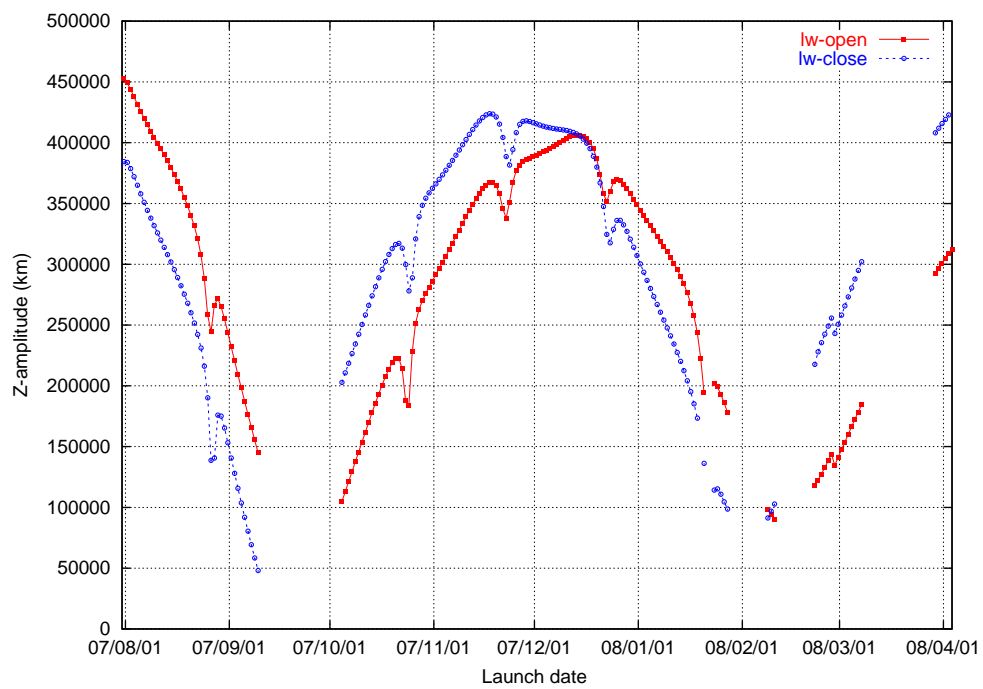


Figure 3.35: Z-amplitude for Herschel

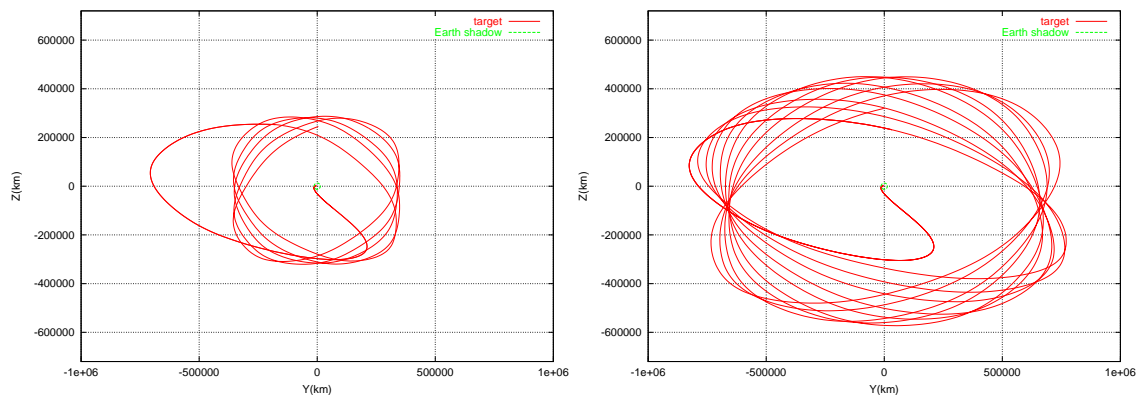


### 3.4.3 Orbit Shapes over Launch Window, Winter 2007/2008

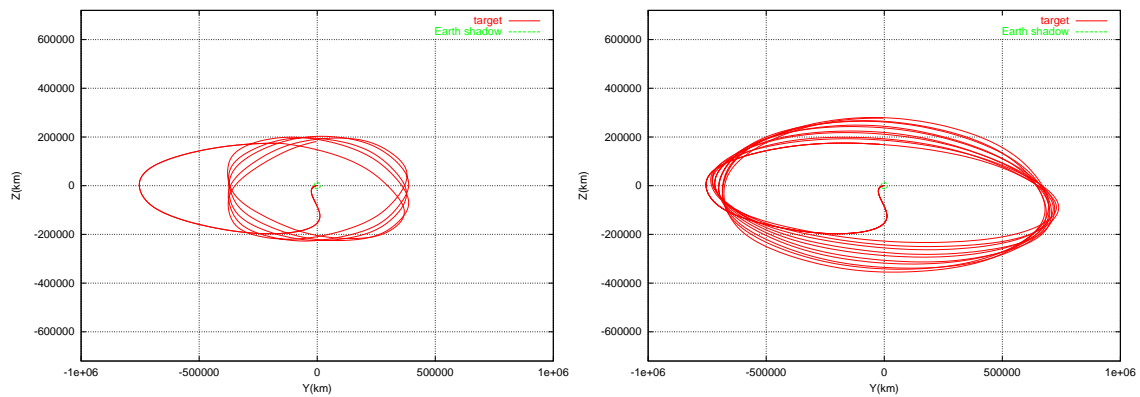
As explained before it is part of the launch concept for Herschel/Planck to start from the same transfer orbit in the frame rotating with the Earth (to reduce the number of flight programs on ARIANE). Therefore mainly depending on the launch date, different orbits around  $L_2$  will be reached.

Figure 3.36 to 3.38 show the yz-plane projection in the rotating frame ( $x$ =sun to Earth,  $y$  positive along Earth velocity, so the  $y$ - $z$  figure is as seen from outside the Earth orbit) of the Herschel (right) and the Planck (left) orbit for a launch about once per month inside the launch window, each time at the opening of the daily launch slot as defined in figure 3.1. The orbits are shown for one day per month from August 2007 to April 2008.

Figure 3.36: Variation of orbit shape for Herschel (right) and Planck (left) August-September 2007

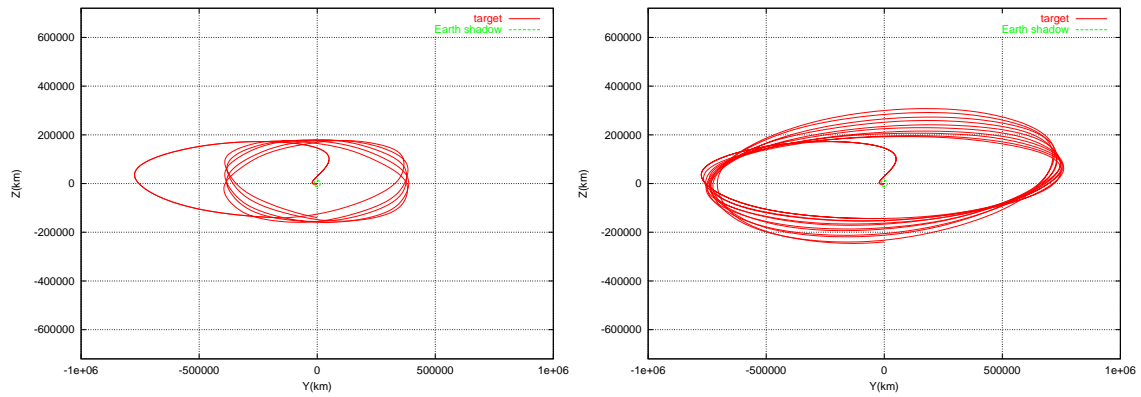


Launch on 2007/8/3 - 12:38:00, equivalent  $\Delta V= 183$  m/s (two manoeuvres)

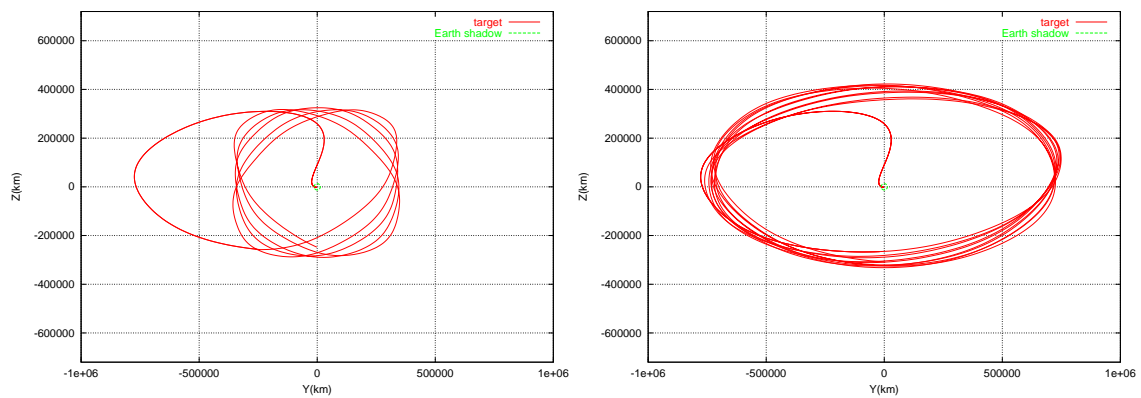


Launch on 2007/9/1 - 12:37:44, equivalent  $\Delta V= 151$  m/s

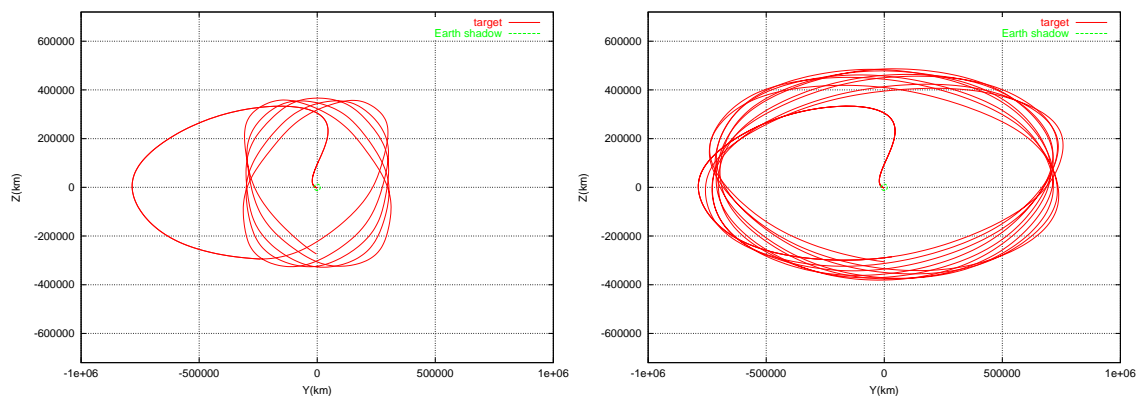
Figure 3.37: Variation of orbit shape for Herschel (right) and Planck (left) October-December 2007



Launch on 2007/10/15 - 13:04:15, equivalent  $\Delta V= 159$  m/s

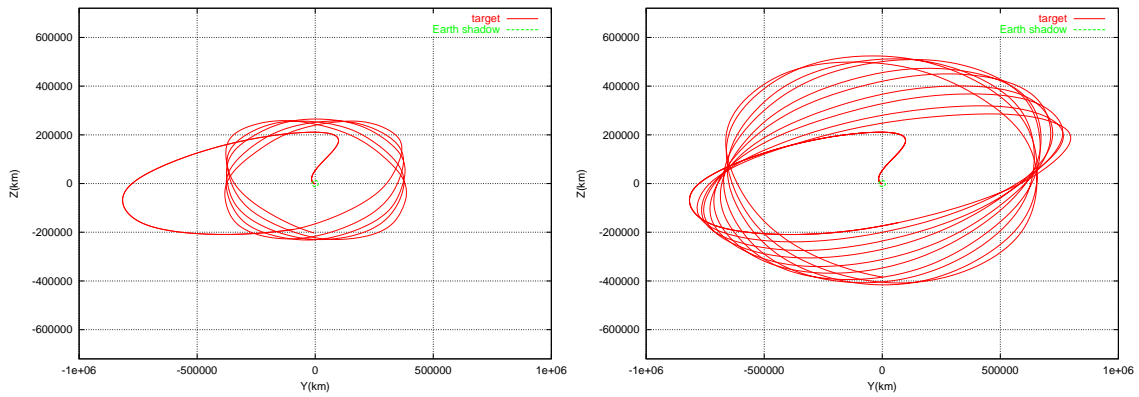


Launch on 2007/11/15 - 13:02:37, equivalent  $\Delta V= 183$  m/s

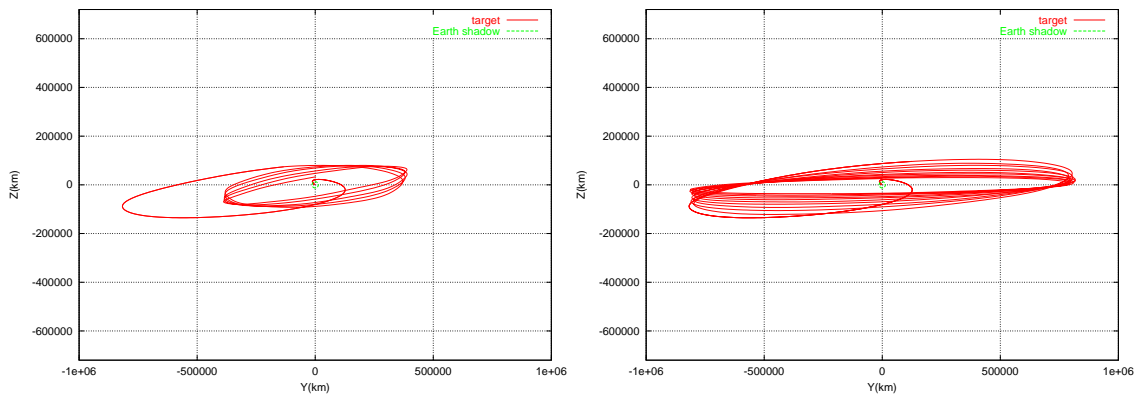


Launch on 2007/12/15 - 13:06:55, equivalent  $\Delta V= 200$  m/s

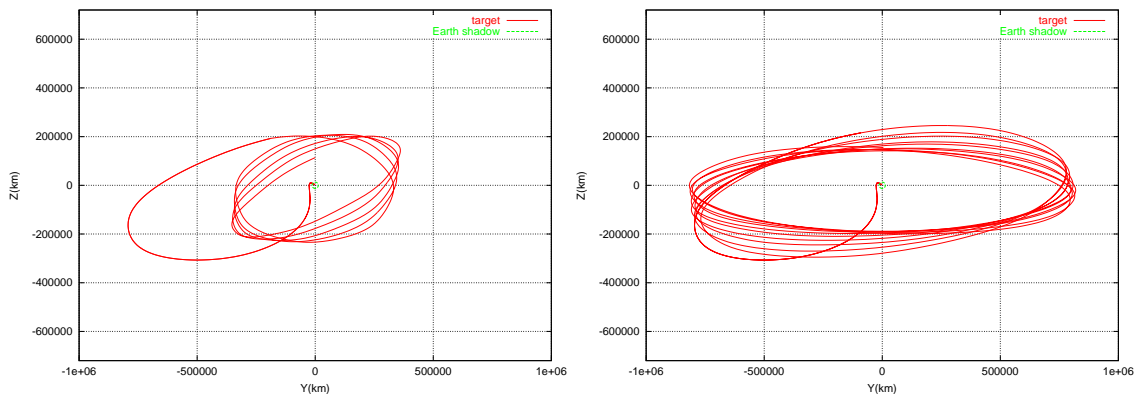
Figure 3.38: Variation of orbit shape for Herschel (right) and Planck (left) January-March 2008



Launch on 2008/01/15 - 13:24:22, equivalent  $\Delta V= 170$  m/s



Launch on 2008/02/22 - 13:43:10, equivalent  $\Delta V= 173$  m/s



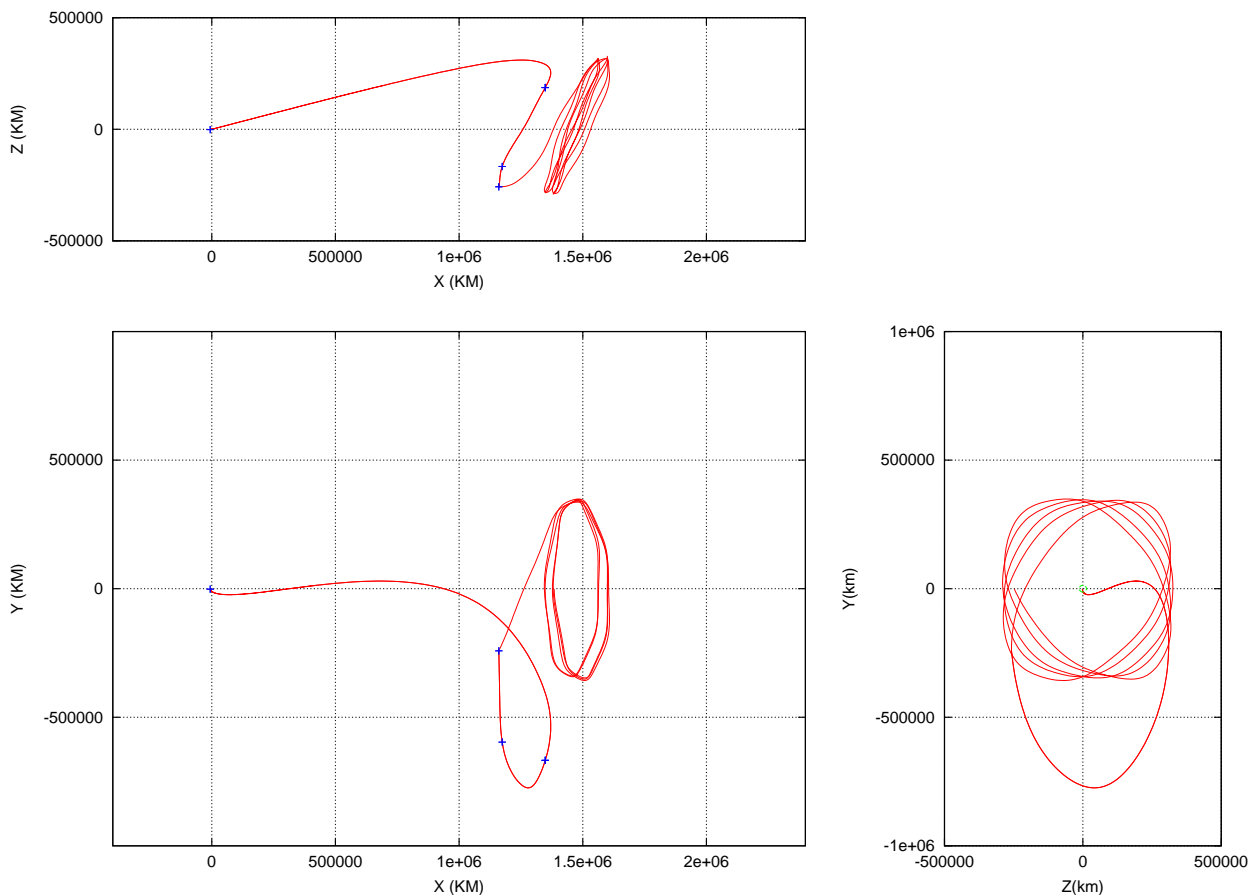
Launch on 2007/03/29 - 13:01:31, equivalent  $\Delta V= 187$  m/s

### 3.5 Reference Orbits for Herschel and Planck

#### 3.5.1 Planck Reference Orbit (Launch on 2007/11/15)

Figures 3.39 to 3.45 display the geometry of a typical pair of transfer orbits for Herschel and Planck starting from the same launch conditions (lift-off on 2007/11/15-13:03 UT, spacecraft separation at 13:22 UT on A5E/CA - optimum). The figures include 2 years of propagation in the operational orbit for Planck and 4.5 years for Herschel.

Figure 3.39: Transfer and Lissajous Orbit for PLANCK, 2007/11/15 launch



All integrations are started at perigee, where the first velocity bisection to find the fuzzy boundary is done. This perigee is hypothetical, as it is before spacecraft separation from the launcher.

The osculating orbital elements at spacecraft separation for an integration with sun + moon (without  $J_2$  nor other harmonics, nor other planets, nor radiation pressure) in the J2000 frame for the reference case are given in table 3.7. The table also gives the orbit reached by Planck and other parameters resulting from the optimisation. The radiation pressure effect is negligible in terms of required perigee velocity. However the  $J_2$  effect will have to be included in the final launch window calculations.

PLANCK ORBIT IN ROTATING FRAME

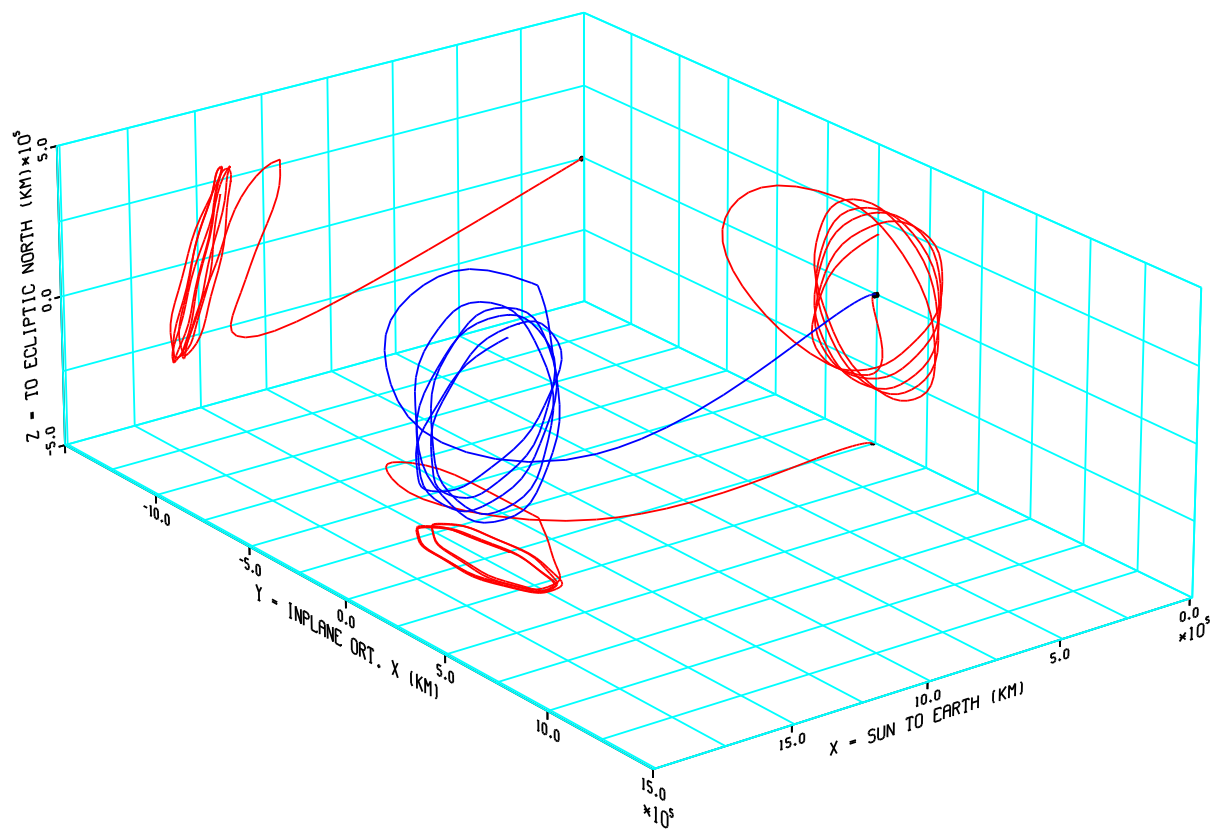


Figure 3.40: Transfer and Lissajous Orbit for PLANCK (3D), 2007/11/15 launch

Table 3.7: Transfer orbital parameters (reference case)

```

LAUNCH PERIGEE 2007/11/15-13:21:40.43 ( 2875.556718)
-----
LIFT OFF TIME                2875.54348
HR,MIN,SEC                   13: 2: 36.6
SUN ASEPECT ANGE AT FJ      25.49998
SUN ASEPECT ANGE AT H3     121.14360

PERIGEE VELOCITY (KM/S)     10.88010
ESCAPE VELOCITY (KM/S)     10.90981
VP-VESC (M/S)               -29.71058

ORBIT AT S/C SEPARATION
-----
SEMIMAJOR AXIS (KM)         615702.72
ECCENTRICITY                 0.9891217
PERIGEE RADIUS (KM)         6697.82
APOGEE RADIUS (KM)          1224707.63
INCLINATION (DEG)           14.00000
R.A. OF ASC. NODE (DEG)     42.77138
ARGUMENT OF PERIGEE (DEG)   207.7540000
TRUE ANOMALY (DEG)          34.6420000

LISSAJOUS ORBIT AFTER INSERTION MANOEUVRE
-----
A1      -11717.41556
A2      -19911.53971
AX      110907.63405
AY      353488.05955
AZ      311616.52713
FIXY    -0.72446
FIZ     201.86978

SOLUTION FROM OPTIMISER
-----
DVP (M/S)      -0.0150517
TI (DAY)       99.6921679
DVI (M/S)      180.1546359
SASPI (DEG)    128.3486379
TU (DAY)       199.3314332
dvsum         180.3353097
BOM           42.7713824
SOM           207.7540000

MIN HEIGHT SHAD. 171847.1514904 IN ORBIT T= 121.2424965
MIN HEIGHT SHAD. 4012.2884094 IN TRANS T= 0.0130152
MIN S-SC-E      13.1614368 AT T= 594.5968928
MAX S-SC-E      14.9968522 AT T= 163.6603018
MOONASP         47.6027219 CLOSEST TO 95, DAY 1.5 TO 2.5
DECMIN         -32.4452347
DECMAX          28.4054288

INSERTION-MANOEUVRE AT 2975.2488857717
-----
AXIAL (M/S)     0.000
FLAT (M/S,DEG) 182.038 -12.089
UPPER (M/S,DEG) 0.000 -12.089
UPPER 2 (M/S)  0.000
COST (M/S)     182.038

EQUIVALENT TOTAL DV (M/S) 182.21820
PENALTY FACTOR IN PERIGEE DV 12.00000

```

Figure 3.41: Transfer and Lissajous Orbit for PLANCK, 2007/11/15 launch (inertial)

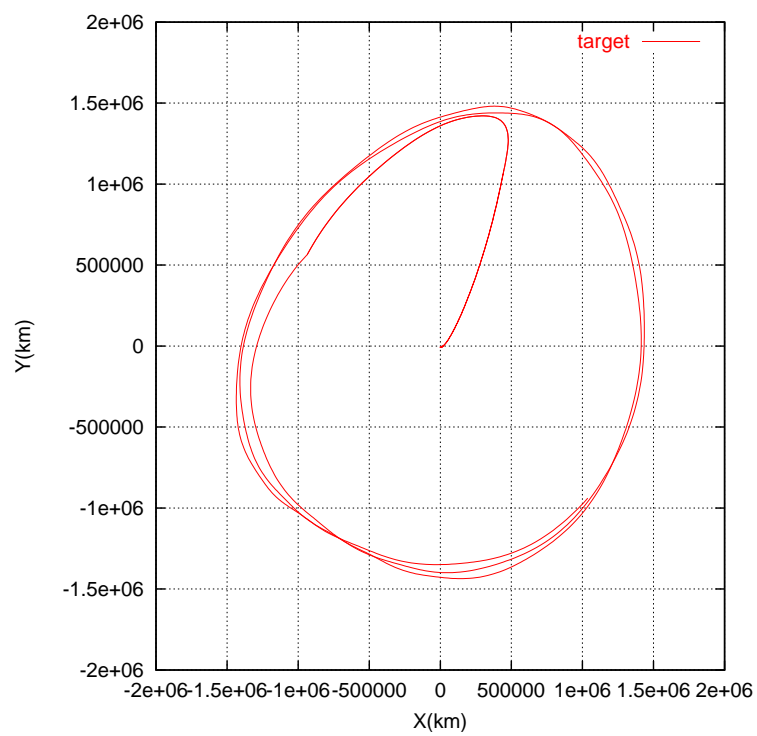
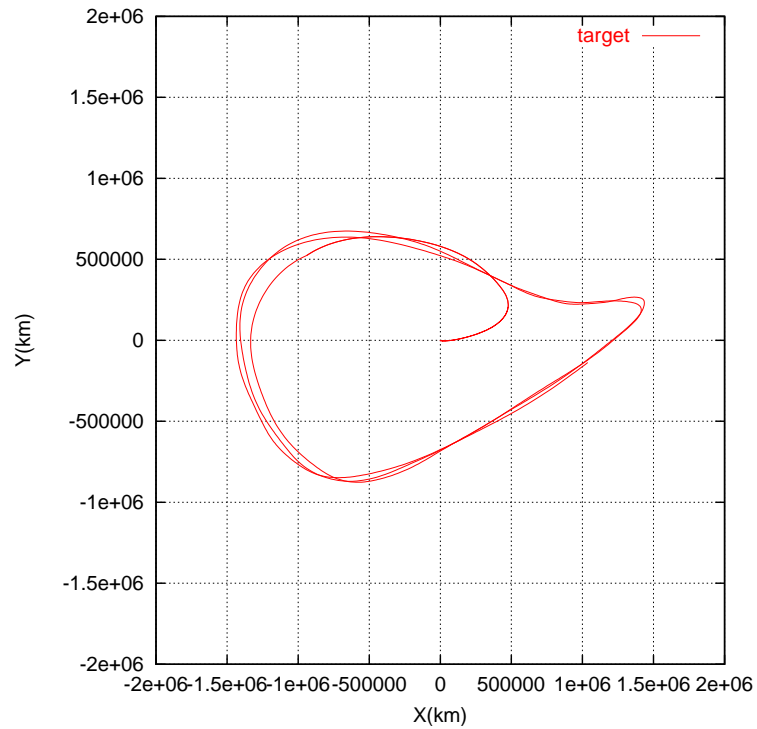
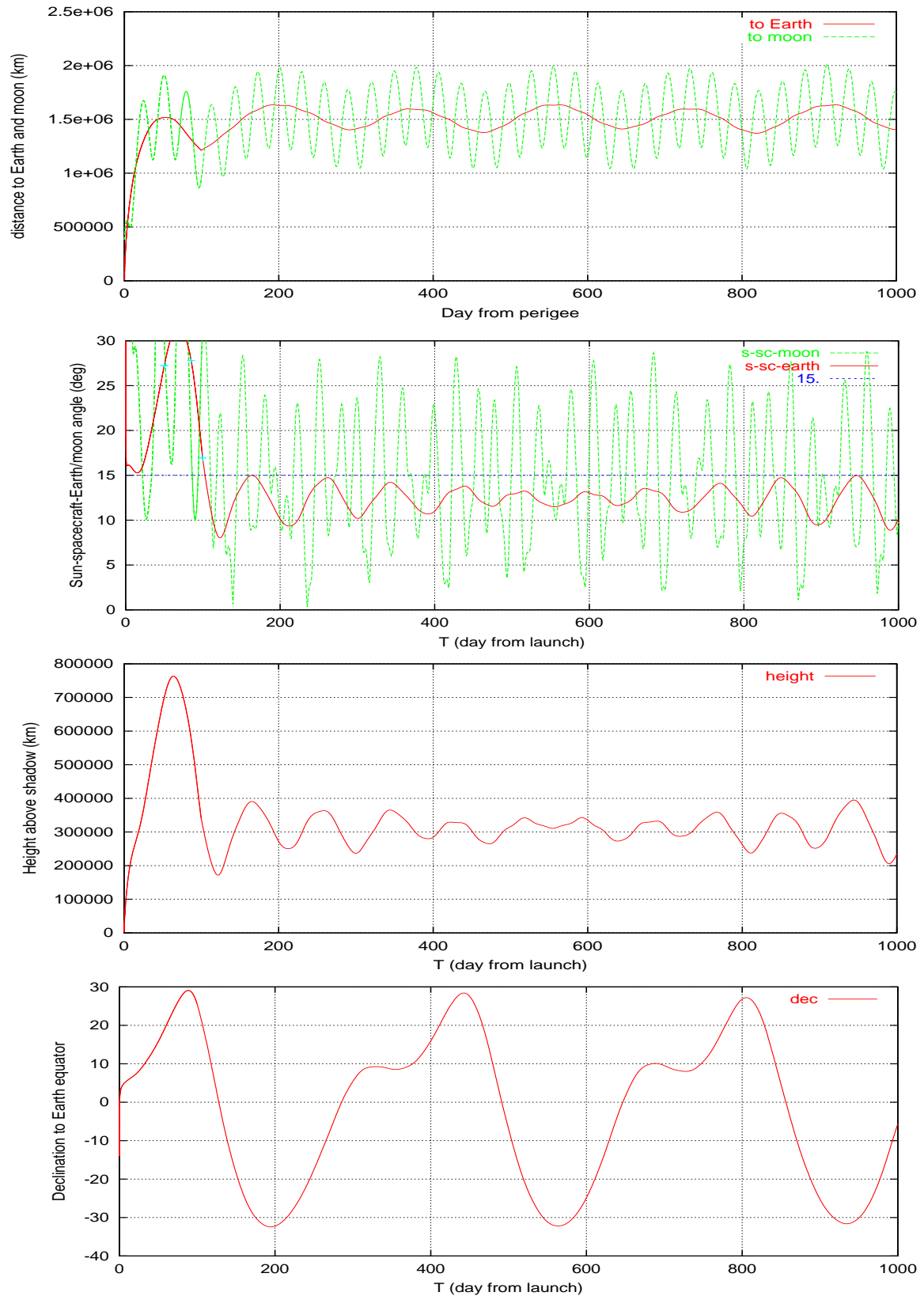


Figure 3.42: Transfer and Lissajous Orbit for PLANCK, 2007/11/15 launch (parameters)



### 3.5.2 Herschel Reference Orbit (Launch on 2007/11/15)

Figure 3.44 to 3.45 shows the Herschel orbit for the reference launch date.

Figure 3.43: Transfer and Lissajous Orbit for Herschel, 2007/11/15 launch (inertial)

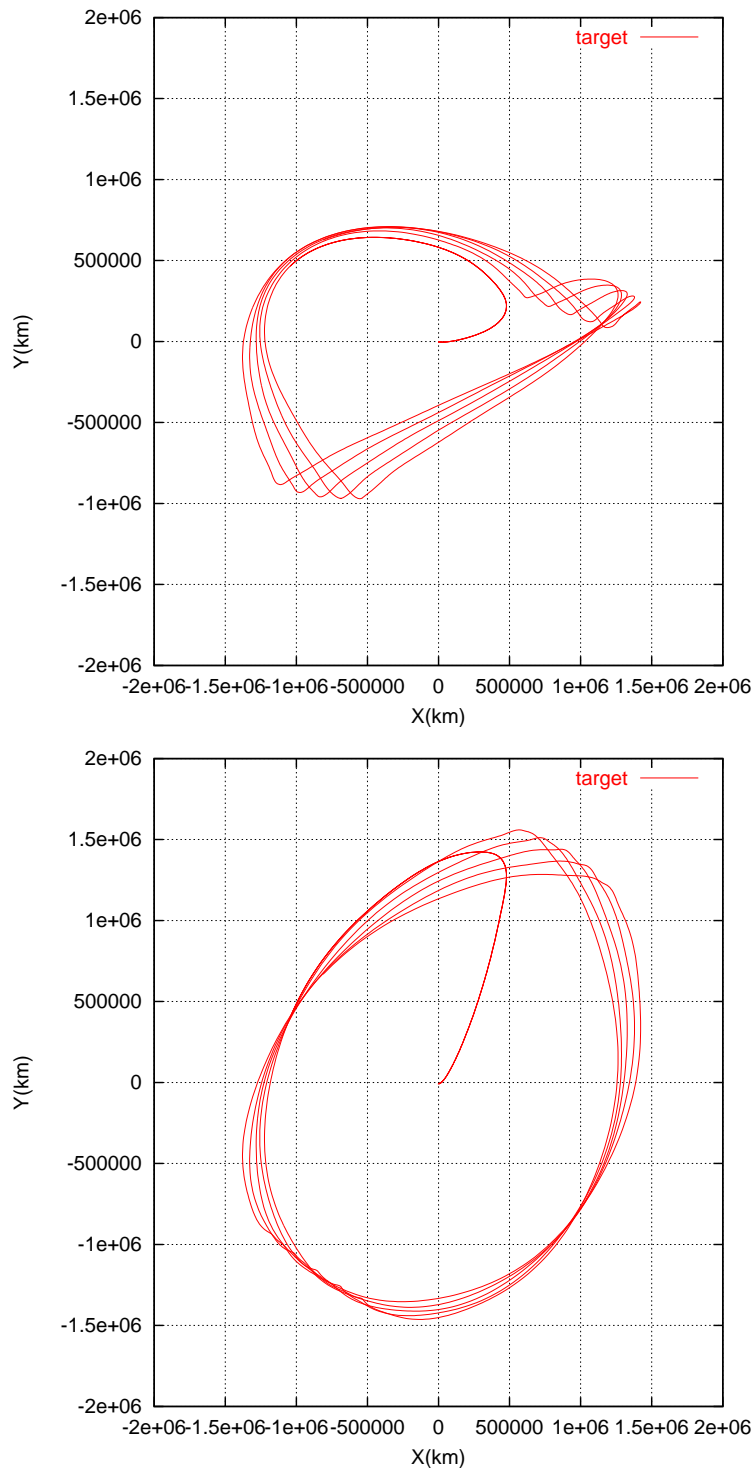


Figure 3.44: Transfer and Lissajous Orbit for HERSCHEL, 2007/11/15 launch

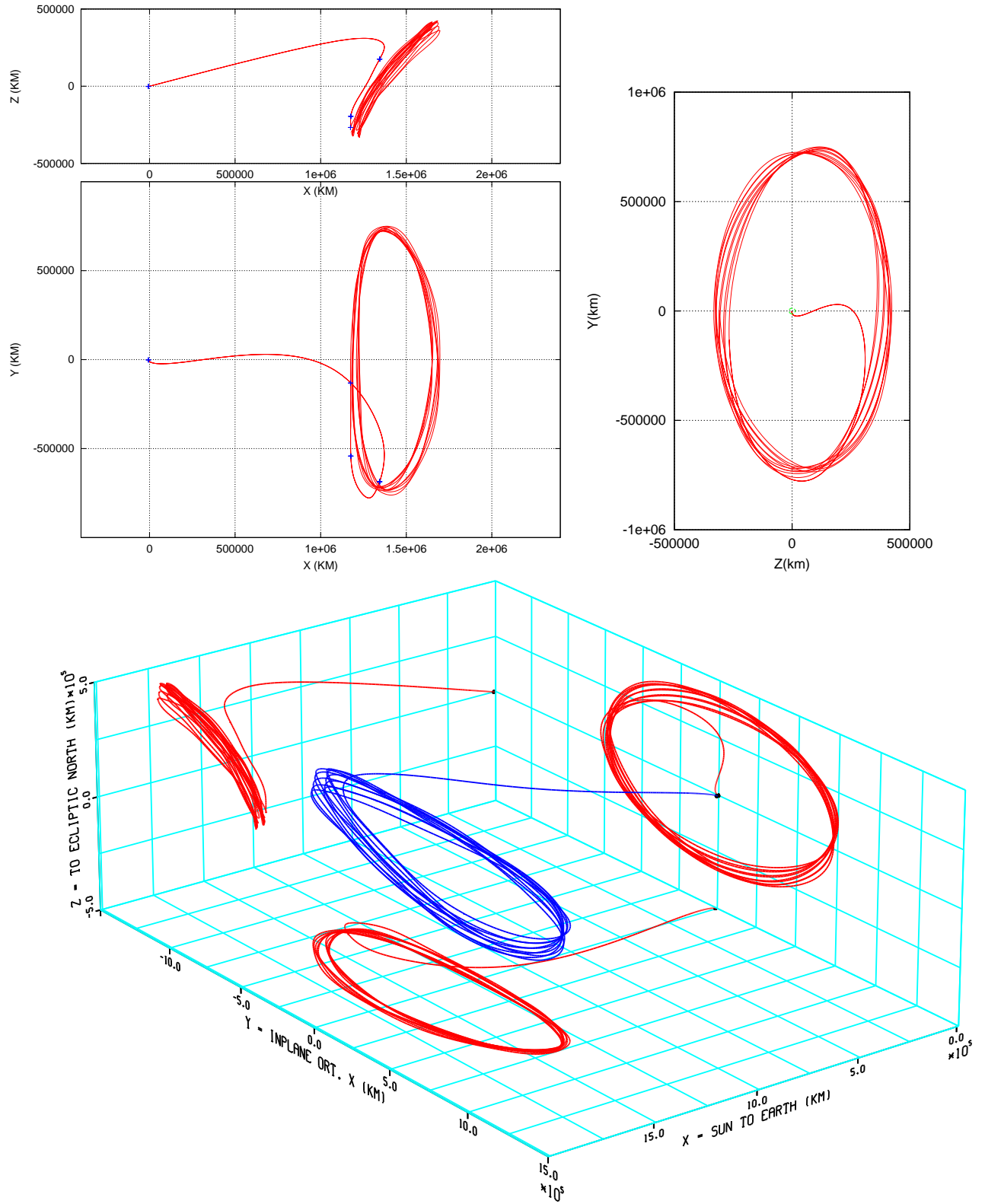
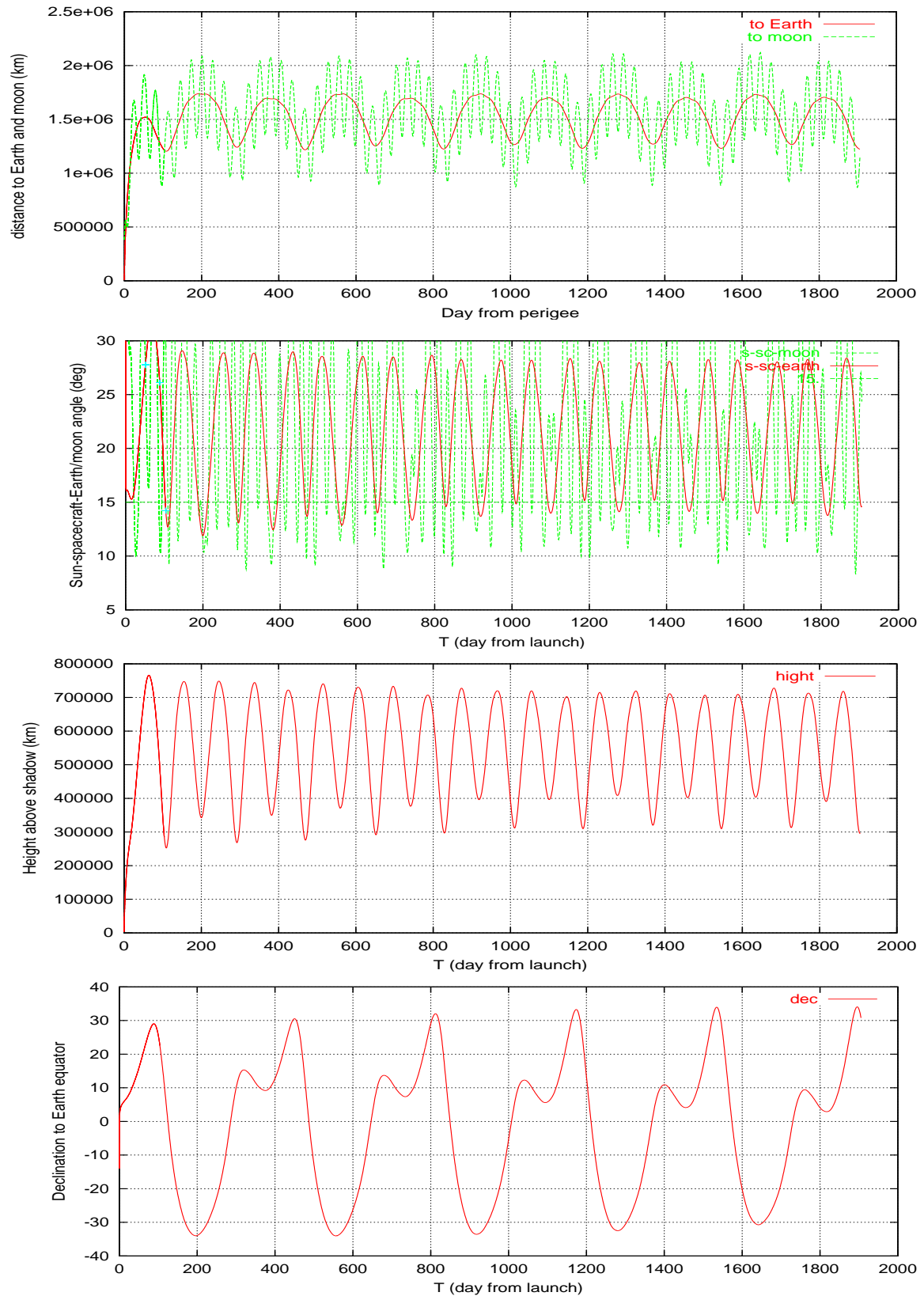


Figure 3.45: Transfer and Lissajous Orbit for Herschel, 2007/11/15 launch (parameters)



### 3.5.3 Ground Station Coverage at Begin of Mission

The ground station coverage for the first week of the Herschel/Planck transfer orbit (both spacecraft still close together) is given in table 3.8. AOS means acquisition of signal, LOS loss of signal. A minimum elevation of  $5^\circ$  from the ground-station has been assumed to be possible, so the first acquisition of the spacecraft will be from the New Norcia station 12.5 minutes after separation from the launcher. For comparison table 3.9 gives the coverage during the first 8 days for  $10^\circ$  minimum elevation.

#	DATE	TIME(UT-99)	HOUR(0)	EVENT	DURATION (hrs)	T0(UTC) = 2875.5609920
2007-11-15	13:40: 9.9	0.206	AOS NEW NORC			
2007-11-15	18:02:23.9	4.576	AOS VILLAFRA			
2007-11-15	20:43:42.8	7.265	LOS NEW NORC	7.1306		
2007-11-15	21:16:31.6	7.812	AOS KOUROU			
2007-11-16	05:20:14.8	15.874	LOS VILLAFRA	11.4000		
2007-11-16	08:45:42.0	19.298	LOS KOUROU	11.5246		
2007-11-16	10:35:48.4	21.133	AOS NEW NORC			
2007-11-16	18:33: 4.5	29.087	AOS VILLAFRA			
2007-11-16	21:32:17.8	32.074	LOS NEW NORC	11.0432		
2007-11-16	21:49:34.0	32.362	AOS KOUROU			
2007-11-17	05:53:13.0	40.423	LOS VILLAFRA	11.3687		
2007-11-17	09:07:20.1	43.658	LOS KOUROU	11.3339		
2007-11-17	10:51:52.7	45.401	AOS NEW NORC			
2007-11-17	18:38:30.2	53.178	AOS VILLAFRA			
2007-11-17	21:41:47.9	56.233	LOS NEW NORC	10.8953		
2007-11-17	21:57:11.5	56.489	AOS KOUROU			
2007-11-18	06:03:57.0	64.602	LOS VILLAFRA	11.5183		
2007-11-18	09:14:42.1	67.781	LOS KOUROU	11.3268		
2007-11-18	10:57:50.7	69.500	AOS NEW NORC			
2007-11-18	18:39:57.8	77.202	AOS VILLAFRA			
2007-11-18	21:45:17.5	80.291	LOS NEW NORC	10.7959		
2007-11-18	22:00: 3.0	80.537	AOS KOUROU			
2007-11-19	06:08:58.6	88.686	LOS VILLAFRA	11.4939		
2007-11-19	09:17:52.6	91.834	LOS KOUROU	11.3992		
2007-11-19	11:00:28.4	93.544	AOS NEW NORC			
2007-11-19	18:39:48.2	101.200	AOS VILLAFRA			
2007-11-19	21:46:24.4	104.310	LOS NEW NORC	10.8721		
2007-11-19	22:00:55.0	104.551	AOS KOUROU			
2007-11-20	06:11:28.0	112.727	LOS VILLAFRA	11.6166		
2007-11-20	09:19: 6.0	115.855	LOS KOUROU	11.3847		
2007-11-20	11:01:28.2	117.561	AOS NEW NORC			
2007-11-20	18:38:46.1	125.182	AOS VILLAFRA			
2007-11-20	21:46:16.4	128.307	LOS NEW NORC	10.8555		
2007-11-20	22:00:42.3	128.548	AOS KOUROU			
2007-11-21	06:12:33.1	136.745	LOS VILLAFRA	11.6339		
2007-11-21	09:19:12.7	139.856	LOS KOUROU	11.3882		
2007-11-21	11:01:30.5	141.561	AOS NEW NORC			
2007-11-21	18:37:11.2	149.156	AOS VILLAFRA			
2007-11-21	21:45:22.5	152.292	LOS NEW NORC	10.7348		
2007-11-21	21:59:49.4	152.533	AOS KOUROU			
2007-11-22	06:12:45.1	160.749	LOS VILLAFRA	11.6602		
2007-11-22	09:18:36.7	163.846	LOS KOUROU	11.4029		
2007-11-22	11:00:55.3	165.552	AOS NEW NORC			

Table 3.8: Ground station coverage during first week in orbit ( $5^\circ$  minimum elevation)

The given HOUR is counted from T0, T0 is the time of spacecraft separation from the launcher (true anomaly =  $33.87^\circ$ ) which happens at 937 km altitude at a longitude and latitude of ( $27.38^\circ$ ,  $-12.29^\circ$ ). DURATION is the duration of the respective coverage interval in hours. The times are given in UTC with the leap seconds taken into account only to 1999.

#	DATE	TIME(UT-99)	HOUR(0)	EVENT	DURATION (hrs)	TO(UTC) =	2875.5608771
2007-11-15	13:41:49.7	0.236	AOS NEW NORC				
2007-11-15	18:31:00.3	5.056	AOS VILLAFRA				
2007-11-15	20:17:31.1	6.831	LOS NEW NORC	6.6082			
2007-11-15	21:37:44.1	8.168	AOS KOUROU				
2007-11-16	04:52:35.1	15.415	LOS VILLAFRA	10.4004			
2007-11-16	08:25:09.4	18.958	LOS KOUROU	11.1443			
2007-11-16	10:59:46.0	21.535	AOS NEW NORC				
2007-11-16	18:59:47.3	29.535	AOS VILLAFRA				
2007-11-16	21:08:01.3	31.673	LOS NEW NORC	10.5450			
2007-11-16	22:09:37.1	32.699	AOS KOUROU				
2007-11-17	05:26:05.5	39.974	LOS VILLAFRA	10.7311			
2007-11-17	08:47:20.9	43.328	LOS KOUROU	12.4172			
2007-11-17	11:17:06.4	45.824	AOS NEW NORC				
2007-11-17	21:15:43.9	55.801	LOS NEW NORC	10.7953			
2007-11-17	19:05:23.6	53.629	AOS VILLAFRA				
2007-11-17	22:17:14.2	56.826	AOS KOUROU				
2007-11-18	05:38:20.7	64.178	LOS VILLAFRA	13.4533			
2007-11-18	11:22:49.0	69.919	AOS NEW NORC				
2007-11-18	08:54:47.5	67.452	LOS KOUROU	14.1406			
2007-11-18	19:06:28.8	77.647	AOS VILLAFRA				
2007-11-18	21:21:30.1	79.897	LOS NEW NORC	14.0307			
2007-11-18	22:19:35.2	80.865	AOS KOUROU				
2007-11-19	05:37:18.3	88.161	LOS VILLAFRA	11.1081			
2007-11-19	08:58:35.6	91.516	LOS KOUROU	12.9519			
2007-11-19	11:27:41.5	94.000	AOS NEW NORC				
2007-11-19	21:07:27.7	103.663	LOS NEW NORC	10.7575			
2007-11-19	19:10:54.7	101.721	AOS VILLAFRA				
2007-11-19	22:22:23.6	104.912	AOS KOUROU				
2007-11-20	08:59:37.0	115.533	LOS KOUROU	11.9569			
2007-11-20	05:51:22.5	112.395	LOS VILLAFRA	15.1482			
2007-11-20	11:54:41.2	118.450	AOS NEW NORC				
2007-11-20	20:55:00.9	127.456	LOS NEW NORC	11.8035			
2007-11-20	22:18:50.3	128.853	AOS KOUROU				
2007-11-20	19:23:25.2	125.929	AOS VILLAFRA				
2007-11-21	05:13:51.2	135.770	LOS VILLAFRA	11.5305			
2007-11-21	11:36:36.2	142.149	AOS NEW NORC				
2007-11-21	09:01:58.0	139.572	LOS KOUROU	16.1777			
2007-11-21	20:10:30.8	150.714	LOS NEW NORC	10.8351			
2007-11-21	22:16:50.1	152.820	AOS KOUROU				
2007-11-21	19:01:28.7	149.564	AOS VILLAFRA				
2007-11-22	04:43:37.7	159.266	LOS VILLAFRA	11.7723			
2007-11-22	11:52:31.9	166.414	AOS NEW NORC				
2007-11-22	09:08:04.0	163.673	LOS KOUROU	17.2740			
2007-11-22	20:04:06.4	174.607	LOS NEW NORC	12.8213			

Table 3.9: Ground station coverage during first week in orbit (10° minimum elevation)

Figure 3.46 gives the ground track over the first day from perigee passage, and the altitude versus geographical longitude, indicating the station coverage. The marks are every 15 minutes.

Figure 3.46: Ground track and altitude over first day of mission (A5E/CA-optimum)

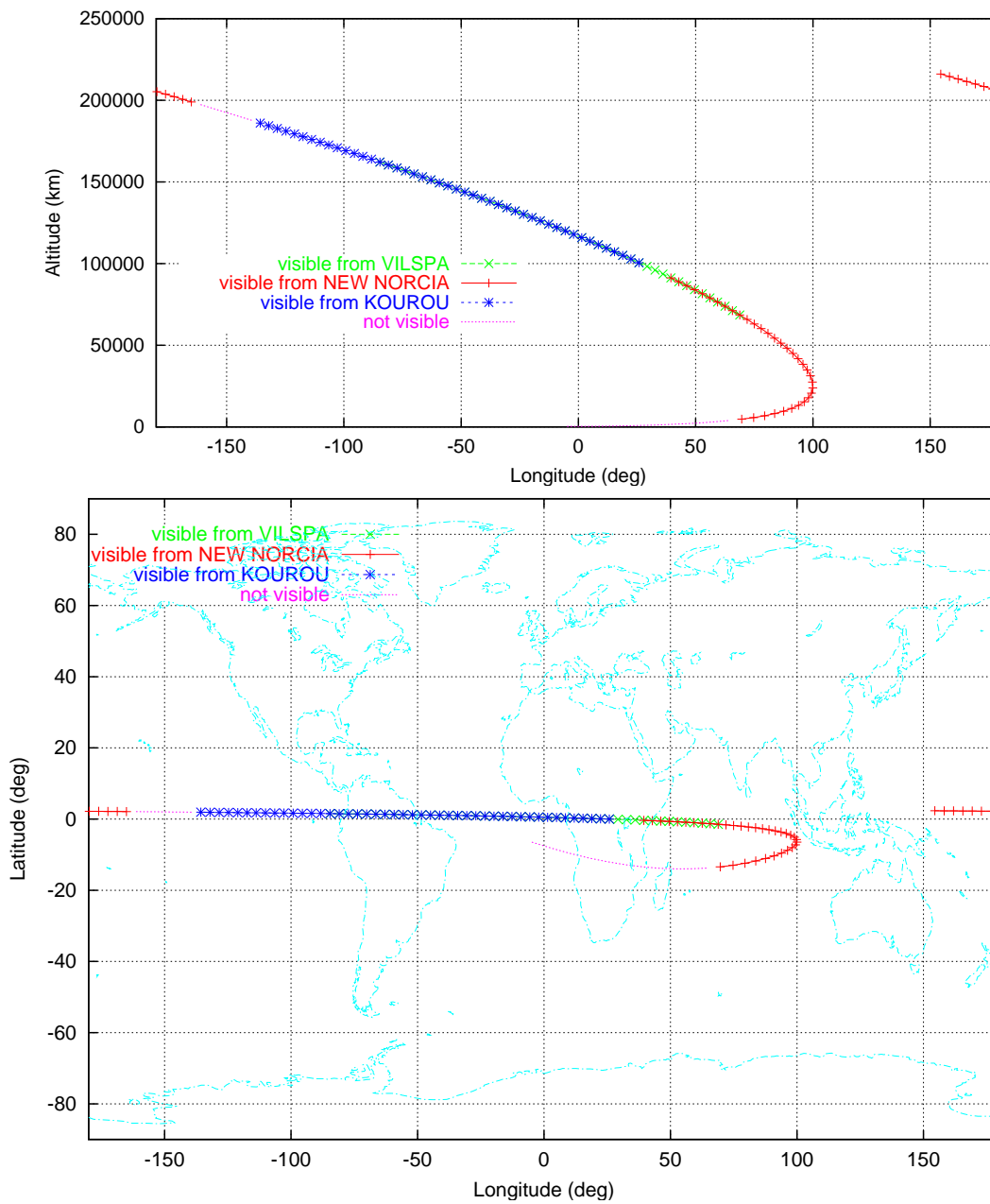


Figure 3.47 shows elevation versus azimuth for the first ground station pass from New Norcia. The station spacecraft slant range at the start of the pass ( $5^\circ$  elevation) is 8000 km. The dispersion 2.5 minutes after acquisition at an elevation of  $12.8^\circ$  is indicated in the figure. The corresponding elevation versus azimuth history from Perth is almost the same (lines cannot be distinguished), in case acquisition will be first done by Perth with its acquisition system.

The same dispersion in elevation and azimuth, presented by 1000 random points generated with the launcher dispersion is shown in figure 3.48. The statistics of this random sample, also including slant range and Doppler, and giving the correlation, and the eigenvalues of the covariance matrix, essentially corresponding to long track and cross track error, are given in table 3.10.

Figure 3.49 finally gives the long track and cross track  $3\sigma$  error as function of time from separation from the launcher. due to the increasing distance the cross track error reduces, the long track error for the first few minutes increases and then reduces.

Figures 3.47 to 3.49 have not been updated from CReMA issue 3.0 for the new launcher dispersion, as any sensible difference is not expected.

Figure 3.47: First tracking path from New Norcia

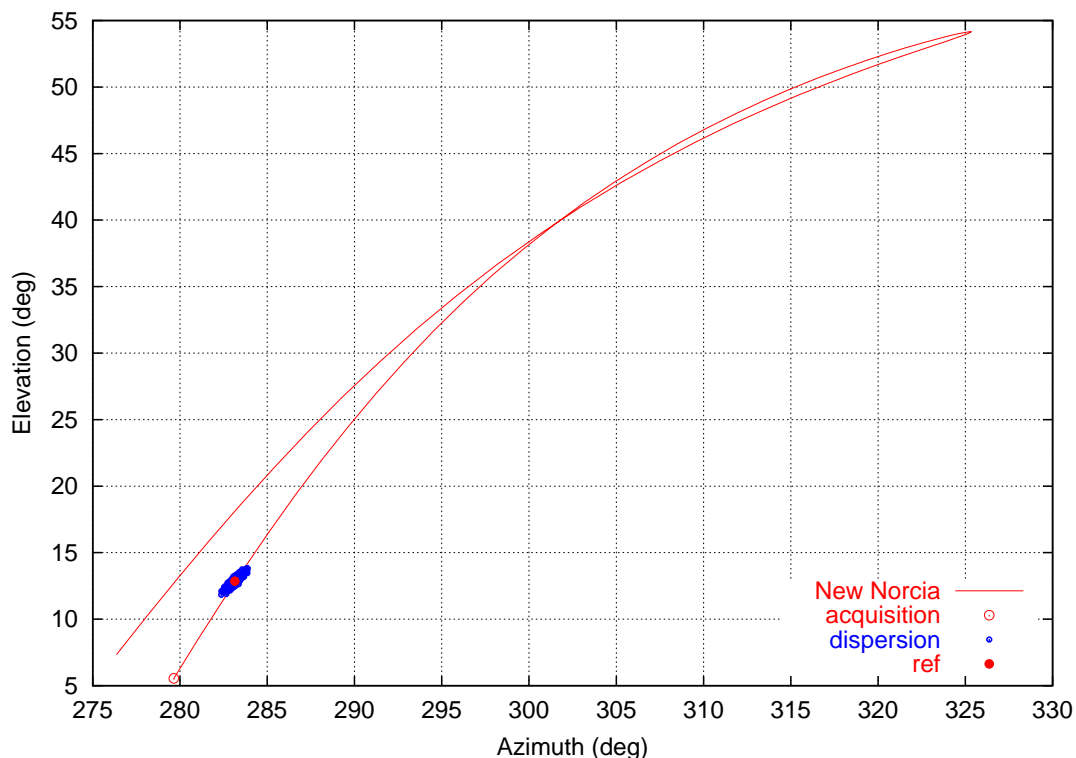


Table 3.10:  $3\sigma$  dispersion at tracking acquisition

AZ	(deg)	0.76078
ELEV	(deg)	0.97435
COR		0.89471
CORANG	(deg)	41.81945
DIST	(km)	131.81751
DOP	(km/s)	0.09963
LONGTRACK	(deg)	1.20528
CROSSTRACK	(deg)	0.27469

Figure 3.48: Dispersion at tracking acquisition from New Norcia

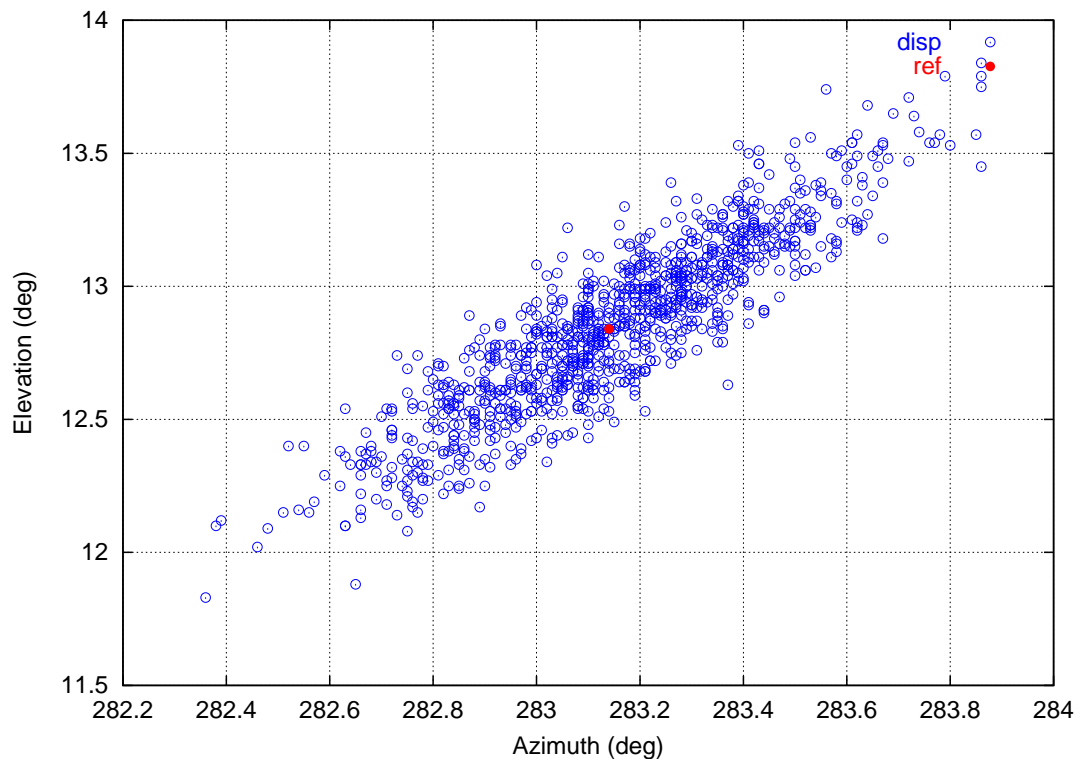


Figure 3.49: Long track and cross track errors as function of time

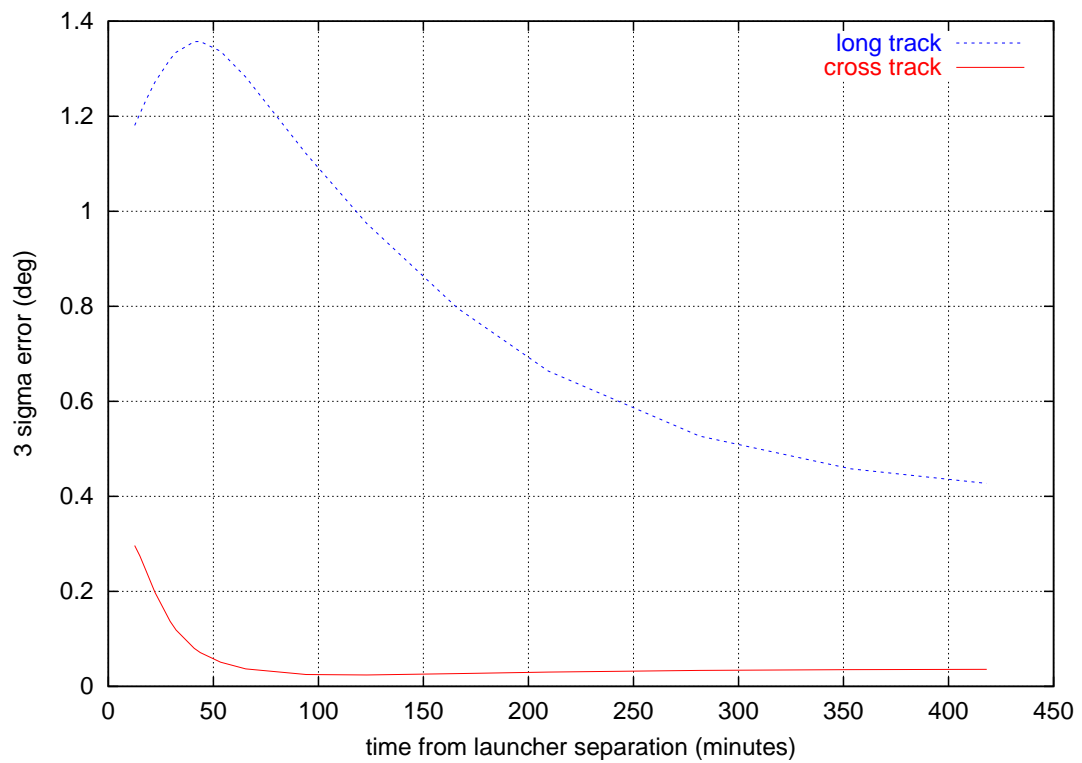


Figure 3.50 shows that the first orbit correction on day 2 is when the spacecraft has already passed the moon distance. This means error amplifying close approaches to the moon are to be avoided. Figures 3.51 and 3.52 show elevation and azimuth from the ground stations. The slant Doppler from the different stations for the first 3 days is shown in figure 3.53. The slant Doppler rate is shown for the first 3 days in figure 3.54 and over the first 8 hours (first contact for A5E/CA will be from New Norcia) in figure 3.55. The sun-spacecraft-station angle over the first 8 hours is shown in figure 3.56.

Figure 3.50: Slant range from ground stations over first 3 days

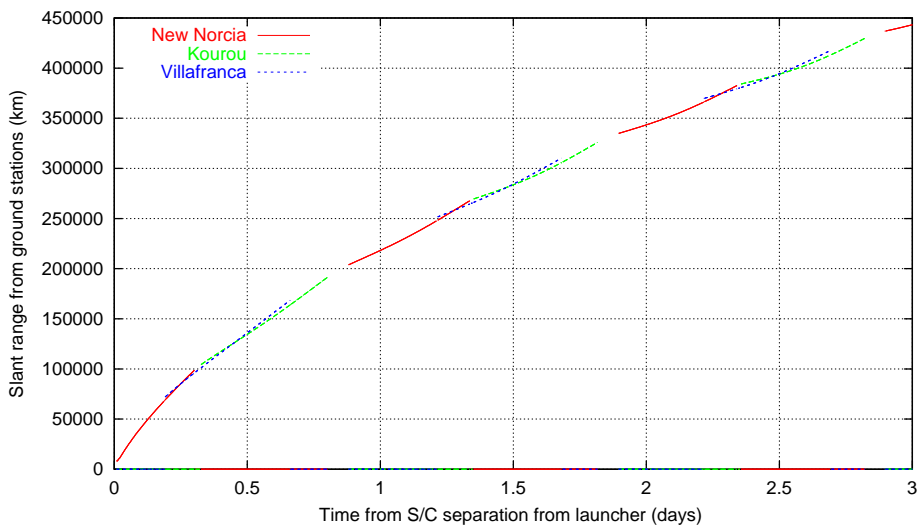


Figure 3.51: Elevation from ground stations over first 3 days

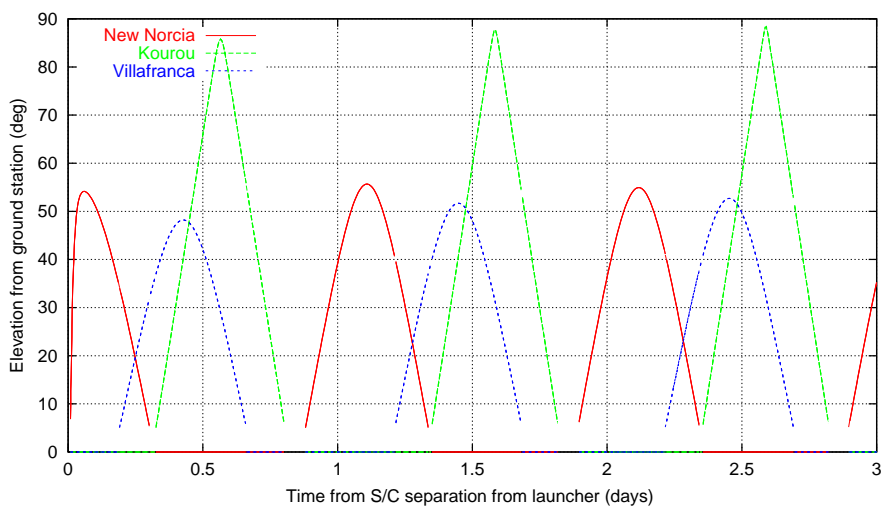


Figure 3.52: Azimuth (North to East) from ground stations over first 3 days

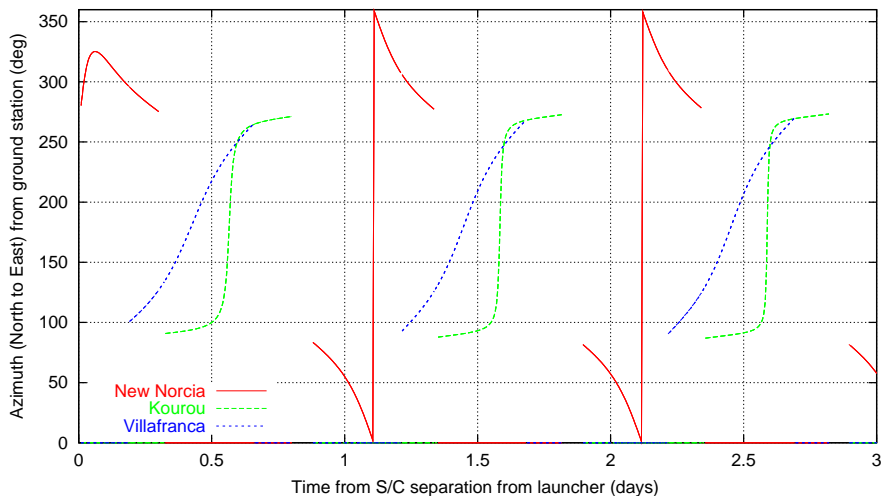


Figure 3.53: Doppler from ground stations over first 3 days

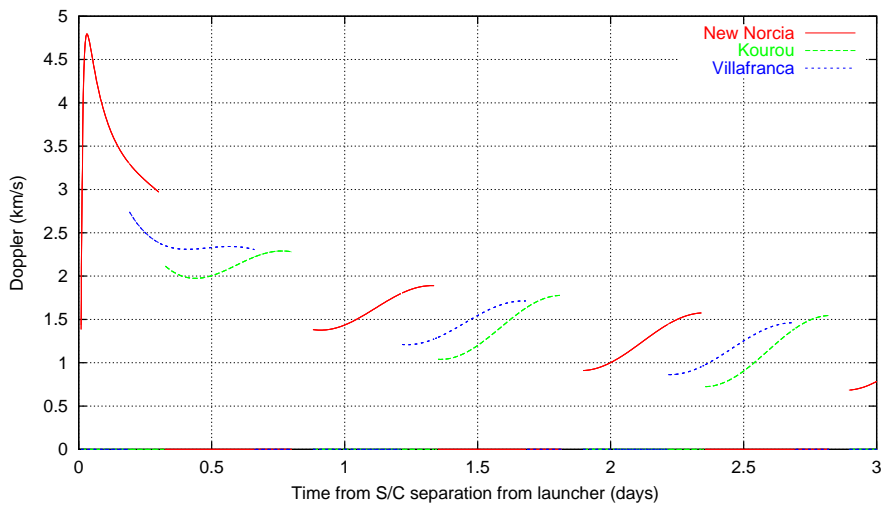


Figure 3.54: Doppler rate from ground stations over first 3 days

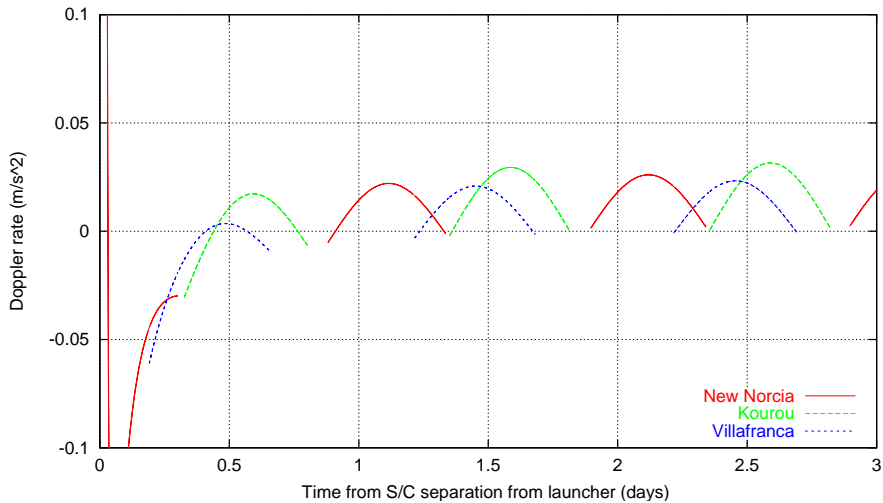


Figure 3.55: Doppler rate over first 8 hours

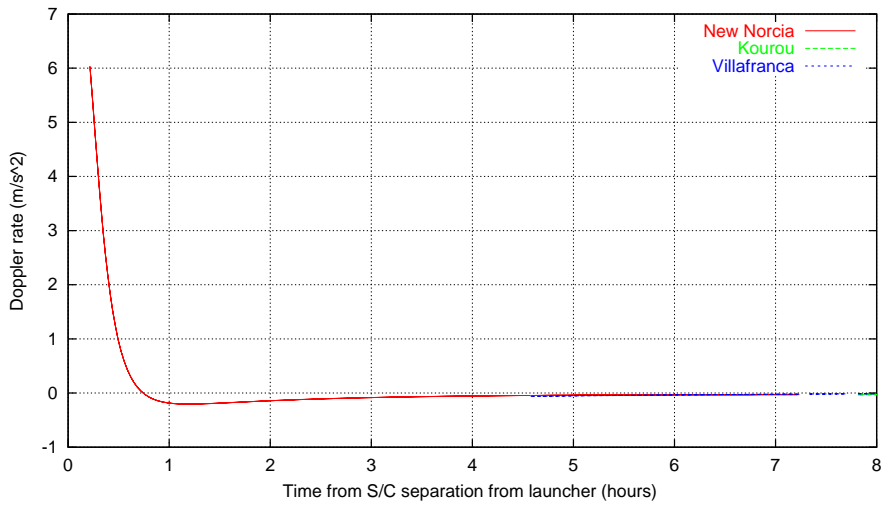
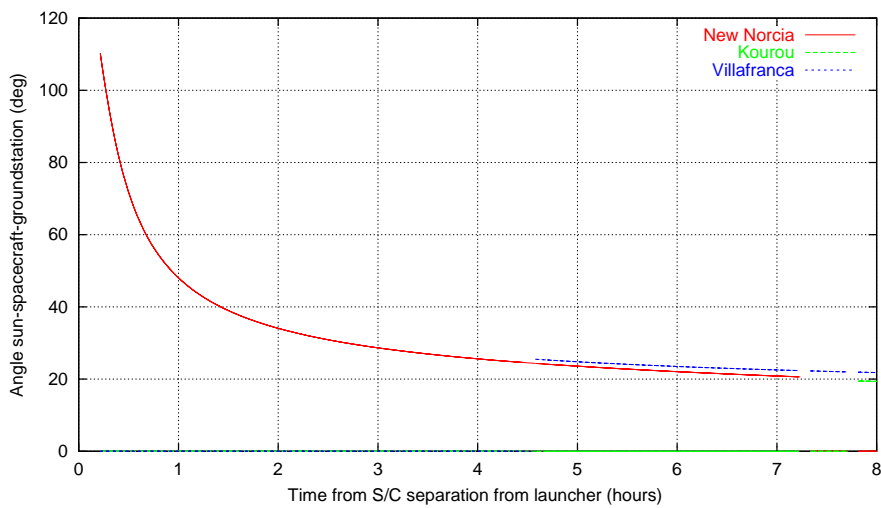


Figure 3.56: Station-spacecraft-sun angle (deg) over first 8 hours



Later in the mission the the Doppler and Doppler rate will be essentially determined by the motion of the ground station, so they will be slightly higher if the station is closer to the equator. Table 3.11 gives the minima and maxima typically reached after the first 50 days for both spacecraft.

	Planck	Herschel
Minimum Doppler	-0.5 km/s	-0.6 km/s
Maximum Doppler	0.5 km/s	0.6 km/s
Minimum Doppler rate	0.035 m/s <sup>2</sup>	0
Maximum Doppler rate	0.035 m/s <sup>2</sup>	0.035 m/s <sup>2</sup>

Table 3.11: Doppler and Doppler rate from after 50 days

### 3.5.4 Ground Station Coverage in Operational Orbit

The ground station coverage from New Norcia and Cebreros over the whole Planck and Herschel mission durations is shown in figures 3.57 and 3.58 for the reference case launched at the opening of the launch window on 15 Nov. 2007. It should be noted that the nominal mission design uses only part of the coverage intervals, the sharing of the New Norcia 35 m station with other projects is to be optimised. The orbit injection (Planck) is 100 days from launch for the chosen reference case. the minimum elevation from the ground station has been taken to be 5°.

In a more systematic way figure 3.30 gave the coverage duration from the 3 ground stations as function of the spacecraft declination to the equator plane. For some launch dates the North/South excursion (in the equator system) may be much higher than for the reference case. The maximum North/South declinations reached over the mission, as function of the launch date have been given for Planck and for Herschel in figure 3.24 to 3.33. Using this figures and 3.30 the range of variation of the station coverage interval duration can be read off for any ESA station.

Picking the worst case north excursion case, on October 17 at the closing of the daily launch slot, figures 3.59 shows that the coverage from New Norcia still remains above 8 hours for Planck and above 6 hours for Herschel. The coverage interval of Planck will extend after that of Herschel for the minima during the time when both spacecraft are operated together, so if Herschel is scheduled first a total of 8 hours will be available. It should be noted that below 15° elevation good tracking cannot be achieved. If one ranging point has to be taken for each spacecraft this should preferably be scheduled at high elevation, this means at the closing of the window for Herschel and at the opening for Planck for the shown case.

Figure 3.57: Ground station coverage from New Norcia, 2007/11/15 launch

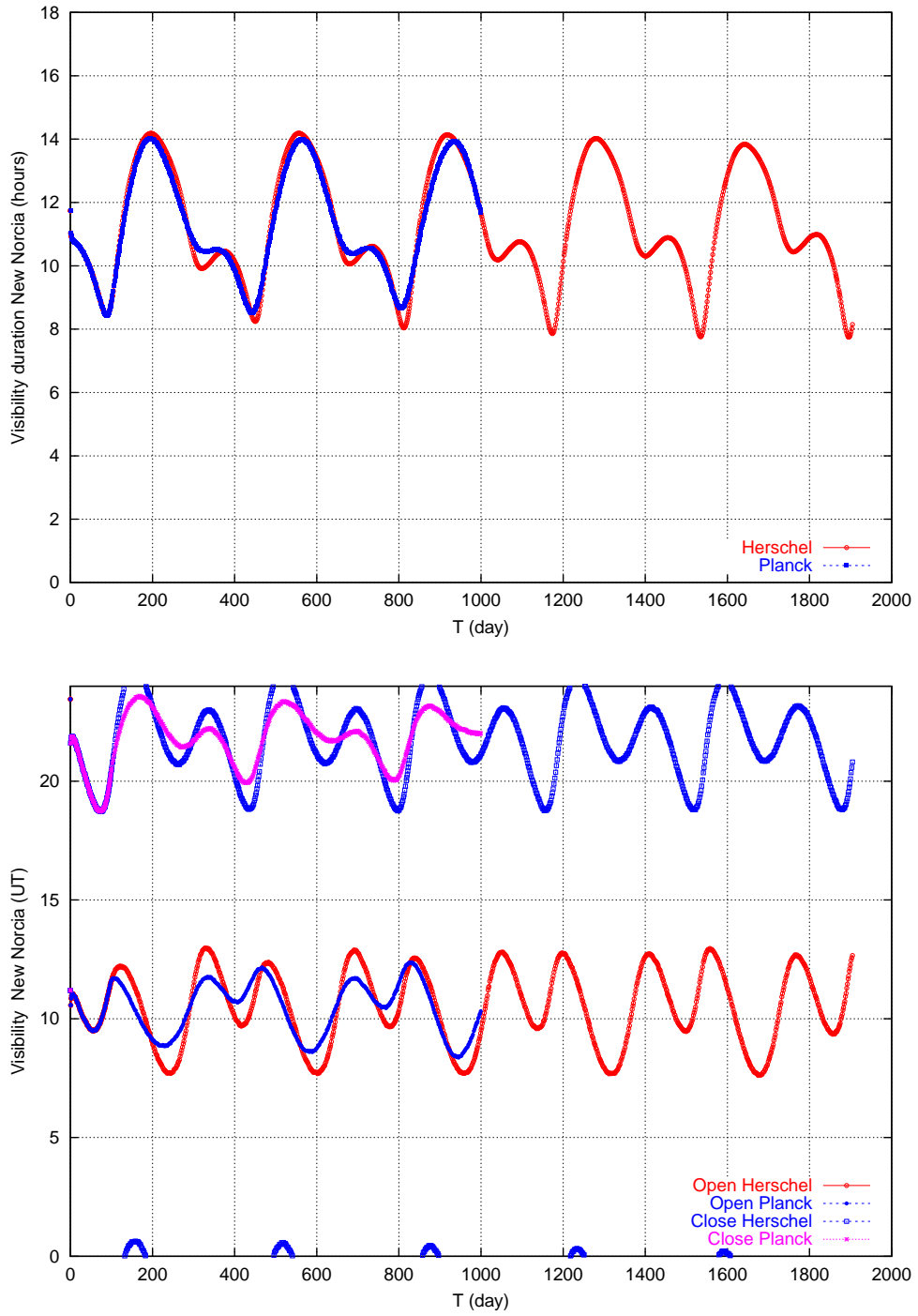


Figure 3.58: Ground station coverage from Cebreros, 2007/11/15 launch

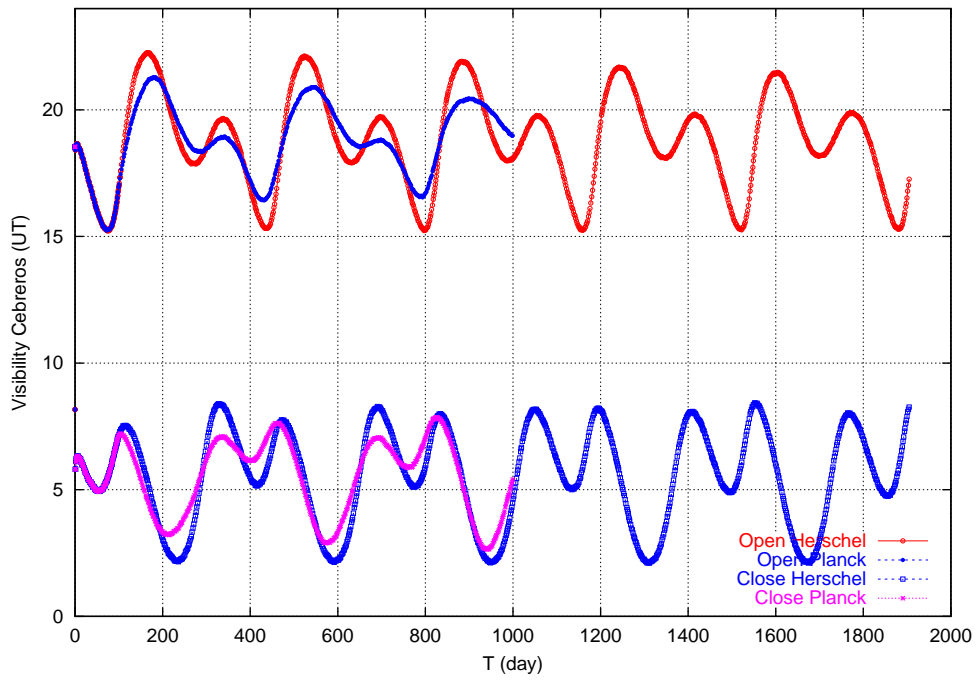
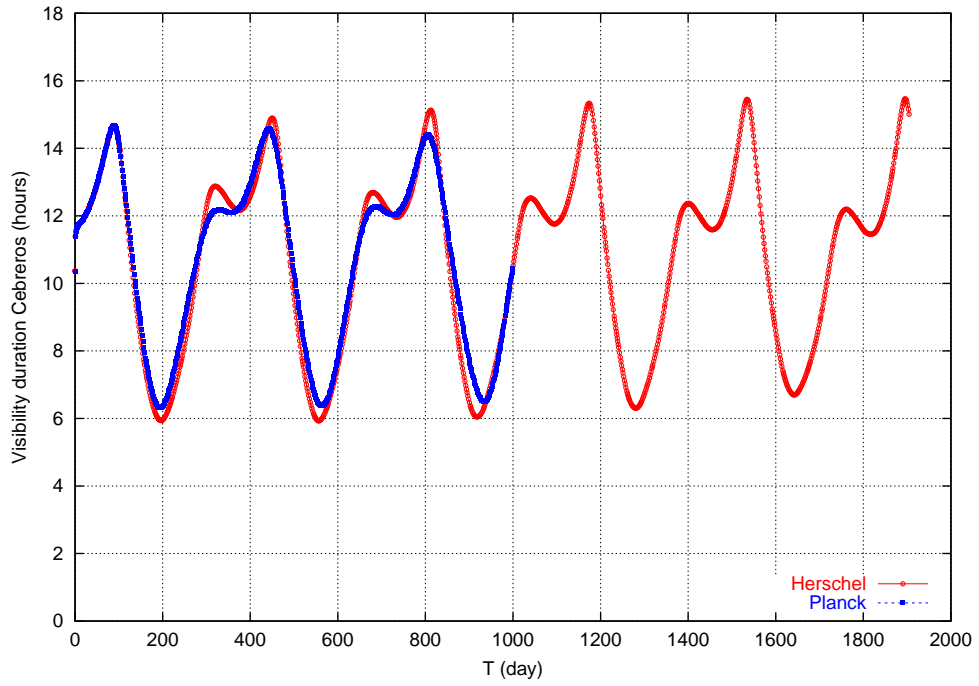
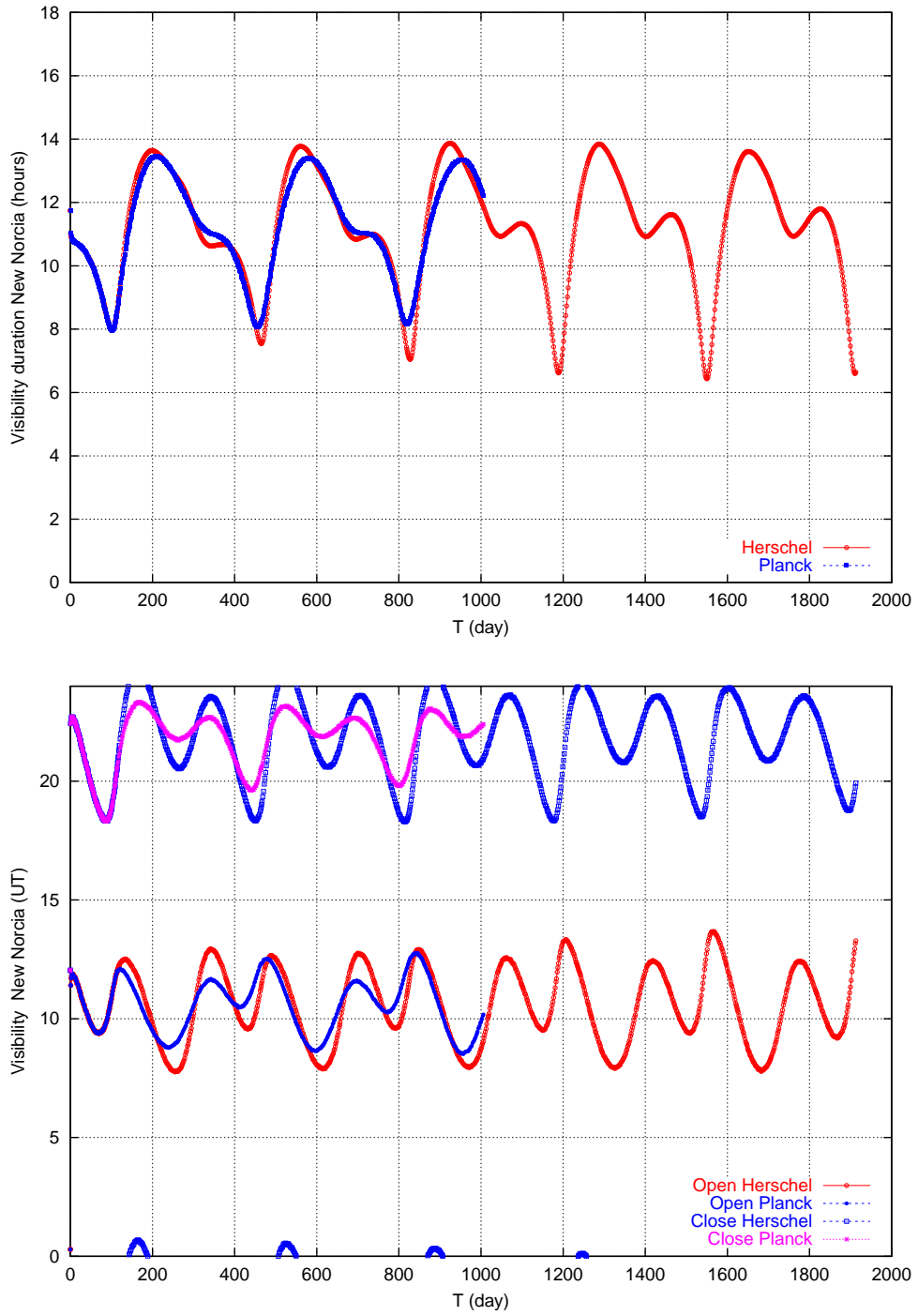


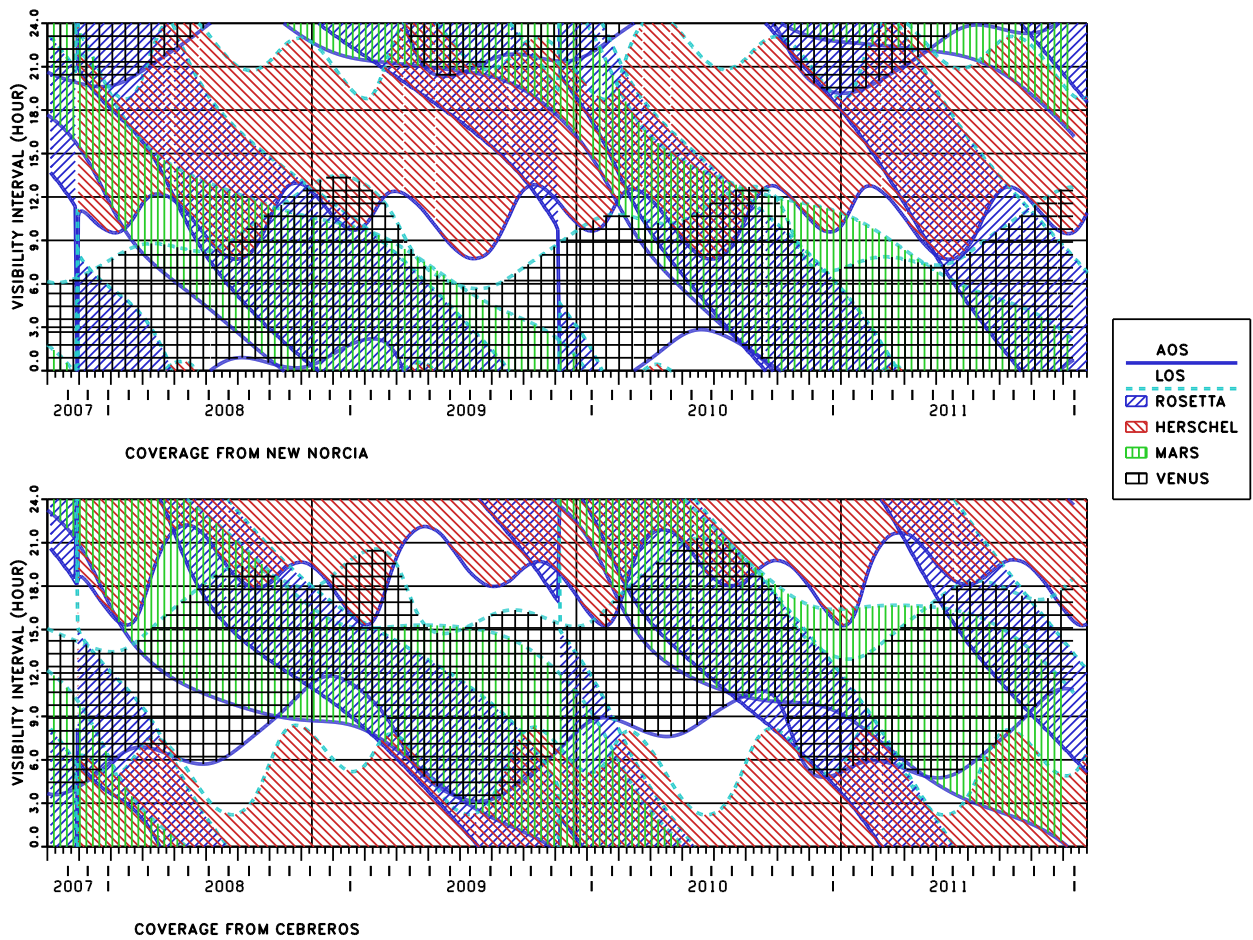
Figure 3.59: Ground station coverage from New Norcia, 2007/10/17 launch, at closing of window



The maximum South excursion for Herschel will be to a declination of nearly  $-45^\circ$  for some launch dates (figure 3.33). Even for  $5^\circ$  minimum elevation, in these cases the coverage interval from Cebreros will close (figure 3.30). In general the declination extrema to the South are about 5 degrees higher than those to the North. In connection with the  $10^\circ$  higher latitude of the Cebreros station compared to the New Norcia station, this leads to worse average coverage from Cebreros than from New Norcia.

Finally figure 3.60 shows that the utilisation of the ESA stations for its different deep space missions in the Herschel time frame, will require some coordination.

Figure 3.60: Ground station coverage of Herschel jointly with Rosetta, Venus and Mars



## 3.6 Eclipses and Occultations by the Moon

### 3.6.1 Duration and Depth of Eclipses by the Moon

From figure 3.42 it can be seen that for Planck the sun-spacecraft-moon angle comes close to zero several times over the mission.

The geometry of the eclipses by the moon can easiest be explained by a very rough consideration. The distance of the spacecraft from the moon will vary from of  $1.0 \times 10^6$  km to  $2.0 \times 10^6$ . The moon disc at this distance will extend over  $0.05^\circ$  to  $0.1^\circ$  half cone angle, whereas the sun disc extends over about  $0.26^\circ$  half cone angle from the spacecraft. This means the moon will shadow up to 13% of the sun disc, and such a partial eclipse happens whenever the sun-s/c-moon angle is below  $0.31^\circ$  to  $0.36^\circ$ , depending on the moon distance.

Figure 3.61 and 3.62 show the duration of the moon eclipses which occur for the different launch dates. Figure 3.63 and 3.64 show the corresponding depth of the eclipses. Figure 3.65 and 3.66 show the percentages of the obscured sun disc for the different launch dates, at the opening and closing of the daily window. The eclipse percentages are "power-normalises" by a factor  $r^{-1.7}$  with  $r$  = sun distance in AU (change of the square law to account for power gain by lower temperature). If the power reduction by an eclipse is  $f$  then the power reduction relative to the power at 1 AU is

$$1 - r^{-1.7} * (1 - f). \quad (3.1)$$

For  $f=0$ , the maximum variation in power due to the Earth orbit eccentricity alone with this assumption comes out to be  $\pm 3\%$ .

It can first be seen that there are launch dates with no eclipse by the moon, and the moon eclipses at the opening of the daily slot are completely different from those at the closing. For some dates there are up to 10 eclipses during the 2.5 years Planck mission. The worst case (10 eclipses) is for a launch at the opening of the daily slot on 2007/9/9, whereas at the closing of the window on the same day there is only one eclipse. Apparently eclipses by the moon cannot be treated in a systematic way like those by the Earth, and a dependence of these results on stochastic deviations from the nominal orbit cannot be excluded.

The very deep eclipses (up to 60%) are during the transfer. From the fact that they appear for different launch dates at the opening and the closing of the launch window it can be concluded that for certain periods every month, eclipses by then moon during the transfer must be verified also for all the internal points in the daily launch window slot, if these represent a danger for the spacecraft.

From figure 3.67 and 3.68 (both AU-normalised) some correlation of eclipse depth and duration can be seen. The few eclipses of more than 8 hours duration are at less the 13% in normalised depth.

Finally figures 3.69 and 3.70 show the product eclipse duration times depth. This number could be typically used to assess battery requirements.

Figure 3.61: Duration of eclipses by the moon at opening of launch window in second half of 2007

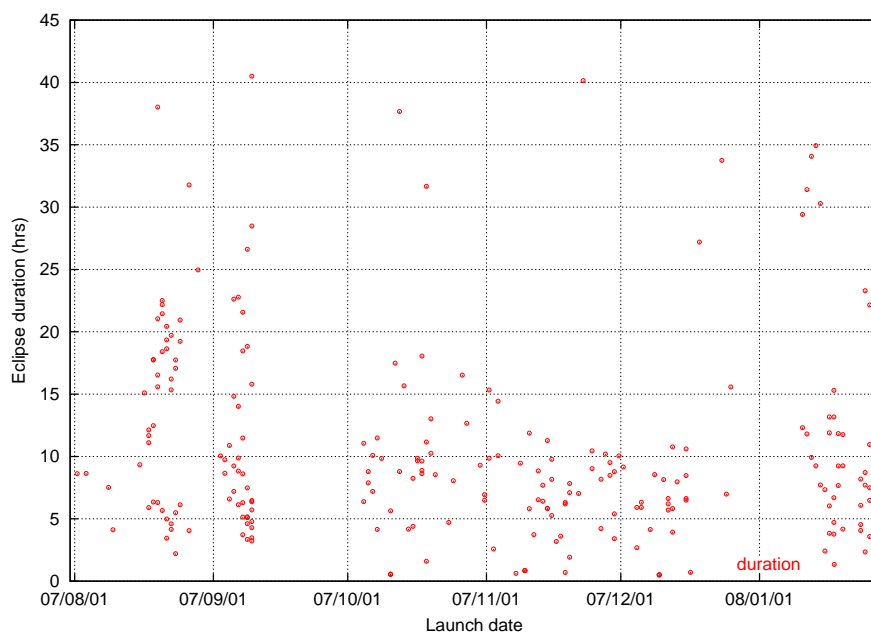


Figure 3.62: Duration of eclipses by the moon at closing of launch window in second half of 2007

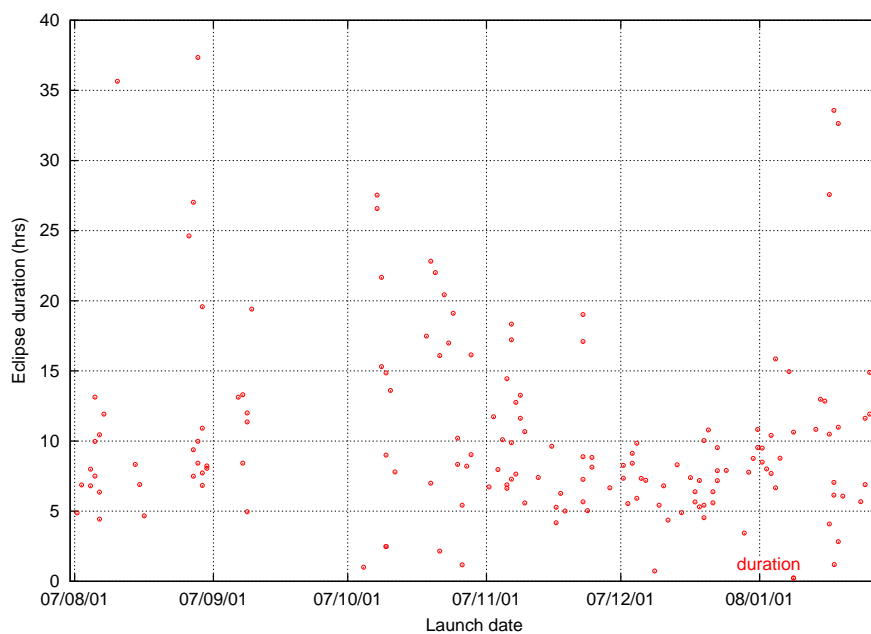


Figure 3.63: Depth of eclipses by the moon at opening of launch window in second half of 2007

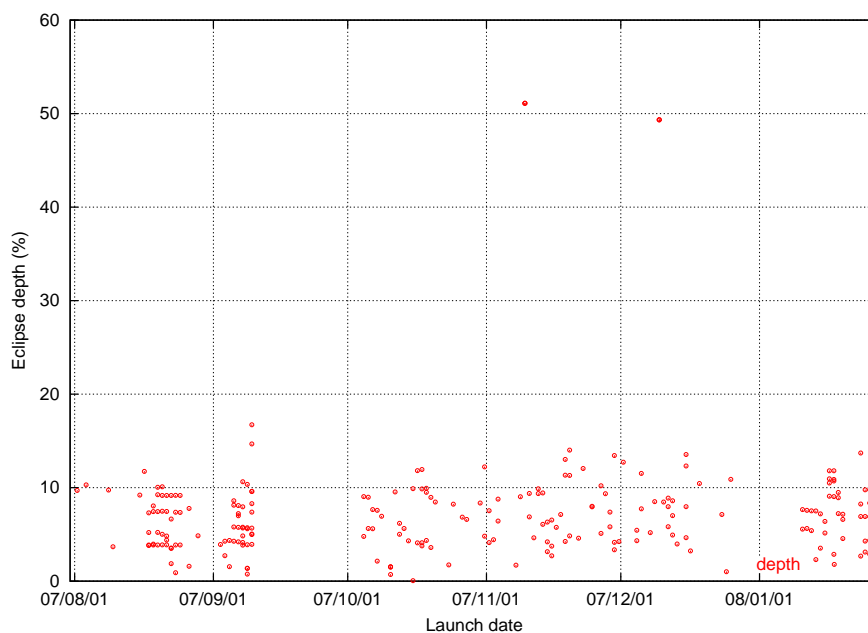


Figure 3.64: Depth of eclipses by the moon at closing of launch window in second half of 2007

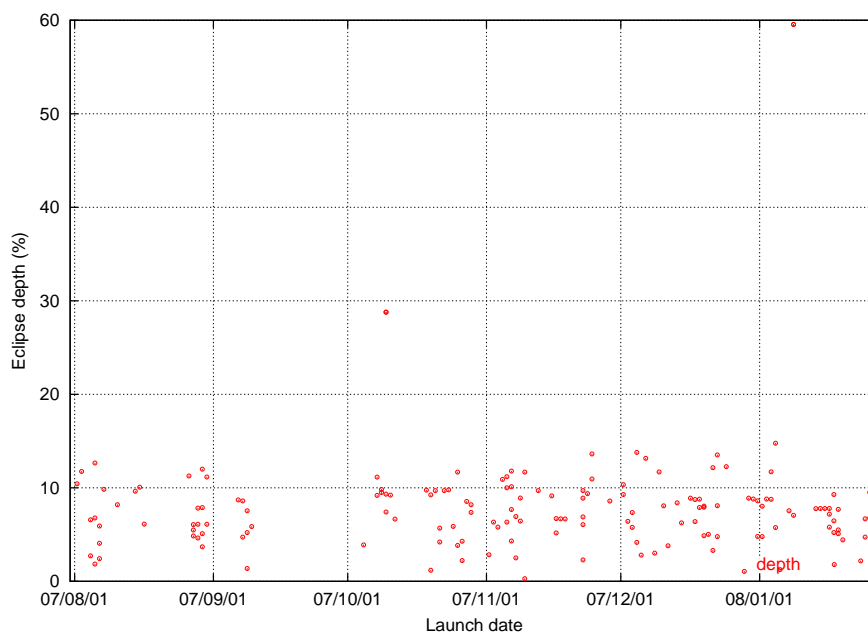


Figure 3.65: Power-normalised depth of eclipses by the moon at opening of launch window 2007

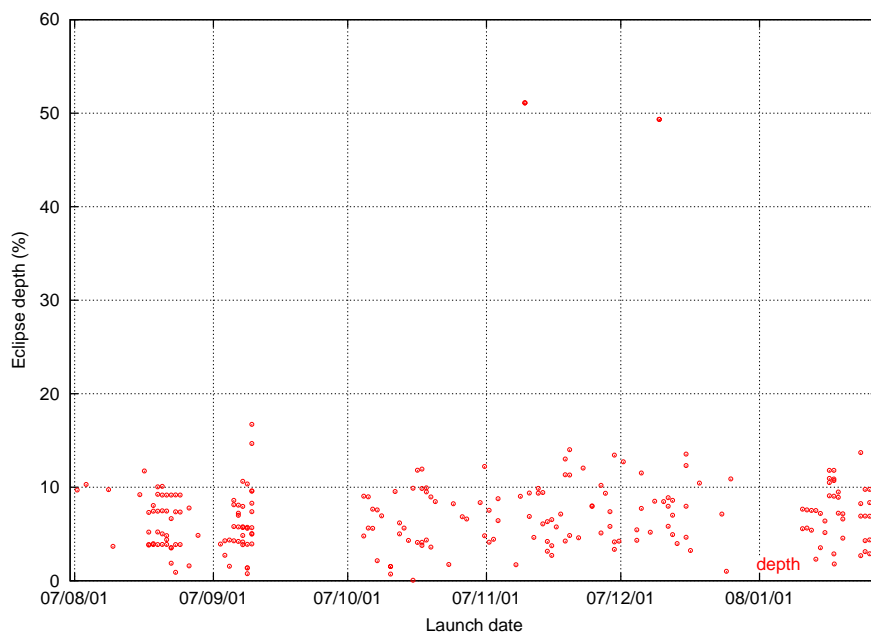


Figure 3.66: Power-normalised depth of eclipses by the moon at closing of launch window 2007

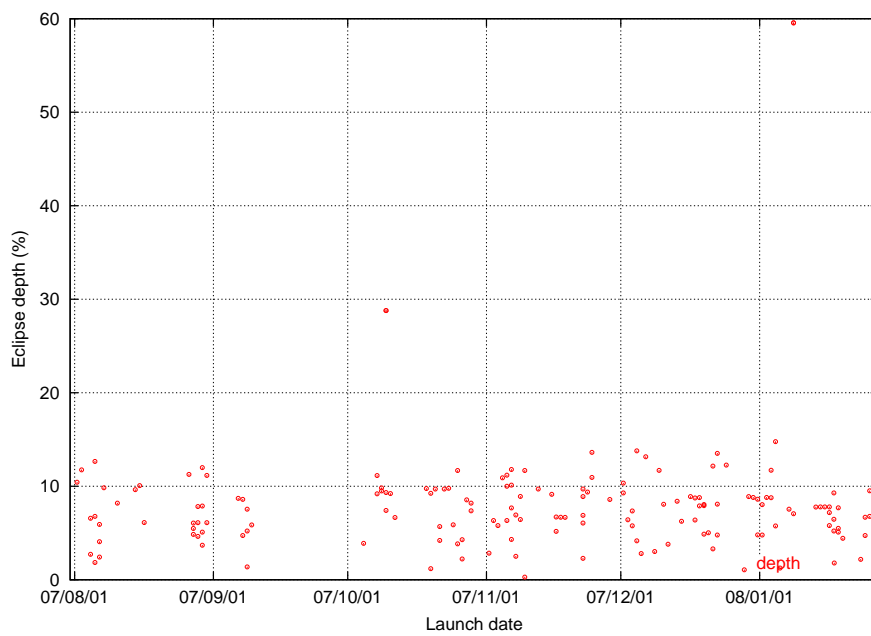


Figure 3.67: Normalised depth of eclipses versus duration (opening of window)

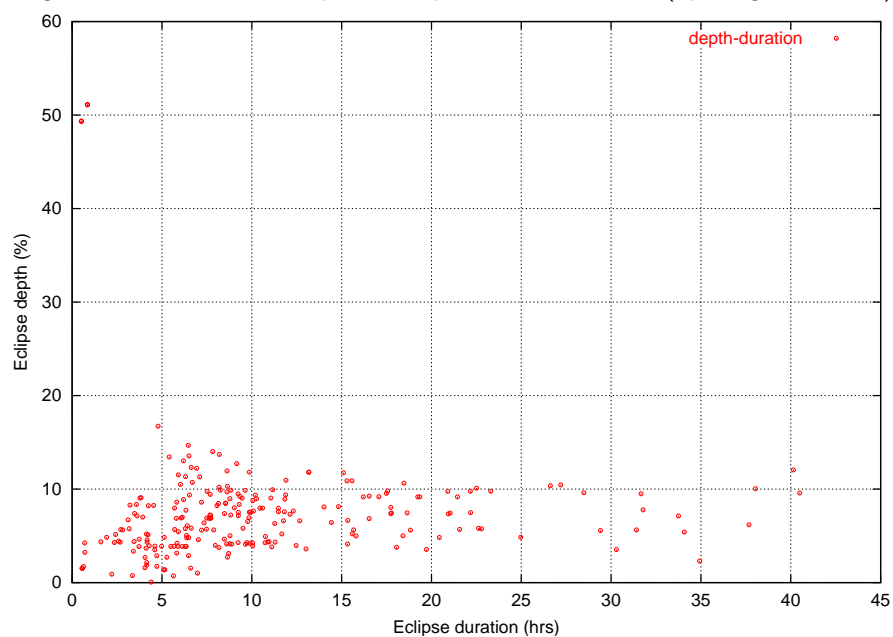


Figure 3.68: Normalised depth of eclipses versus duration (closing of window)

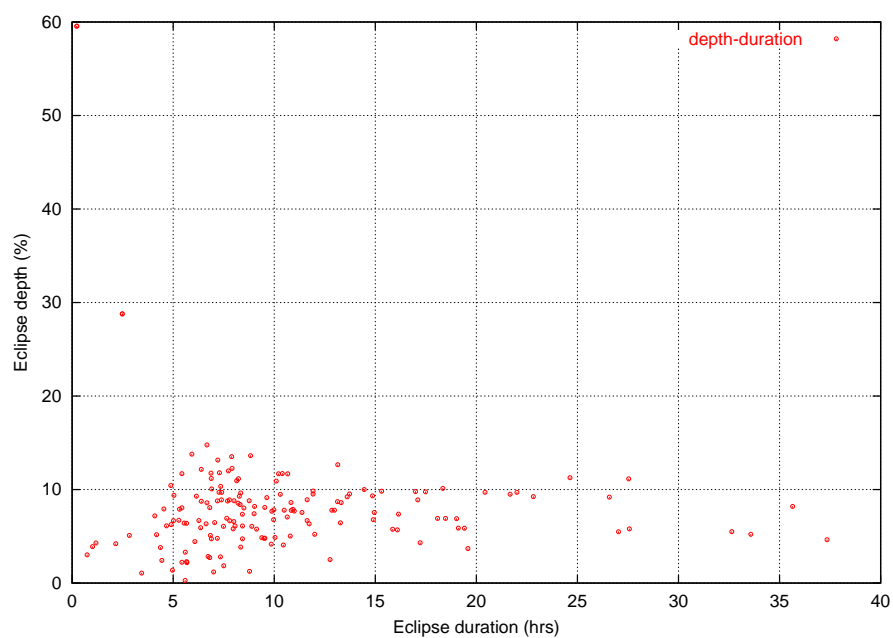


Figure 3.69: Duration times depth of eclipses by moon (opening of window)

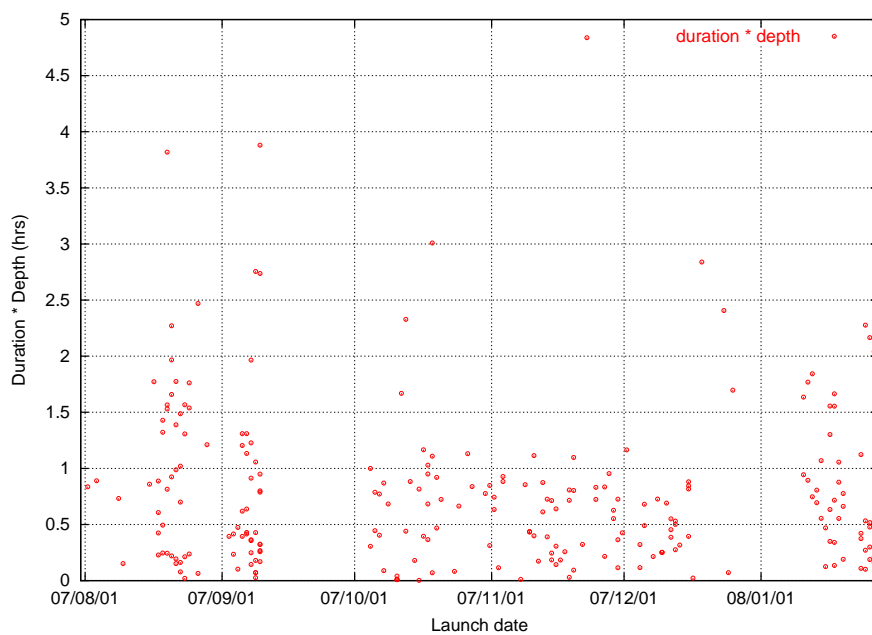
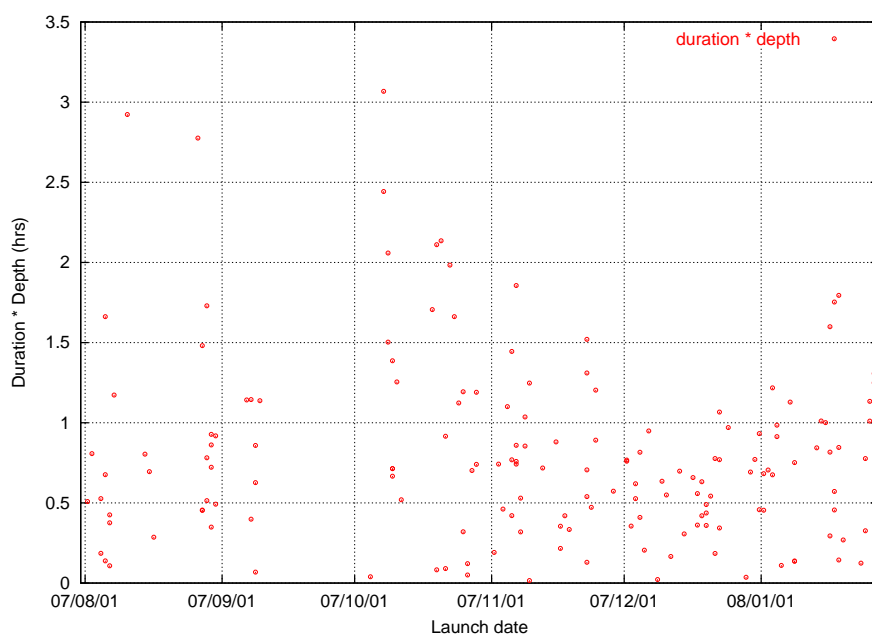


Figure 3.70: Duration times depth of eclipses by moon (closing of window)



### 3.6.2 Avoidance of Eclipses by the Moon by Manoeuvres

This section gives a feasibility discussion for example cases, it has not been updated from CReMA issue 3.0. Figure 3.71 and 3.72 show the time history of the normalised depth of the eclipses for two extreme cases (calculations of CReMA issue 3.0) namely for a launch on 2007/9/7 and on 2007/9/9 at the closing of the daily window each. In the first case one eclipse is particularly long, the second case has particularly many (9) eclipses. The time is counted from the start of each of the eclipses

Figure 3.71: Depth of eclipses by the moon for eclipses on 2007/9/7, closing of window

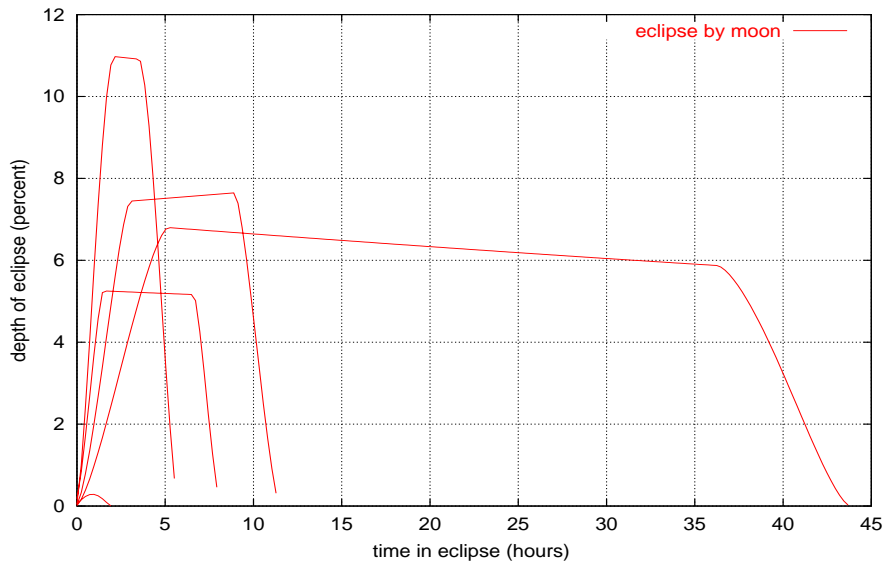
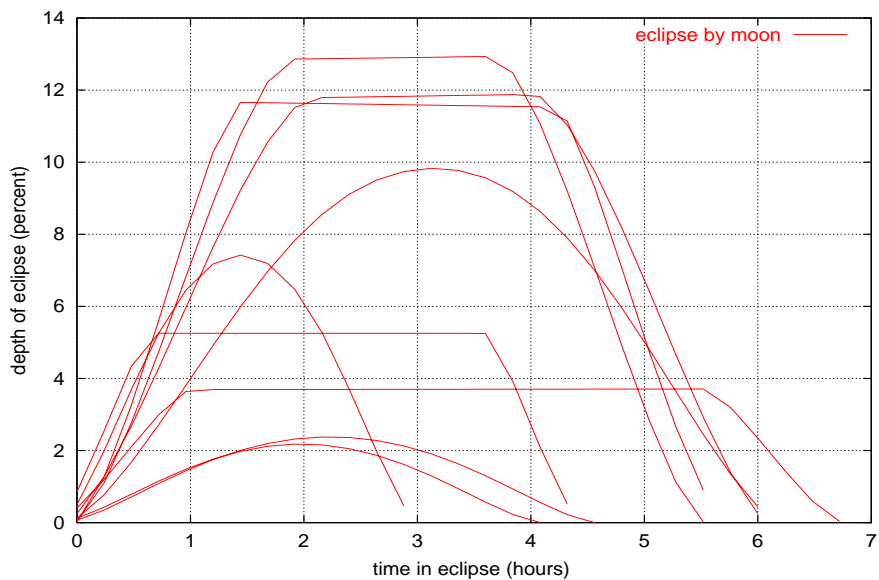


Figure 3.72: Depth of eclipses by the moon for eclipses on 2007/9/9, closing of window



Figures 3.73 and 3.74 show that the orbits for a September 7 and 9 launches are rather close to the ecliptic plane, and thus the moon orbit plane. To some extent this explains why these cases suffer most from eclipses by the moon.

Figure 3.73: September 7 orbit at closing of window

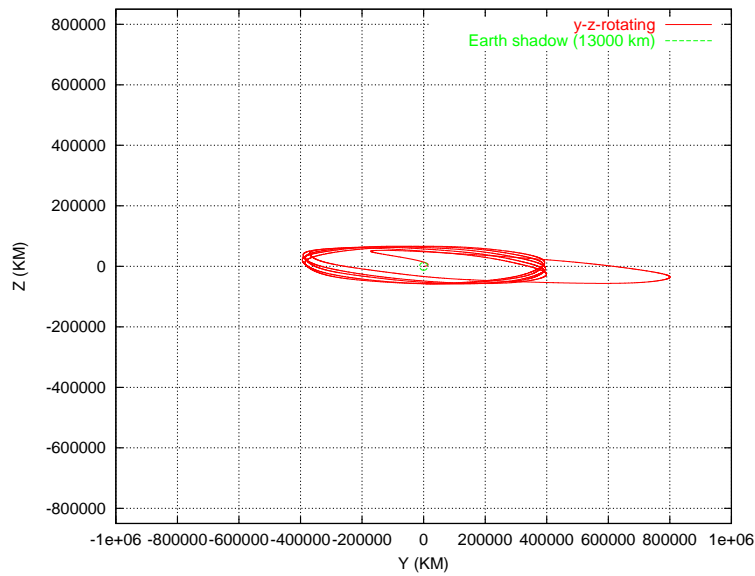
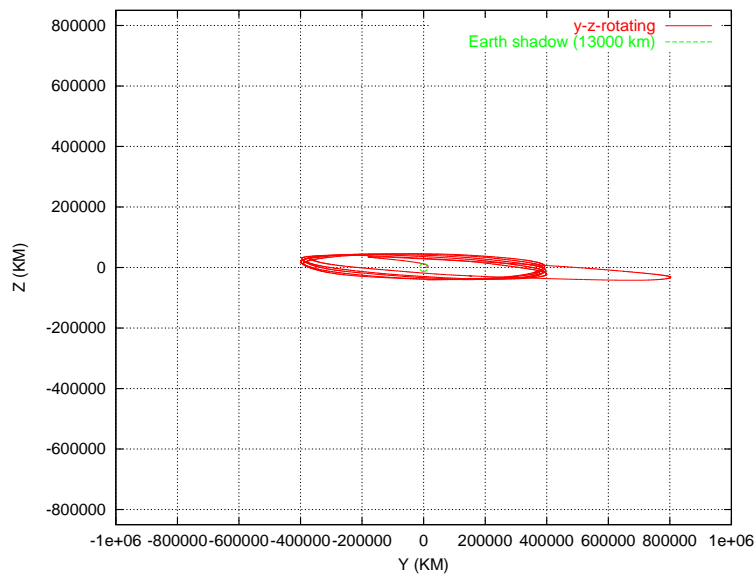


Figure 3.74: September 9 orbit at closing of window



The lunar eclipses appear rather irregular. They also change completely if the orbit amplitudes are slightly changed. From this it cannot be concluded that eclipses by the moon can be easily avoided. However it can be assumed that the rather rare eclipses of over e.g. 12-15 hours, or also the rare eclipses with a depth of over 10% can possibly be avoided by changing the orbit slightly. A limit imposed by spacecraft design should be defined for operations. A general strategy to avoid lunar eclipses may be possible, however is TBD.

A first approach to assess such an avoidance strategy for extreme eclipses has been taken as follows:

- A manoeuvre of a fixed size (5 m/s) is applied at a fixed time (scan over times in first revolution, 10 days step) in a fixed direction in the plane spanned by the non-escape direction and the out-of-ecliptic vector.
- The orbit is re-generated (including the insertion manoeuvre optimisation before that eclipse avoidance manoeuvre)
- Length and depth of the eclipse are re-evaluated.

After some testing with arbitrary directions in the non-escape plane a pure z-manoevure was preferred. Figure 3.75 shows the normalised eclipse depths for the October 9 case at the closing of the daily launch window as function of the day on which the z-manoevure is done.

Table 3.12 (explanation of columns in annex) shows the details of all the eclipses (0.5 hours resolution) for a 5 m/s manoeuvre in +z-direction on day 140, compared to the case without that manoeuvre. It can be seen that the deep eclipses on day 280 and 633 have disappeared with the manoeuvre, but others have appeared newly and they have become more. Clearly general conclusions cannot be drawn from this un-systematic first assessment, however it can be confirmed that the lunar eclipses are very sensitive to manoeuvres.

Long duration eclipses can be similarly removed.

Figure 3.75: Normalised eclipse depth as function of time of 5 m/s z-manoevure

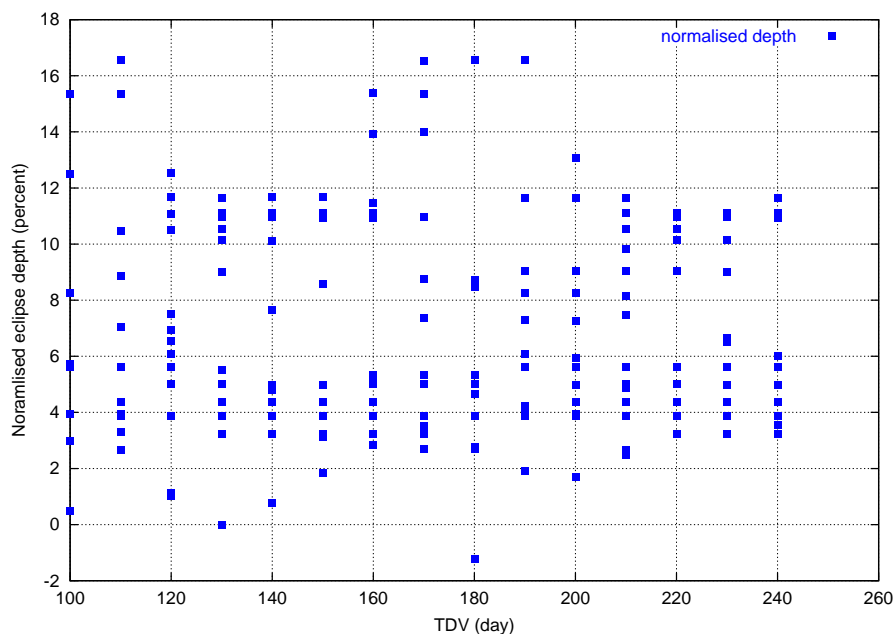


Table 3.12: Eclipses without and with 5 m/s z-manoevre on day 140 (Sept 9 launch)

Without manoeuvre:

#	MJLAUNCH	DVTOT	DAYECLI	SHADDUR	MOONSIZE	SSCEMIN	DEPTH%	SUNDIST(AU)	DEPTH%AU	9/ 9
2808.5651	161.6435	121.4127	4.8000	0.0616	0.0105	5.2547	0.991546	3.877257		
2808.5651	161.6435	210.5727	6.7200	0.0508	0.0818	3.7053	1.011886	5.620358		
2808.5651	161.6435	280.4127	5.2800	0.0938	0.1285	12.9330	1.025305	16.554460		
2808.5651	161.6435	399.3851	3.3600	0.0787	0.2172	7.4132	1.008432	8.725386		
2808.5651	161.6435	492.6595	5.7600	0.0909	0.0369	11.6597	0.992704	10.553037		
2808.5651	161.6435	564.5995	4.8000	0.0501	0.2502	2.3602	1.008649	3.779238		
2808.5651	161.6435	633.8795	6.2400	0.0901	0.1380	11.8755	1.023959	15.352080		
2808.5651	161.6435	854.5684	3.8400	0.0605	0.2738	2.1506	0.992659	0.917284		
2808.5651	161.6435	987.7284	6.2400	0.0857	0.1967	9.7770	1.022104	13.068830		

With manoeuvre:

#	MJLAUNCH	DVTOT	DAYECLI	SHADDUR	MOONSIZE	SSCEMIN	DEPTH%	SUNDIST(AU)	DEPTH%AU	9/ 9
2808.5651	161.6265	121.4144	4.8000	0.0616	0.0153	5.2545	0.991546	3.877143		
2808.5651	161.6265	137.9132	2.4000	0.0984	0.3371	1.1300	0.993240	-0.016614		
2808.5651	161.6265	210.5332	5.2800	0.0507	0.2194	3.5855	1.011876	5.501208		
2808.5651	161.6265	374.0398	4.3200	0.0771	0.0301	8.7162	1.015702	11.102099		
2808.5651	161.6265	399.3998	4.3200	0.0788	0.0160	8.8511	1.008428	10.142314		
2808.5651	161.6265	475.0167	4.8000	0.0569	0.1420	4.4924	0.992399	3.245522		
2808.5651	161.6265	492.6567	5.2800	0.0909	0.1096	11.6391	0.992704	10.532248		
2808.5651	161.6265	564.6567	7.6800	0.0501	0.0360	3.5896	1.008666	4.993588		
2808.5651	161.6265	728.8133	4.3200	0.0776	0.1300	8.8678	1.018442	11.655418		
2808.5651	161.6265	754.0733	3.8400	0.0801	0.0786	9.2157	1.011529	10.967667		
2808.5651	161.6265	918.3147	8.1600	0.0496	0.0107	3.5023	1.005359	4.375156		
2808.5651	161.6265	982.4347	7.6800	0.0627	0.1660	5.7014	1.021154	8.998193		

### 3.6.3 Eclipses by the Moon on Herschel

For Herschel there was only one launch date (Feb. 16) which at the opening of the daily launch window led to an eclipse by the moon in the operational orbit. It can therefore be said that Herschel will have no eclipses by the moon in the operational orbit, assuming this aspect is taken into account in the final launch window refinement. Eclipses by the moon during the transfer happened only for launches on 2007/10/9 and 2008/1/8 at the opening of the daily slot. They will have to be verified over the full launch window slot. Possibly some launch dates will have to be removed from the launch window.

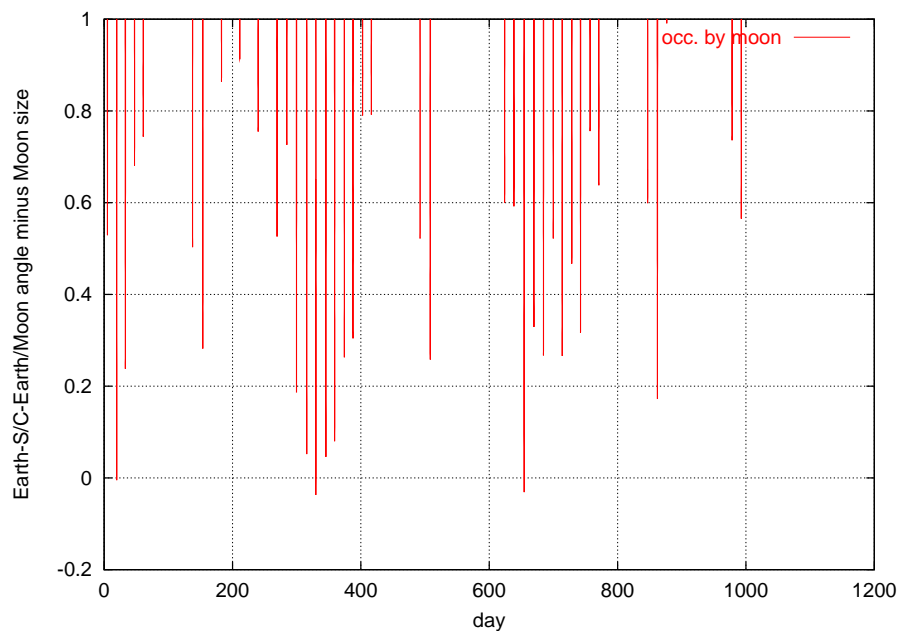
### 3.6.4 Conclusions on Eclipses by the Moon

- For Herschel there are no eclipses by the moon in the operational orbit except for one launch date.
- For Planck there will be typically two eclipses by the moon per year. In extreme cases there may be up to about 10 eclipses during the 2 years mission.
- Depth and duration of the eclipses are correlated, such that eclipses over 13% normalised depth will not last more than 10 hours.
- Eclipses by the moon cannot be avoided for Planck in a systematic way like the Earth eclipses (at least no method has been constructed up to now). However long eclipses by the moon or particularly deep eclipses can be avoided.
- It is recommended to cover eclipses of up to 10 hours, with a depth up to 13% (normalised to the power at 1 AU) by the spacecraft design, and to allocate 5 m/s in the propellant budget to avoid the others. It should be noted that the 5 m/s allocation should also allow to cover dispersed cases.
- Also very long eclipses (up to 60 hours) occur for some launch dates during the transfer. These can be removed by shortening or shifting the daily launch slot for some launch dates.

### 3.6.5 Occultations by the Moon

The moon may also interrupt the communication link to the ground station. Figure 3.76 shows the Earth-spacecraft-moon angle minus the angular size (half cone angle) of the moon as seen from the spacecraft, for a 2007/9/9 launch case (old CReMA 3.0 reference). It can be seen that this angle will become less than zero only once per year. The duration of such an occultation by the moon is about 1 hour.

Figure 3.76: Occultations by the moon



## 4 Navigation and Orbit Maintenance

This chapter covers the navigation process (orbit determination and orbit control) during the transfer and during the operational orbit at  $L_2$ . It summarises and updates [14].

### 4.1 Assumptions

#### 4.1.1 Tracking

The following assumptions have been done on the measurement system:

- Tracking exclusively from New Norcia.
- The duration of the tracking pass restricted to 3 hours.
- Doppler measurement frequency one every 10 minutes. This assumption is slightly pessimistic, actually measurements every minute at the assumed accuracy will be available.
- Two Range measurements per tracking pass at the beginning and at the end, cases with one point at the beginning and with Doppler only are included.
- Doppler noise 0.1 mm/s ( $1-\sigma$ ) above  $15^\circ$  elevation.
- Range Bias 20 m ( $1-\sigma$ ). The range bias is estimated for one station pass, then the error is re-initialised.
- Range noise 2 m ( $1-\sigma$ ) above  $15^\circ$  elevation.
- Measurement noise amplification by a factor of 10 (1 mm/s and 20 m respectively) for elevations lower than  $15^\circ$
- Ground-station coordinate bias ( $1-\sigma$ ):
  - X-component: 0.3 m
  - Y-component: 0.3 m
  - Z-component: 1 m.

Also the ground station biases are re-initialised after each day, but this is irrelevant.

#### 4.1.2 Noise

In the estimation process the state vector (position and velocity) has been extended to include the additional dynamic model parameters:

- The Solar radiation pressure (combined with the reflectivity coefficient): with 10% steady state standard deviation, 1 day auto-correlation time. For Herschel a surface of  $23.1 \text{ m}^2$  and a mass of 2700 kg have been assumed, for Planck  $13.8 \text{ m}^2$  and 1300 kg. In both cases the reflectivity coefficient has been set to 1.1.
- Three independent 3-dimensional non-gravitational acceleration processes along the coordinate axes causes e.g. by attitude control forces and gas leakage: with  $6 \times 10^{-12} \text{ km/s}^2$  steady state standard deviation, and 3 different auto-correlation times of 1, 5, and 10 days.
- It should be noted that these assumptions do not cover the effects of the radiation pressure variation by changing the Herschel yaw angle, and of helium venting and of the wheel off-loading manoeuvres on Herschel. These effects are not predictable, assuming the observation schedule will not be fixed long time in advance. Therefore they must be covered in the study on orbit maintenance. This is done in section 4.5. The above errors are assumptions for the knowledge error on the dynamic model input to the orbit determination. It has been assumed that at the time of orbit determination the pointing direction of the telescope will be known, so the accelerations will be known to the assumed level.



At the RAMP follow on meeting in June 2004 it has been explained that the guidance system only controls the first 5 orbital elements. The covariance in  $f$  and  $T$  is the result of a statistical sample representing the dispersions in launcher performance.

The covariance analysis uses as input the transformation of the covariance matrix at spacecraft separation to a local frame (along track, cross track, radial) at perigee. This matrix is given in table 4.3 (in km,s).

Table 4.3: Launcher dispersion in local frame at perigee

5856.548660845	-12.979251980	1902.520056266	-1.607730086	-0.035908649	-4.787068396
-12.979251980	6.796461667	-12.931091140	0.010988866	0.007909012	0.010861215
1902.520056266	-12.931091140	1948.239572067	-1.646321590	-0.036269326	-1.552899471
-1.607730086	0.010988866	-1.646321590	0.001391446	0.000030818	0.001312247
-0.035908649	0.007909012	-0.036269326	0.000030818	0.000011302	0.000029659
-4.787068396	0.010861215	-1.552899471	0.001312247	0.000029659	0.003917550

## 4.2 Navigation During Transfer

### 4.2.1 First Orbit Correction on Day 2

The launcher dispersion has to be removed by a correction manoeuvre as soon as possible. The first orbit correction manoeuvre can only be done after the orbit determination process has been successfully completed. An agreed assumption on the time when the manoeuvre can be done at the earliest is 2 days from perigee, this is at a distance of about 340000 km from the Earth, so around moon distance. The details of the orbit determination do not play a role for the first orbit correction. The orbit will be known accurately compared to the launcher dispersion effect.

The estimate of the correction  $\Delta V$  to remove the launcher dispersion has originally been obtained by two different methods.

- First a "Linear Navigation" algorithm was used. This method uses a scheme combining linear covariance analysis (for orbit determination) with linear guidance. The targeting is done to the nominal position vector at the Lissajous orbit insertion. A method like this is commonly used for interplanetary navigation mission analysis. For the Lissajous orbit transfer, the statistics of a second maneuver at the target position, to match the velocity, was calculated in addition.
- An alternative "Monte Carlo" method for the guidance was developed using the same scheme as the one introduced for the station keeping in the Lissajous orbit. That is, removal of the velocity component along the escape velocity. The implementation of this second algorithm follows the following steps:
  1. Generation of a set of random state vectors by using the covariance matrix in orbital elements at spacecraft separation.
  2. Propagation of the state until the day of the correction (nominally day 2).
  3. Calculation of the new optimum transfer from there to the L2 for each case. The correction maneuver is assumed to be performed parallel to the instantaneous velocity, and is calculated by a bisection method which leads to a non-escape orbit.
  4. Generation of the statistics of the correction manoeuvre and the modified insertion manoeuvre from the random sample.

In Issue 3.0 of this CReMA, to use the input from Arianespace in a way with minimum modifications, but also to properly take into account the effects by the moon (notice that day 2 is reached at 340000 km radius), the Monte-Carlo method had been used to estimate the first orbit correction  $\Delta V$ . The result of the Monte-Carlo method confirmed the result of the linear method with some variation depending of the launch date due to the moon influence. The Herschel transfer orbit has not been changed, so the previous results still apply. The Planck transfer orbit now deviates slightly from the Herschel stable manifold orbit, from day 2. It has been calculated by a complex optimisation which was not done on a random sample,

Time (Days)	Mean (m/s)	Std (m/s)	91% (m/s)	95% (m/s)	99% (m/s)
1	7.960	5.927	16.826	19.047	25.395
2(Nom)	10.632	7.920	22.124	25.526	34.033
3	12.795	9.534	26.707	30.301	41.083
5	16.613	12.389	34.883	39.578	52.990
10	25.683	19.198	53.741	61.115	83.238
15	35.482	26.598	75.510	102.152	116.954

Table 4.4: Correction  $\Delta V$  as function of the execution time

it is simply too heavy computationally. Rather the linear method has been applied for Planck, but the variations as function of the launch date have been kept as previously calculated.

The statistics of the first correction manoeuvre for the reference launch date on 2004/11/15 at the opening of the launch window on that day, using the linear method for this case, are presented in table 4.4 for different manoeuvre execution times.

Apparently the update of the covariance matrix at launcher separation by Arianespace leads to a slight reduction in the requirement for the first orbit correction manoeuvre compared to that of CReMA issue 3.0. The verification over the full launch window has not been repeated. Rather the requirement has been verified using the linear method at the opening and closing of the daily window for a few launch dates which require the maximum propellant allocation on Planck for the deterministic manoeuvres. This is shown in table 4.5.

Date	Mean (m/s)	Std (m/s)	91% (m/s)	95% (m/s)	99% (m/s)
07/10/21 - open	10.257	7.592	21.950	26.317	33.596
07/10/21 - close	9.918	7.397	21.296	25.536	32.601
07/11/18 - open	10.812	7.942	23.057	27.643	35.285
07/11/18 - close	12.222	9.123	26.250	31.477	40.187
07/12/15 - open	10.481	7.745	22.414	26.873	34.304
07/12/15 - close	11.376	8.493	24.437	29.301	37.409

Table 4.5: Launch date dependence of first orbit corrections

It appears that the allocation for the correction manoeuvre on day 2 could be reduced to 40 m/s. However figure 4.1 prepared with the Monte-Carlo Method, not updated from the old launcher dispersion of CReMA issue 3.0, shows a relative variation of 12 m/s with higher maxima at other dates. Therefore a margin of 5 m/s has been kept in the allocation to cover the influence of the moon and an increase in the insertion manoeuvre due to stochastic effects during the transfer, in fact the previous allocation of 45 m/s on both spacecraft for a manoeuvre on day 2 remains appropriate.

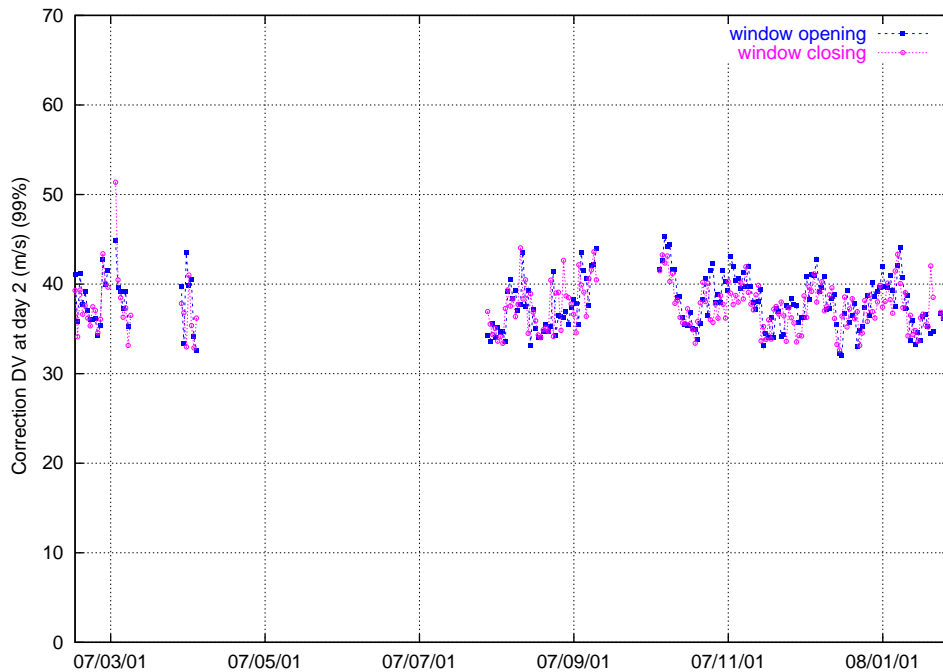


Figure 4.1: Launch Dispersion  $\Delta V$  at day 2 (99-percentiles) over the launch window (old dispersion)

#### 4.2.2 Later Stochastic Transfer Orbit Correction Manoeuvres

A second "trim manoeuvre" will be necessary a few days after the launcher dispersion removal manoeuvre, mainly to remove the error remaining from the rather large first correction. For a first correction on day 2 this manoeuvre has been assumed to be done on day 12. Another two correction manoeuvres have been assumed to be scheduled 20 and 10 days before the Planck orbit insertion manoeuvre. By this scheduling a position error at insertion to the Lissajous orbit (time  $T_{inj}$ ) below 10 km ( $1\sigma$ ) can be reached. Table 4.6 gives the  $\Delta V$  statistics for these manoeuvres using the linear navigation algorithm. The table also includes the correction to the insertion manoeuvre on day 99.696. In general this will disappear by re-optimising the target orbit, or choosing a different orbit for Herschel, but it has been covered by taking some margin.

Time (Days)	Mean (m/s)	Std (m/s)	91% (m/s)	95% (m/s)	99% (m/s)
2.000	10.397	7.730	22.505	25.853	33.105
12.000	1.110	0.773	2.272	2.637	3.418
80.000	0.317	0.226	0.657	0.763	1.021
90.000	0.021	0.009	0.033	0.037	0.045
99.696	1.852	0.984	3.309	3.701	4.682

Table 4.6: Transfer Orbit Corrections

It has been observed that for some launch dates the size of the second correction (on day 12 above) depends on the day of execution. Figure 4.2 shows this dependence for a launch at the opening of the launch window on 6 October 2007. Evidently there is a singularity in the guidance matrix around day 9.5, however when choosing the time of the correction manoeuvre differently, the allocation of 3 m/s remains sufficient.

For Planck an additional allocation of propellant must be made to correct the orbit after the rather large orbit injection manoeuvre (of e.g. up to 210 m/s). It can be assumed that this correction is done soon after the injection and also that the injection manoeuvre, which is not time critical, is decomposed in two

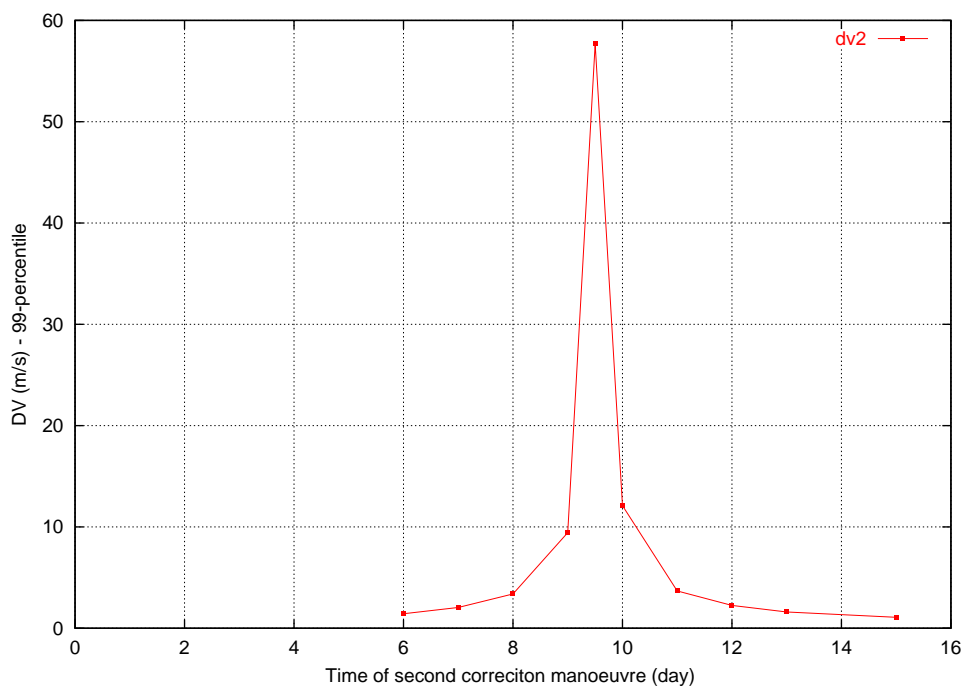


Figure 4.2: Possible time dependence of second orbit correction manoeuvre

parts, with some tracking in between, such that the second part can be tuned to calibrate the first part. An allocation of 2 m/s has been made.

The propellant estimates for the transfer mid-course corrections do not depend on the details of the tracking schedule and accuracy. Three station tracking has been assumed in the performed simulations. The assumptions on the system noise modelling however influence the propellant estimates. It must be noted that the details of the perturbations on the orbit created by the spacecraft itself are not yet taken into account, e.g. the effect of wheel off-loading manoeuvres which are not performed in a pure torque mode. In such a case it is recommended to allocate the same amount of propellant used as for these attitude manoeuvres for additional orbit corrections.

### 4.3 Orbit Determination in the Operational Lissajous Orbits

#### 4.3.1 Reference Operational Orbit

The reference orbit for the navigation studies in the final orbit has been taken at the opening of the launch window on 2007/2/15 (not updated from CReMA 3.0). The orbit as generated by the launch window software, has been stored on an orbit file using the standard software of ESOC Flight Dynamics (Hermite polynomial interpolation). From there a grid of points every 10 days has been interpolated over a given time interval. The multiple shooting method then is used to generate a reference orbit for all navigation and orbit control studies.

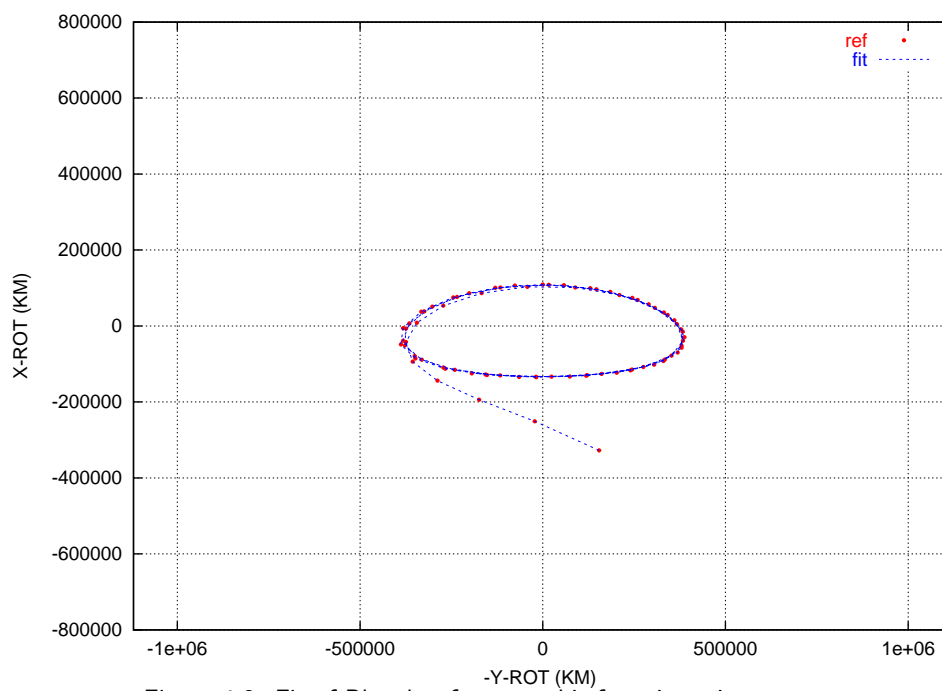


Figure 4.3: Fit of Planck reference orbit from insertion manoeuvre

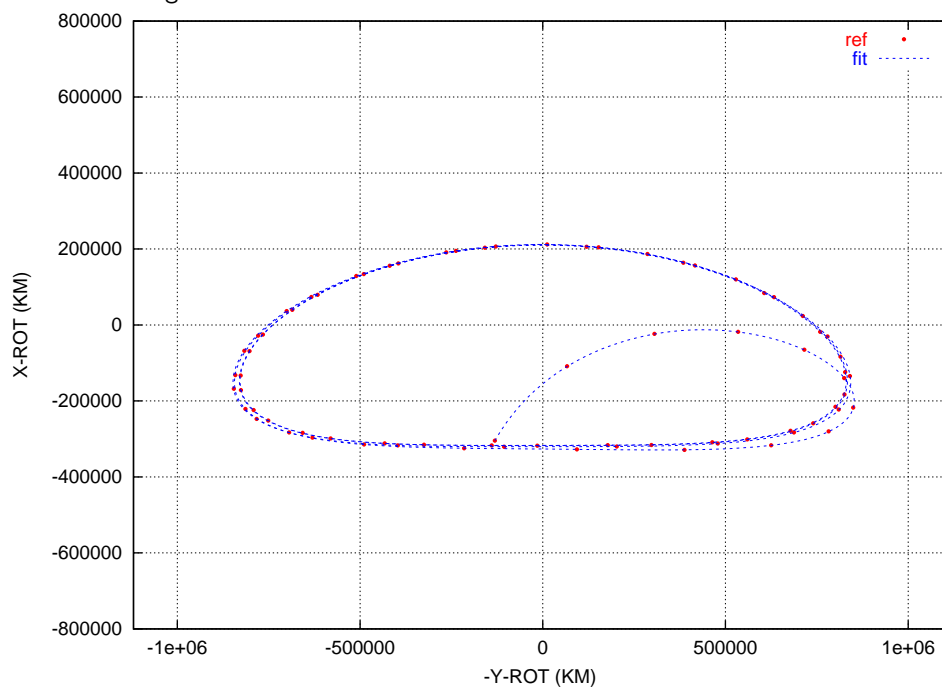


Figure 4.4: Fit of Herschel reference orbit from day 20

The Multiple Shooting method takes those  $n+1$  points as initial guess. It then integrates forward from each of these points (using a completely different orbit generator than the one used in the launch window calculations) to the next grid time, also solving the variational equations numerically and storing the state transition matrices. It then linearises and solves a system of  $6*n$  linear equations in  $6*(n+1)$  variables, to match the final points of the forward integration steps with the initial points of the next. The 6 remaining degrees of freedom are used to minimise the root sum square of the  $6*n$  corrections to the states (the velocity is normalised in km/day and no other scaling is applied). This process converges quickly, and with the latter addition ("pseudo-inverse") leads to a solution close to the initial.

The method can be used in different variants. Prescribing the initial position reduces the degrees of freedom to 3, this is used in one of the orbit control modes. Prescribing the final position as well solves a two point boundary value problem ("Lambert solver for Libration point orbits").

Figures 4.3 and 4.4 shows how the multiple shooting fits the initial orbit for Planck and Herschel, on that scale the differences cannot be seen. In fact in the multiple shooting the radiation pressure has been turned on, which was not the case in the launch window generation (this demonstrates that the radiation pressure can be ignored in the launch window calculation). The start point for routine operations is assumed at the insertion manoeuvre for Planck, and 20 days after launch for Herschel respectively. The plots start at these points. The position deviation of the multiple shooting fit from the original reference orbit remains below 500 km for Planck and below 2000 km for Herschel.

### 4.3.2 Knowledge of Operational Orbit

During the transfer to  $L_2$ , orbit determination has to be performed to estimate the state for the re-targeting, so as part of the spacecraft operations. In the Lissajous orbit when the scientific payload is operated, the reached orbit accuracy is important not only to calculate the target conditions for the orbit maintenance but also for the payload. All reference assumptions have been given in section 4.1.

The orbit determination process for three different scenarios has been studied:

- Tracking using Doppler exclusively.
- Tracking using both Doppler (every 10 minutes) and Range every 3 hours (twice per pass)
- Tracking using both Doppler (every 10 minutes) and Range only once per pass (at BOM)

Range measurements cannot be done at the same time as telemetry transmission for the Herschel-Planck telemetry systems so there is an interest to minimise ranging activities. Table 4.7 summarises the level of variations of the  $1-\sigma$  errors over two years. In the orbit determination study the orbit control algorithm (3), removal of linearised escape component, has been used. This is a slightly pessimistic assumption.

		Herschel Dop.	Herschel Dop.+1 Ran.	Herschel Dop.+2 Ran.	Planck Dop.	Planck Dop.+1 Ran.	Planck Dop.+ 2 Ran.
Position	(km)	8 - 53	2 - 22	1 - 24	10 - 38	1 - 13	0.5 - 13
Velocity	(mm/s)	8 - 18	4 - 13	3 - 12	7 -14	4 - 11	3 - 10
Distance	(km)	6	0.05	0.045	6	0.04	0.03

Table 4.7: Orbit Determination Accuracy

Figure 4.5 to 4.8 present the errors projected into the three axis of the plane of the Sky frame. The peaks are at zero declination. The plane of sky frame is defined as follows:

- X-axis. Along the radial direction Earth-S/C
- Y-axis. Orthogonal to X-axis and contained in the Earth equator
- Z-axis. Completing a right-handed system

It can be seen that the main contribution to the total error comes from the error orthogonal to the viewing direction, with a domination error out of the equator plane, due to the lack of dynamic coupling. This means that any additional measurement directly related to this plane of the sky (i.e. angular astronomic measurement) would drastically improve the orbit determination accuracy.

Without any ranging the position error may become up to 40 km, the radial distance then is badly observable, the error it remains above 6 km. If one range point per station pass is taken as baseline scenario, a position accuracy of 22 km and a velocity accuracy of 1.3 cm/s is achieved for both spacecraft. Most of the time the position error will be below 5 km. The radial distance will be directly observable, its error is below 50 m in steady state. This is important e.g. for the spacecraft clock synchronisation. A second range point per station pass does not contribute much.

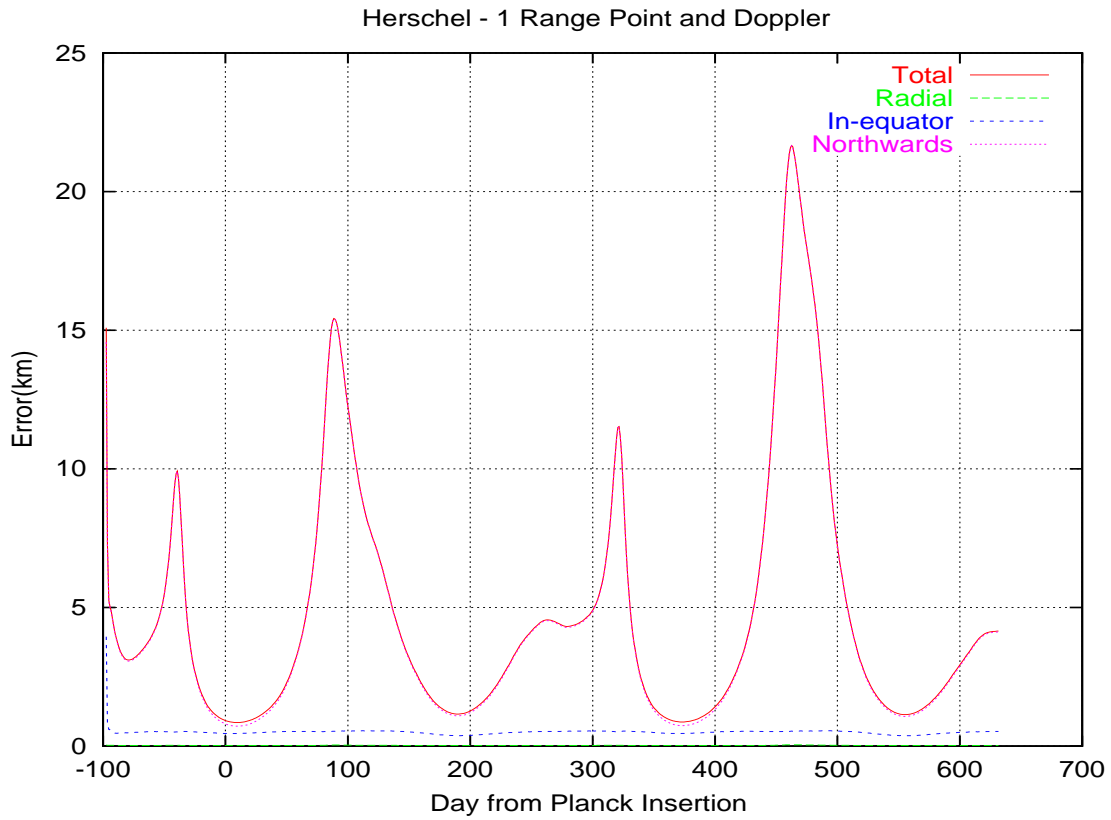


Figure 4.5: Position determination accuracy for Herschel. Doppler and 1 point Range

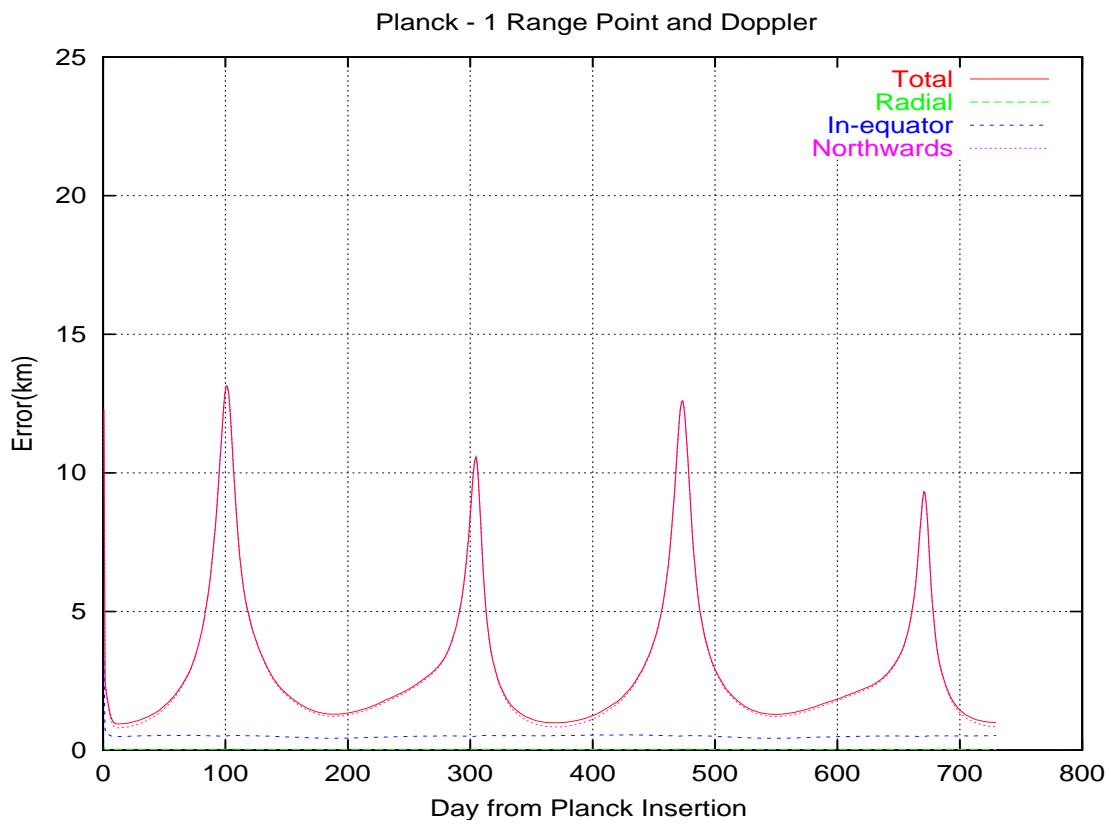


Figure 4.6: Position determination accuracy for Planck. Doppler and 1 point Range

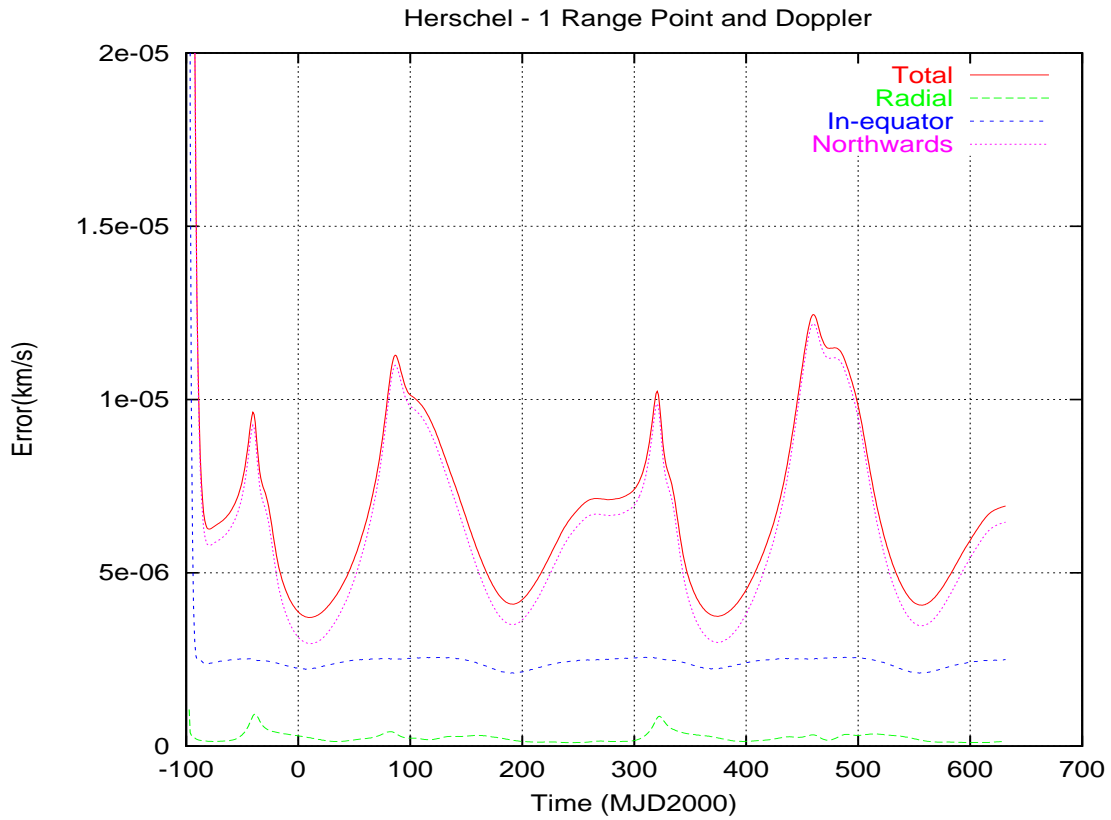


Figure 4.7: Velocity determination accuracy for Herschel. Doppler and 1 point Range

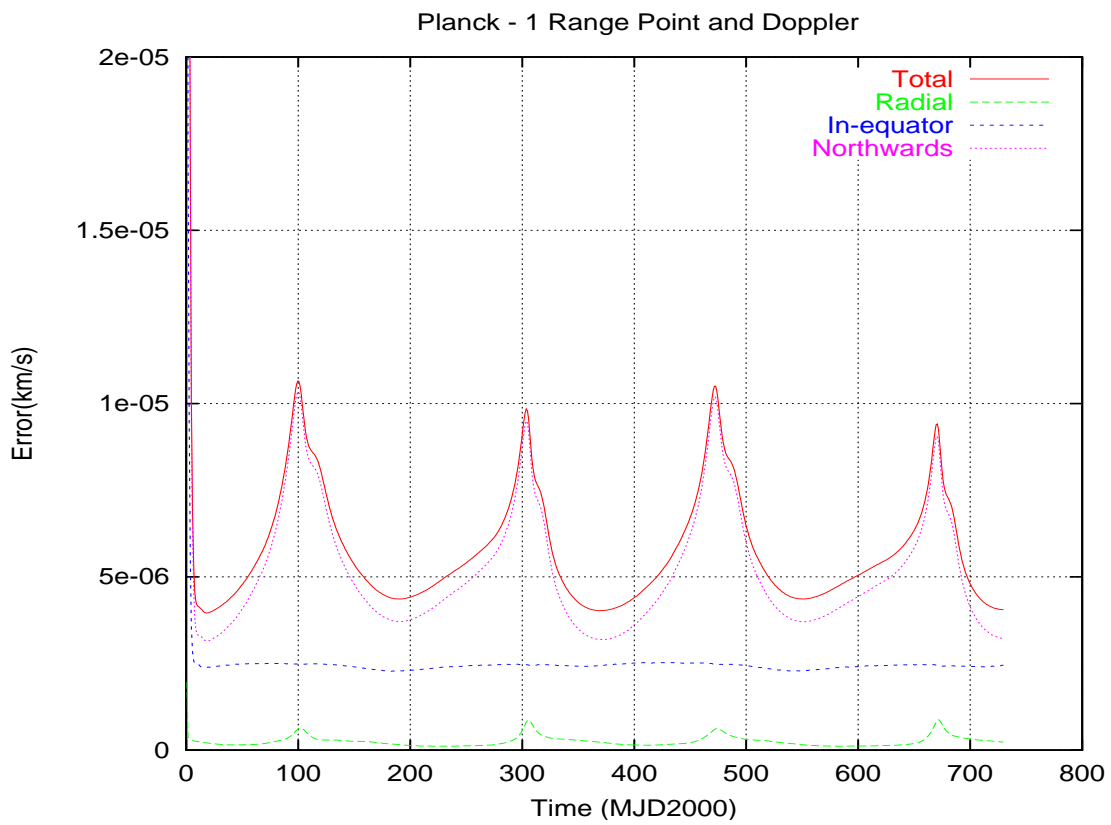


Figure 4.8: Velocity determination accuracy for Planck. Doppler and 1 point Range

## 4.4 Orbit Maintenance

### 4.4.1 Choice of Orbit Control Method

From the tracking data any deviations from the desired motion around  $L_2$  will be observed. Deviations in the escape direction (see chapter 2 for definition) will have to be removed without too much time delay, the spacecraft has to be targeted back to a quasi-periodic motion around  $L_2$ . Several orbit maintenance strategies to achieve this have been tested:

1. **Classical interplanetary navigation** with a shifting target position. Every manoeuvre is calculated by targeting to a future position on the nominal trajectory. This method originates from targeting e.g. to a fly-by at a planet or a minor body [1]. For Libration point orbits, the choice of the time to the target position is a parameter to be optimised, it has first been chosen at 30 days ahead.
2. **Linear Quadratic Control (Bellman)**. This uses pre-calculated control gains linearising along a reference trajectory and minimising a quadratic functional weighting state deviations and manoeuvre size. This method might be useful for an on-board controller, but for the actual implementation on ground it seems to be restrictive.
3. **Cancellation of the escape component** calculated with linear theory. This has been based on the ideas derived for the construction of the Libration point orbits (see chapter 2). However a term to control the position deviation has been added. Only the linear approximation has been used to calculate the size of the manoeuvres, different from the orbit construction (see method 5 below) where a bisection iteration along the unstable direction covers the non linear effects.
4. **Parallel shooting** To reconstruct the future orbit, in this control mode, the parallel shooting method has been used. This means, the current position together with the future positions of the original reference orbit are used to fit a new orbit. This method conceptually is not much different from method 1, it keeps the orbit close to the nominal.
5. **Construction of a free non-escape orbit** at each manoeuvre time as described in chapter 2. This means the position is fixed and a velocity increment along the escape direction is calculate by a bisection method until the predicted orbit does neither escape towards the sun (radius above  $2.5 \times 10^6$  km) nor towards the Earth (radius below  $8 \times 10^5$  km). This method resembles the original orbit construction method.

Table 4.8 compares the different control methods for the small amplitude Planck orbit and the large amplitude Herschel orbit. In both cases 2 years of orbit maintenance have been studied as one arc of the control method. Both start on the stable manifold, for Planck directly after the insertion manoeuvre, for Herschel 20 days after launch. The insertion manoeuvre execution error has been ignored, for both cases the same initial dispersion (=knowledge) of 15 km in position and 5 cm/s (spherical) in velocity has been assumed. It can be assumed that the insertion manoeuvre of Planck is properly decomposed, such that its execution error is below the assumed initial dispersion in velocity.

The time between correction manoeuvres has been assumed to be at least 30 days in this section, the first manoeuvre is 10 days after the start of the simulation (from insertion for Planck).

Strategy	1: Classical	2: Bellman	3: Escape direct.	4: New nominal	5: Free
Planck	1.28 m/s	diverges	1.9 m/s	0.90 m/s	0.75 m/s
Herschel	1.31 m/s	diverges	8.0 m/s	0.86 m/s	0.60 m/s

Table 4.8: Station keeping  $\Delta V$  for 2 years (maximum of 20 simulations)

Figure 4.9 shows the accumulated  $\Delta V$  and the single  $\Delta V$  for 20 simulations along the Herschel reference orbit with method 5 (free non-escape orbit).

To limit the CPU time, the results have been obtained by running a 20 cases Monte Carlo simulation only. This is certainly not sufficient to represent 99-percentiles, however it gives a clear indication. Also the

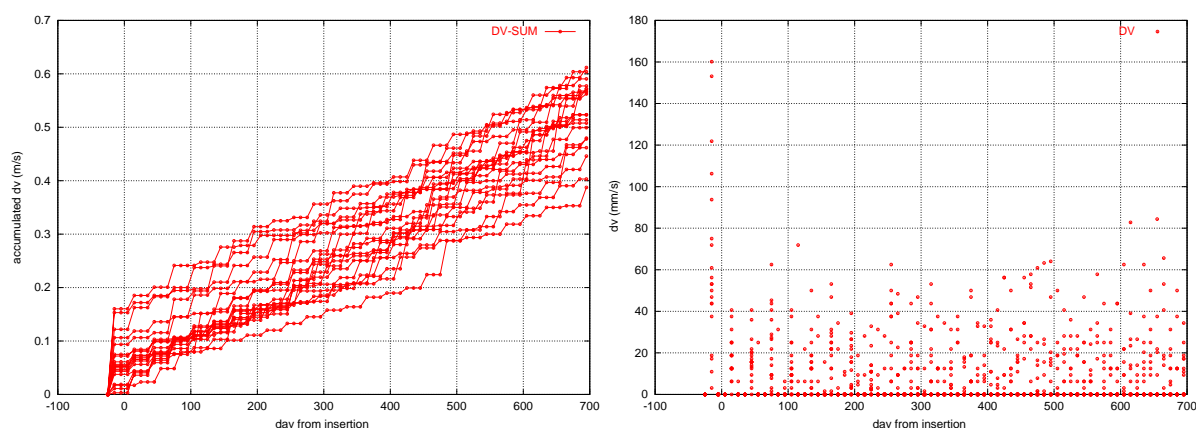


Figure 4.9: Accumulated and single  $\Delta V$ 's over 2 years with method 5 (Herschel)

number of Doppler measurements has been reduced from one every 10 minutes to one every hour, without changing the error assumptions. This reduces the obtained orbit accuracy slightly. It has been verified that the results on the orbit control are not influenced by that. For each case a full orbit determination process is simulated.

It can be seen from table 4.8:

- The Bellman method (2) diverges for the large time interval. This does not mean that it could not be applied for shorter intervals after some thinking, but it will be disregarded as already explained above.
- The Escape direction method (3) is obviously not sufficient on the large amplitude Herschel orbit. It should be noted that only the linear approximation is used to calculate the size of the correction manoeuvre. The method appears to be self-corrective, however this "self-correction" of the method error (nonlinearities) requires a considerable  $\Delta V$ .
- Of the two methods following a reference orbit the method (4) using the parallel shooting seems to require slightly less propellant than method (1) targeting to the position 30 days ahead. For both methods the correction manoeuvres are far from being aligned to the escape direction. This explains the higher cost compared to method (5).

First conclusions can be drawn as follows:

- The method (5) freely re-generating a future non-escape orbit at each orbit control gives the lowest overall  $\Delta V$  requirement.
- If separate propellant allocations are made to cover the effects of wheel off-loading and helium venting as discussed in section 4.5 and if in particular the remaining acceleration noises remain below the limits assumed, an allocation of 0.6 m/s per year is sufficient for this method (result of simulations still doubled).
- Orbit Control on the stable manifolds (far enough from Earth) works exactly as on the Lissajous orbits.
- For a 30 days control interval, the single  $\Delta V$ 's will be less than 10 cm/s.
- The classical position targeting method (1) and the parallel shooting method (4) require twice as much  $\Delta V$  than method (5). Method (4) performs slightly better than method (1), however in case guidance relative to a nominal orbit is desired, method (1) may be preferred because of its conceptual simplicity.

#### 4.4.2 Orbit Predictability

For both methods (1) and (4) the controlled orbit remains within 100 km of the planned orbit except for the initial phase as a result of the large dispersion started from (see figure 4.10 for the position targeting method 1). So for all nominal operational purposes the orbit can be assumed to be frozen for the whole mission for Herschel and also for Planck to a 1 second level in event times. It should be noted that for this case the propellant allocation to compensate for the effects of the helium venting and the wheel off-loading will be maximum (see table 4.11

Figure 4.11 shows that for the free non-escape control (5) over one year the orbit remains well within 1000 km from the nominal. 1000 km at  $L_2$  distance represents an angle of  $0.04^\circ$  and thus a time of 10 seconds in Earth rotation, e.g. in station acquisition time. If 10 seconds predictability is sufficient, method (5) can be used for Planck with up to a year lead time and the event sequence for the next period of another year ahead can be frozen. In most cases the predictability will be better.

The orbit predictability for Herschel will be mainly limited by the Helium venting effect as the directions of the accelerations by the Helium venting depend on the observation directions. Figure 4.12 shows a case with 10 simulations for Herschel, setting a system noise with accelerations of  $10^{-10}$  km/s<sup>2</sup> in all components and 10 days correlation times. This will not be representative, as the modelling of the noise processes in orbit determination and orbit control has not been separated. However it indicates the order of magnitude of deviations from the originally planned orbit. A prediction time scale of a few months to an accuracy of the order of 1000 km seems still to be possible, with helium venting and free non-escape orbit control.

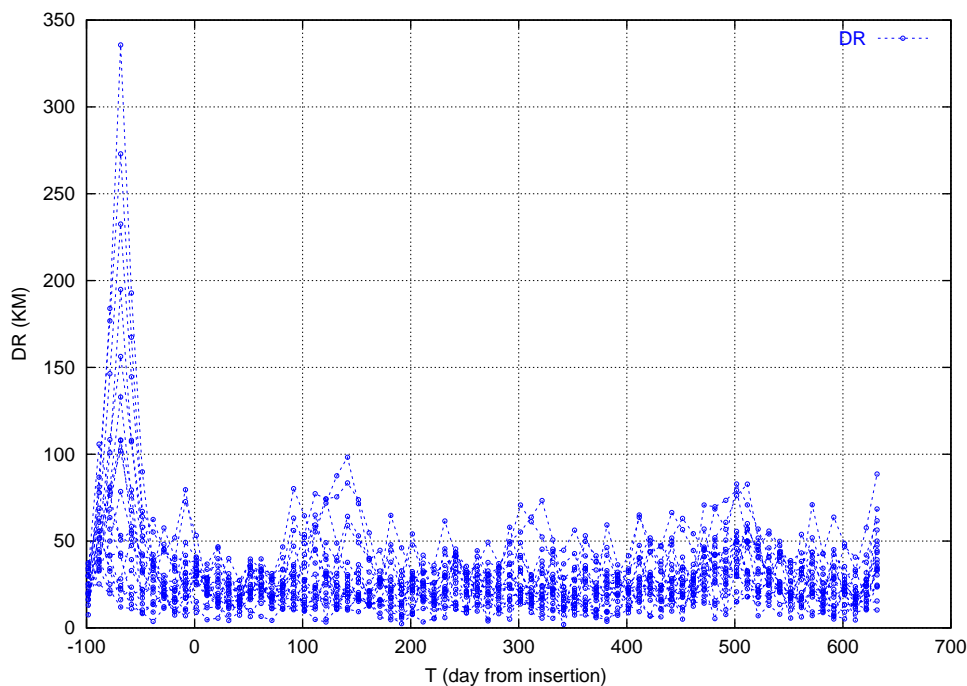


Figure 4.10: Orbit predictability for prescribed reference orbit (Herschel)

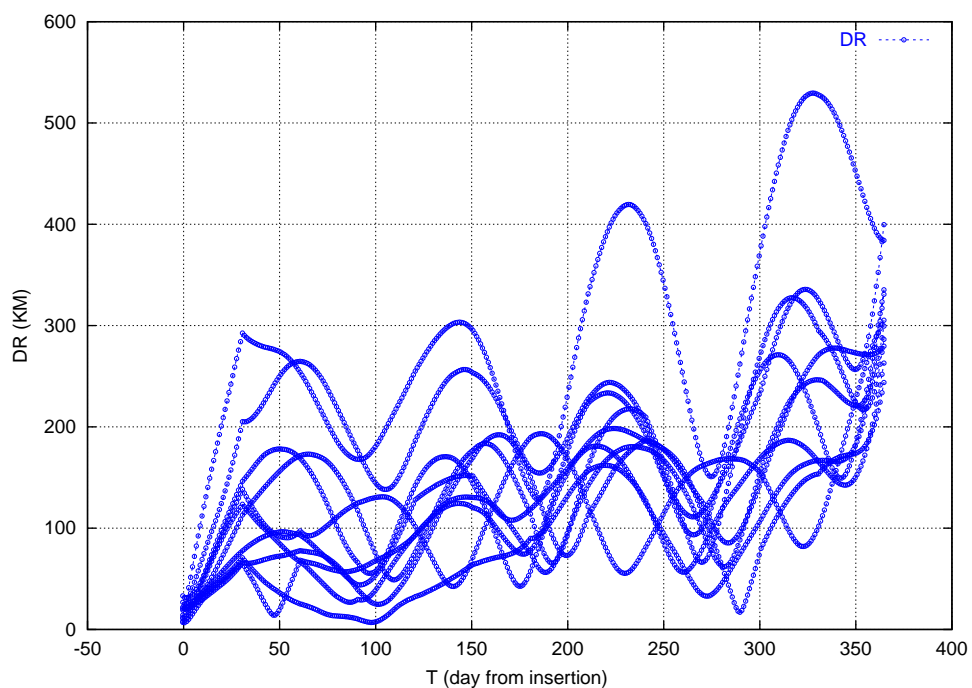


Figure 4.11: Orbit predictability for free non-escape control (Planck)

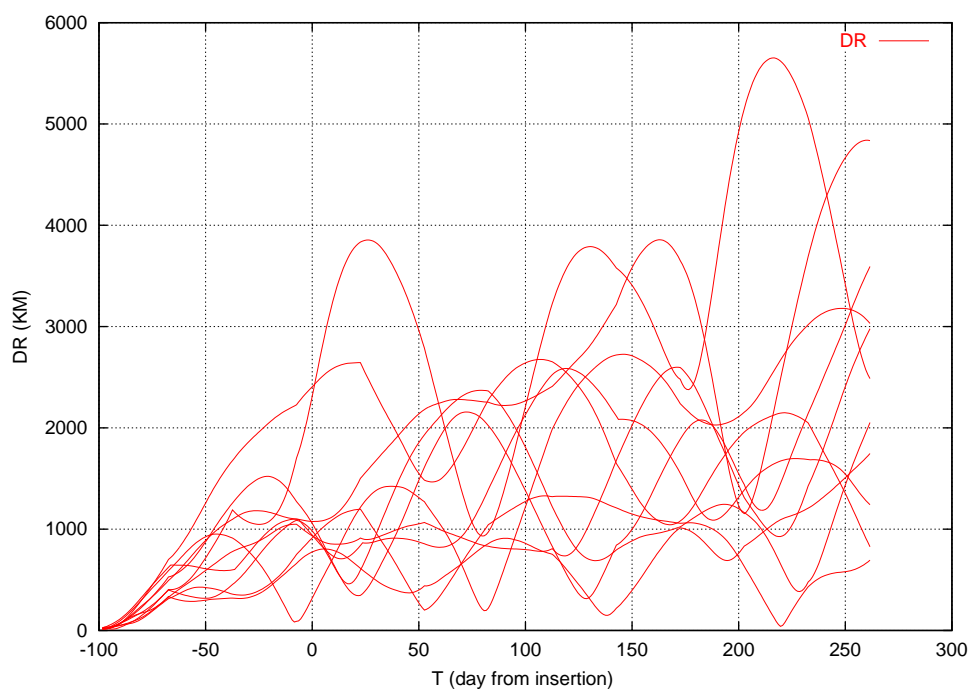


Figure 4.12: Orbit predictability for free non-escape control (Herschel)

### 4.4.3 Influence of Noise

Figure 4.13 compares the Herschel reference case (10% radiation pressure error - 23 m<sup>2</sup>, 2700 kg, reflectivity set to 1.1) with a simulation with 20% radiation pressure error (without the helium venting!). The results are given for position re-targeting control algorithm (1) and the free non-escape control (5). Figure 4.14 gives the same comparison doubling the radiation pressure error for Planck (13.8 m<sup>2</sup>, 1300 kg).

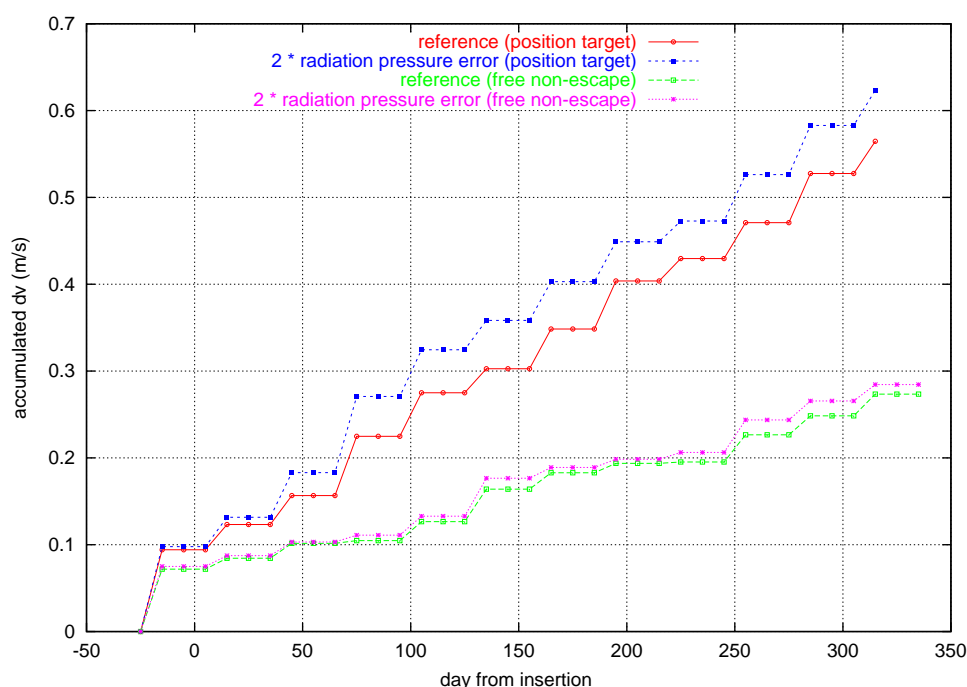


Figure 4.13: Double radiation pressure noise (Herschel)

In figure 4.15 the coordinate acceleration system noise (to cover e.g. random effects of the wheel off-loadings) has been doubled. The reference case assumes three three dimensional coloured noise processes (uncorrelated in coordinate directions) with the same steady state standard deviation of  $6 \times 10^{-12} \text{ km/s}^2$  but with 3 different auto-correlation times (1, 5 and 10 days).

Figure 4.16 compares the reference case in which the manoeuvre execution error of the manoeuvre below 10 m/s has been assumed at  $1 \sigma = 2.5\%$ , with a case with 0.5% manoeuvre execution error.

It can be seen that:

- The manoeuvre execution error does not play a role.
- Method (5) is not very sensitive to the radiation pressure effect, in the one simulation case in figure 4.14 more noise even leads to a smaller  $\Delta V$ .
- The dominating sensitivity at the current level of noise assumptions is to the coordinate acceleration noise. This means it should be carefully verified if the spacecraft satisfies the assumption, in particular on Herschel the effects of helium venting, wheel off-loading and also the changes of the sun aspect angle (pitch) during the observations will dominate the effects perturbing the orbit. These will be discussed independent of the orbit determination process in section 4.5.

### 4.4.4 Time between Manoeuvres

Figure 4.17 give a comparison for different times between the orbit maintenance manoeuvres, again both for method (1) and method (5).

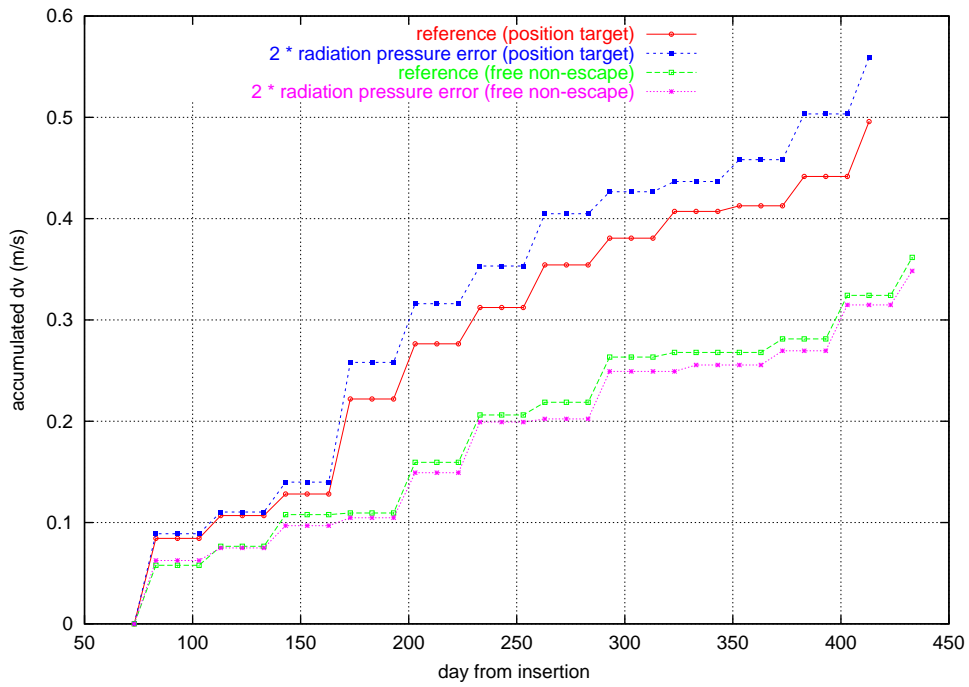


Figure 4.14: Double radiation pressure noise (Planck)

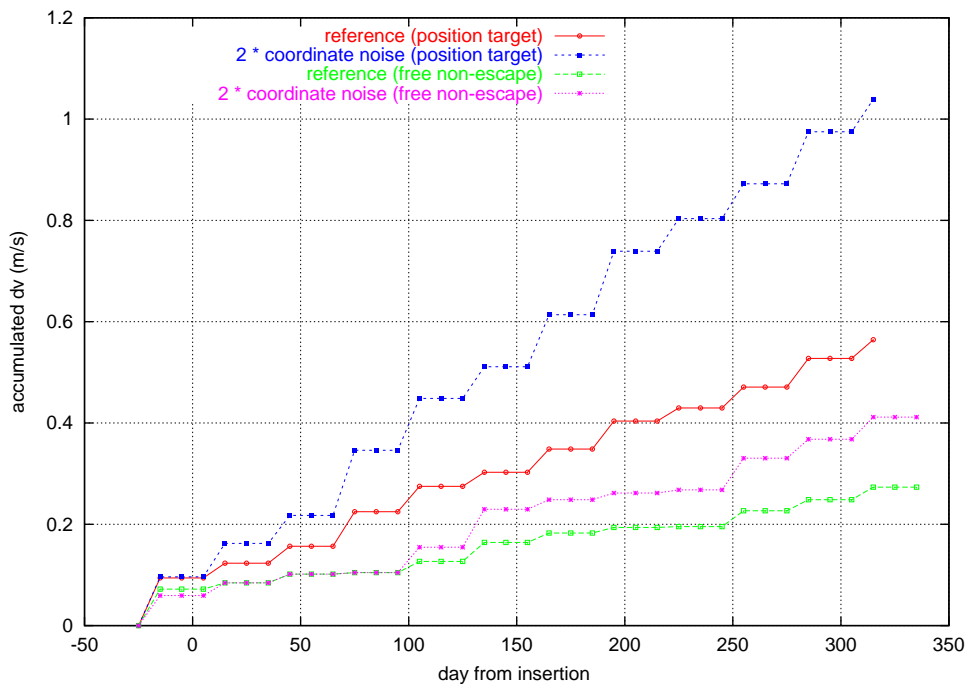


Figure 4.15: Double coordinate acceleration noise

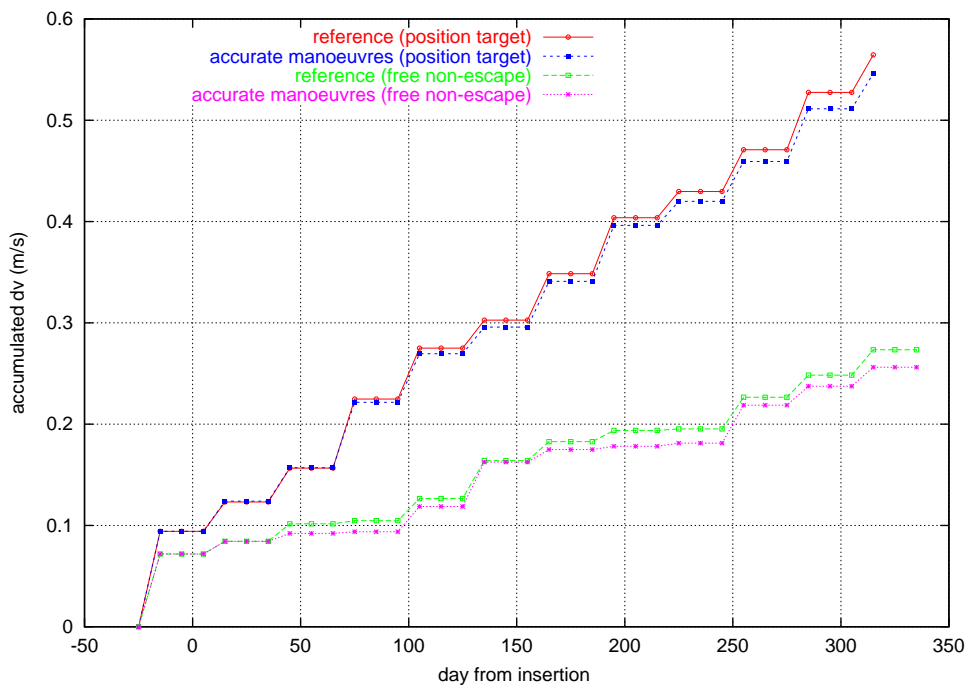


Figure 4.16: Smaller manoeuvre execution error

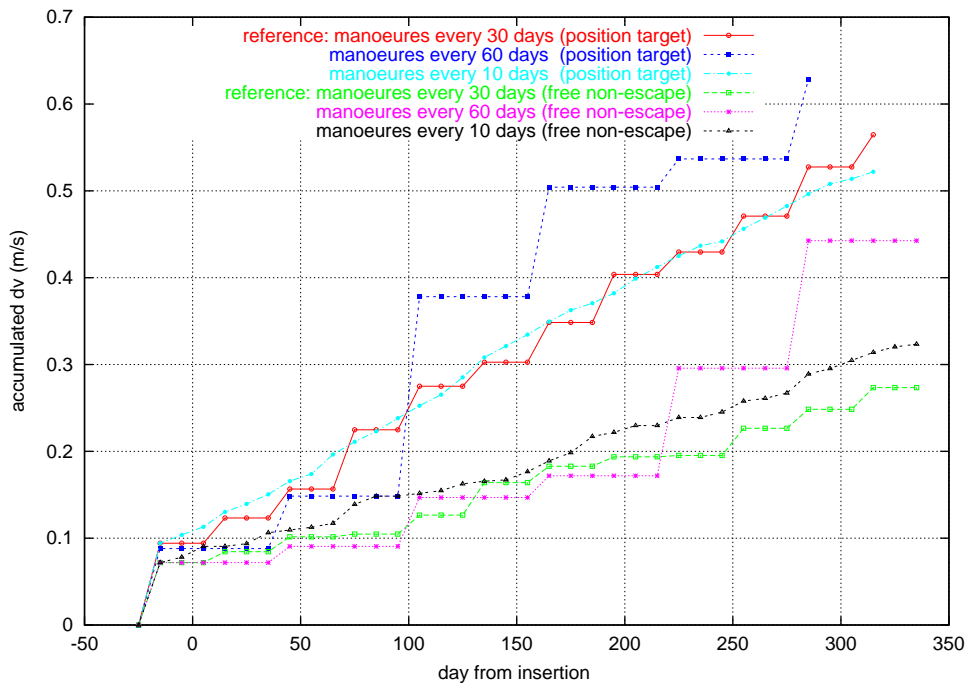


Figure 4.17: Time between manoeuvres (Herschel)

It can be seen that for method (1), the position targeting, times of 10 or 30 days between manoeuvre lead to the same result in overall  $\Delta V$ . In both cases the position targeting lead time has been assumed to be 30 days. For time intervals of 60 days between the manoeuvres the targeting lead time has been changed to 60 days, in this case for 30 days lead time the total  $\Delta V$  after 1 year was higher ( $\approx 1.4$  m/s).

For method (5), the free non-escape orbit control, 10 days or 60 days control intervals are worse than 30 days. However for the case with a much higher coordinate acceleration noise ( $10^{-10}$  km/s<sup>2</sup> with 10 days auto-correlation) it appears preferable to perform the orbit maintenance manoeuvres more frequently according to figure 4.18.

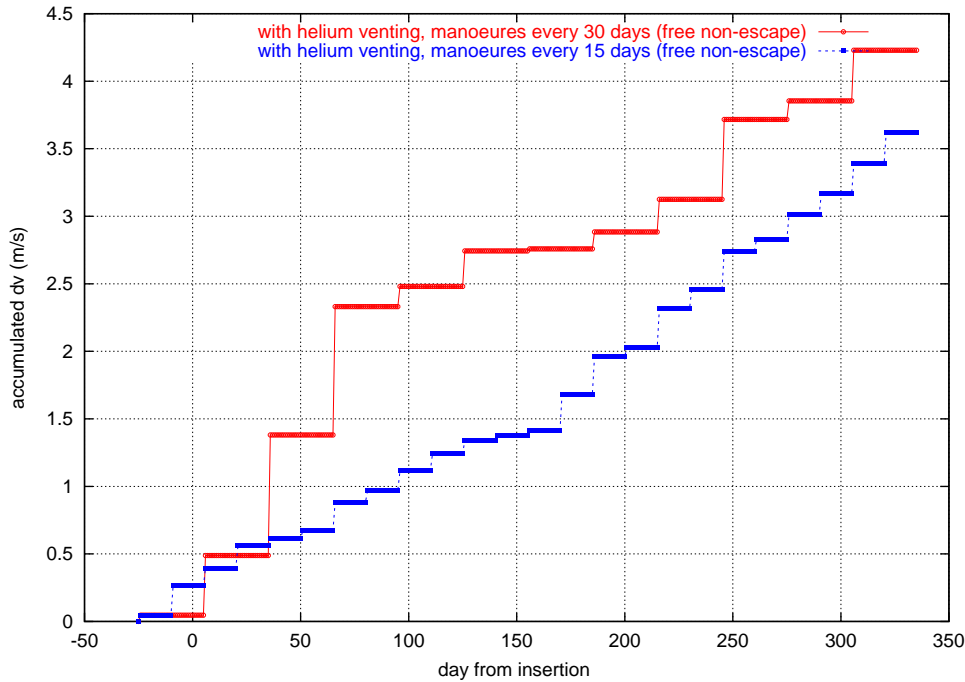


Figure 4.18: Time between manoeuvres (Herschel with helium venting)

## 4.5 Orbit Maintenance with Wheel Off-loading and Helium Venting for Herschel

The effect on the orbit of the wheel-offloading on Herschel has been studied in [12]. After the first issue of [12] the S/C design had evolved such that the results given there became obsolete. This section will cover the new scenario including the contribution of the helium venting system which were not considered before.

### 4.5.1 Wheel off-loadings

The Herschel reaction wheel system will continuously counteract the momentum to maintain the inertial S/C attitude. After a certain time the wheels must be discharged to keep their rotation speed within a certain limits.

According to [15] the range of variations for the torque due to the Solar pressure for each component in the body fixed frame is:

- $-13\mu N < T_x < 9\mu Nm$
- $120\mu N < T_y < 274\mu Nm$
- $-24\mu N < T_z < 27\mu Nm$

For the Helium venting system a detailed description of the disturbance torque sources is given in [17]. The expected variations along each component are the following:

- $\Delta T_x = 20\mu Nm$
- $\Delta T_y = 45\mu Nm$
- $\Delta T_z = 3\mu Nm$

Combining both contributions and assuming the worst possible scenario, the maximum residual torque acting on the S/C will be:

- $\Delta T_x = 33\mu Nm$
- $\Delta T_y = 125\mu Nm$
- $\Delta T_z = 30\mu Nm$

With the residual torque  $T$  with these limits, the angular momentum to be discharged from the wheels will be the accumulated according to:

$$\vec{H} = \int_{t_1}^{t_2} \vec{T} dt \quad (4.1)$$

with  $t_1$  and  $t_2$  the times of two consecutive wheel off-loading maneuvers.

During a wheel off-loading maneuver this angular momentum will have to be generated by actuating the spacecraft thrusters. The effect of the wheel off-loading maneuvers in terms of torque but also force, so effect on the trajectory, will depend on the thrusters configuration and the spacecraft attitude selected for the off-loading manoeuvre.

A matrix ( $E_T$ ) defines the torque created by every thruster acting during one second. For an arbitrary combination of thrust durations (defined by the vector  $\vec{s}$ ) this matrix will provide the angular momentum in the spacecraft body frame according to

$$\vec{H}_{sc} = E_T \cdot \vec{s} \quad (4.2)$$

The effects of the thrusters in terms of force is given by another matrix  $E_F$ . This matrix provides with the force in the spacecraft body frame created by every thruster acting during one second. For an arbitrary combination of thrusting times, the matrix will then provide the linear momentum in the spacecraft body frame as follows:

$$\vec{T}_{sc} = E_F \cdot \vec{s} \quad (4.3)$$

- The thrust-on vector  $\vec{s} = \{s_i, i = 1, 4\}$  is the vector containing the thrusting time for all the thrusters. The Herschel S/C has a set of 4 thrusters (C1,C2,C3,C4) for the attitude control.
- The Matrix  $E_T$  for Herschel is given in table 4.9 (mail from Mr. Anders Elfving on 2003/06/27).

Thruster	Tx(N)	Ty(N)	Tz(N)
C1	27.85	29.30	-19.50
C2	-27.85	-28.73	-19.50
C3	27.85	-28.73	19.50
C4	-27.85	29.30	19.50

Table 4.9:  $E_T$  Matrix for Herschel

- The Matrix  $E_F$  for Herschel is given in table 4.10 (mail from Anders Elfving on 2003/06/27).

Thruster	F <sub>x</sub> (N)	F <sub>y</sub> (N)	F <sub>z</sub> (N)
C1	11.47	0.0	16.38
C2	11.47	0.0	-16.38
C3	11.47	0.0	-16.38
C4	11.47	0.0	16.38

Table 4.10:  $E_F$  Matrix for Herschel

The components in inertial frame of the  $\Delta V$  will depend on the S/C attitude at the time of the wheel off-loading, e.g. defined by a rotation matrix  $R$  from body frame to inertial frame. Assuming the wheel off-loadings are carried out during the communication periods to preserve more time for observations, the S/C can be assumed to be in Earth pointing mode. This means there remains only one degree of freedom for the S/C attitude, the angle of rotation around the S/C-Earth direction (yaw).

With this, the accumulated angular momentum in the inertial frame has to be compensated by the wheel off-loading manoeuvre and the resulting linear momentum are

$$\vec{H} = R \cdot \vec{H}_{sc} = R \cdot E_T \cdot \vec{s} \quad (4.4)$$

$$\vec{T} = R \cdot \vec{T}_{sc} = R \cdot E_F \cdot \vec{s} \quad (4.5)$$

For a given S/C attitude, the problem of calculation the equivalent  $\Delta V$  of each wheel off-loading is then reduced to the calculation of the combination of thrusting times (vector  $\vec{s}$ ) required to counteract the accumulated angular momentum ( $\vec{H}$ ) with minimum usage of fuel.

In a mathematical way the problem can be expressed as follows:

$$\sum_{i=1,4} s_i = \text{Minimum} \quad (4.6)$$

$$s_i \geq 0, i = 1, 4 \quad (4.7)$$

Because of the symmetric configuration of the Herschel Reaction Control System, the actuation of the four thrusters with the same impulse generates a pure force without any torque. All the solutions to the previous set of equations can then be expressed as a parameterisation from a particular solution:

$$\vec{s}^{opt} = \vec{s}^0 + \lambda \vec{u} \quad (4.8)$$

with:

- $\vec{u} = (1, 1, 1, 1)$  combination of impulses with zero torque
- $\vec{s}^0$  a particular solution (i.e.  $s^0_1 = 0$ ) of equation 4.4

The final solution will be that one with a minimum sum of the impulses of all the four thrusters. This is achieved for (one thruster off):

$$\vec{s}^{opt} = \vec{s}^0 - \min_{i=1,4} s^0_i \vec{u} \quad (4.9)$$

The equivalent  $\Delta V$  (approximation with constant mass  $M$ ) will then be given by the expression:

$$\Delta \vec{V} = \frac{R \cdot E_F \cdot \vec{s}^{opt}}{M} \quad (4.10)$$

#### 4.5.2 Effect of the Helium exhaust flow

The helium nozzles have been arranged such that the resulting nominal torque compensates the torque produced by the Solar radiation pressure. The random residuals of the torque have been included in the previous section. However the force originated by the helium flow will also have a direct major perturbing effect on the orbit.

The average Helium flow per nozzle will be 1 mg/s. The gas outlet temperature for the nominal orbit phase of 66 K will result in an exhaust velocity in the vacuum of 500 m/s. The resulting force will then be 0.5 mN per Nozzle. Both small Nozzles are mounted on the xy plane with an angle of 98° with respect to the X direction (telescope viewing direction) almost opposite to each other. This results in a total force of 140  $\mu N$  along the +X direction with both nozzles operating. This force depends on the spacecraft attitude, so the observation schedule, and must be included in the orbit analysis.

#### 4.5.3 Treatment of the orbit perturbations

The nominal values presented in the previous section will not be exactly reproduced during real operations. The variations on the Solar torque and force will be mainly due to S/C attitude changes. Centre of gravity displacements will also cause variations on the Solar torque. The He mass flow change or nozzle misalignment among others will cause variations both in the torque and force associated to the the venting process.

The nominal force created by the Solar radiation pressure may be included in the propagation for the generation of the nominal orbit but the effect of the deviations with respect to the nominal will have a perturbing effect not known a priori. In the case of the Helium venting the 360° freedom for the yaw angle (rotation around the Sun direction) does not allow a priori estimation of the expected force orientation during operations (apart from being contained in the plane perpendicular to the S/C Z-axis).

On the other hand the accumulated momentum originated by the imbalance between the He venting torque and the Solar radiation pressure must be stored in the Wheel Reaction System. The wheels must then be regularly off-loaded and as explained above, this will have an effect on the orbit maintenance. These two perturbing effects must be studied and included in the propellant budget for the orbit maintenance.

#### 4.5.4 Perturbing Forces

The forces (in the sense of deviations from a priori nominal) produced by the Solar radiation pressure and the He venting system will have to be introduced as perturbations into the dynamic model. As mentioned before a nominal value of the solar radiation pressure force along the Sun-L<sub>2</sub> direction will be included in the orbit generation. No nominal direction for the Helium venting force will be considered in this analysis, as the changes on the S/C attitude during operations (mainly in pitch and yaw) will have a direct impact on the projection of the nominal forces along the inertial axes and in particular along the escape direction. For the Helium venting another effect will be the variation in the mass flow (14% in [17]) .20 $\mu N$  of additional  $\Delta F_x$  must be considered due to this effect.

The reference forces in the S/C body fixed frame are then as follows:

- $F_z = -125\mu N$  due to Solar Radiation Pressure [15].
- $F_x = 140\mu N + 20\mu N = 160\mu N$  due to He venting.

The orbit maintenance shall compensate the projection of the resulting force along the escape direction that will be given by the following expression:

$$F_{esc} = u_1(-F_z \sin(\alpha) + F_x(1 - \cos(\alpha))) + u_2 \sin(\beta)(F_z \cos(\alpha) + F_x \sin(\alpha))$$

where:

- $F_z$  is the force due to Helium venting (160 $\mu N$  in the worst case).

- $F_x$  is the force due to Solar Radiation Pressure ( $125\mu N$ ).
- $u_1, u_2$  are the components of the escape direction the in X-Y plane of the  $L_2$  rotating frame.
- $\alpha$  is the pitch angle of the S/C Z-axis versus  $L_2$ -Sun direction
- $\beta$  is the yaw angle (rotation around the Sun direction).

#### 4.5.5 Simulation results

A Monte Carlo simulation has been run using the following random variables:

- Accumulated Momentum, with the maximum values derived in section 4.5.1 taken as  $3\text{-}\sigma$  values.
- S/C attitude during observations, given by pitch angle ( $\pm 30^\circ$  uniform distribution) and yaw angle ( $\pm 180^\circ$  uniform distribution).
- S/C attitude during wheel off-loading, given by the yaw angle around the Earth pointing direction (also simulated through a uniform distribution).

The wheel off-loadings are assumed to be done once per day however the wheel loading is calculated using equation 4.1. With the helium venting torque compensation for the Herschel wheel capacities, off loading intervals may be in the order of 3 days.

In addition worst cases (S/C attitude for maximum projection of the resulting acceleration along the escape direction) for perturbing force and wheel off-loading have been analysed. Another case is included, assuming that the orbit maintenance follows a reference orbit, this means all perturbation are to be completely removed from the orbit by manoeuvres (method 1 or 4).

The results of the simulations in terms of required  $\Delta V$  per year to compensate the different perturbing effects are presented in table 4.11.

Case	Helium	Wheels
Worst case	1.85	1.00
random (99%)	1.70	0.85
to reference orbit	2.15	1.48

Table 4.11:  $\Delta V$  budget for orbit maintenance, m/s per year

It may be concluded then that an additional allocation of 2.6 m/s ( $1.70\text{m/s}+0.85\text{m/s}$ ) per year will then cover these stochastic effects with a level of confidence of 99%. In the worst case, 2.9 m/s per year have to be allocated, and in case a reference orbit is followed 3.6 m/s will be necessary.

#### 4.5.6 Helium venting during LEOP

Before closing the big nozzle, the total He mass flow will be split in one part coming out through the big nozzle and another part through the small nozzles. The corresponding forces expected for each type of nozzle can be seen in [17]:

- 7.28 mN for the big nozzle
- 1.54 mN for each small nozzle

Taking into account the nozzles orientation, this will result in a total force of 6.85 mN along the S/C X-axis. The expected duration of this period of large mass flow will be around 30 days [17]. The total equivalent  $\Delta V$  corresponding to the previous figures (integration of force along time) is 6 m/s. In order to minimise the trajectory perturbation, the S/C should be oriented such that this  $\Delta V$  has no component along the escape direction. It is then recommended to orient the big nozzle along the out of plane direction.

#### 4.5.7 Required Increase of Maintenance $\Delta V$

The torque compensation by the Helium venting system has a considerable effect on the orbit. The current propellant allocation for orbit maintenance on Herschel (1 m/s per year) will not be sufficient. Admitting that the worst case assumption later in this study is conservative, it is proposed to increase the propellant allocation to 3.0 m/s per year. This then covers the wheel off-loading effects, the helium venting, and other random effect as given in table 4.8 (0.45 m/s per year). The analysis of orbit predictability of section 4.4.2 will also not hold any more. The best choice of the orbit maintenance time interval for Herschel (30 days before) will also have to be reconsidered.

#### 4.6 Effect of Spin Axis Slew Manoeuvres for Planck

For the Planck spacecraft the spin axis (one revolution per minute) is kept pointing to the sun. The libration point  $L_2$  moves around the sun with the Earth, so the angular momentum vector of the spacecraft has to be moved at an average rate of about  $1^\circ$  per day in the ecliptic plane. This will be done firing different possible combinations of pairs of the 1 N attitude control thrusters, once per hour. The phase angle over the spin period of that firings will be optimised to obtain the required torque, the thruster opening times will typically be 0.25 s.

With the torque the thrusters will also generate a force on the spacecraft. The required change of angular momentum will be along the  $y$ -axis in the pseudo-inertial frame  $(x,y,z)$ , rotating with the Earth around the sun. From this the acceleration on the spacecraft can be defined in the same frame. The total linear momentum per day (in kg m/s) for the slew manoeuvres for the two selections of thruster pairs (A1-B1 and A2-B2) then comes out as given in table 4.12. The resulting  $\Delta V$ 's for the Planck spacecraft mass

Thrusters	$I_x$	$I_y$	$I_z$
A1-B1	2.08	0.036	-5.34
A2-B2	2.27	0.048	-5.74

Table 4.12: Linear momentum per day (kg m/s) of slew manoeuvres

of 1154 kg, can then simply be represented by an acceleration, constant in the  $(x,y,z)$  frame as given in table 4.13. Only the case A1-B1 has been taken.

$a_x$	$a_y$	$a_z$
$2 \times 10^{-11}$	$3.6 \times 10^{-13}$	$-5.3 \times 10^{-11}$

Table 4.13: Acceleration by slew manoeuvres ( $km/s^2$ )

For the radiation pressure a spacecraft surface of  $12.95 \text{ m}^2$  and a reflectivity of 1.5 has been assumed. Figure 4.19 shows that the acceleration by the slew manoeuvres is of the same order of magnitude as the radiation pressure.

Figure 4.20 shows the effect of these accelerations on the orbit (projection to  $x$ - $y$ -plane, Earth centred),

The difference to the orbit without radiation pressure and the slew manoeuvres cannot be seen. This is the prime result. The monthly effect of the moon and the yearly effect of the eccentricity of the Earth orbit around the sun can be seen in the figure. But clearly the slew manoeuvres must be included in the dynamic model used for the orbit construction, like the radiation pressure.

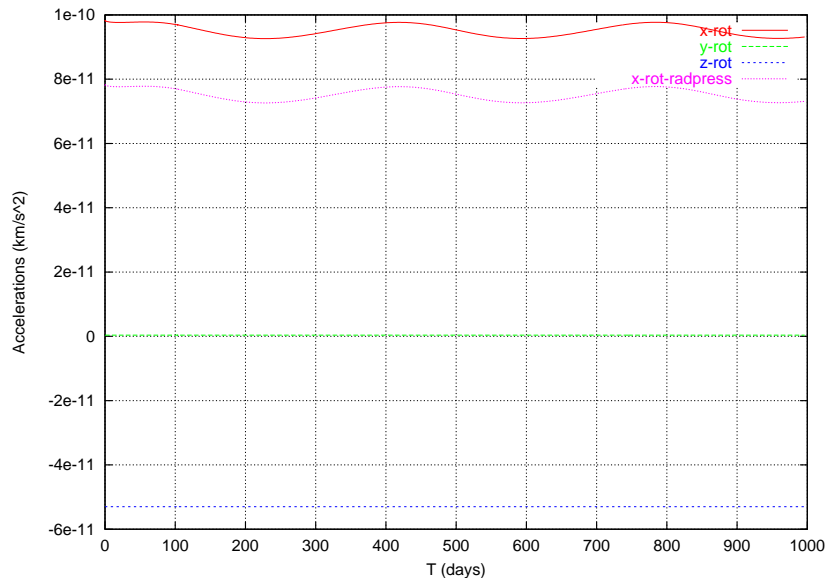


Figure 4.19: Accelerations by radiation pressure and slews

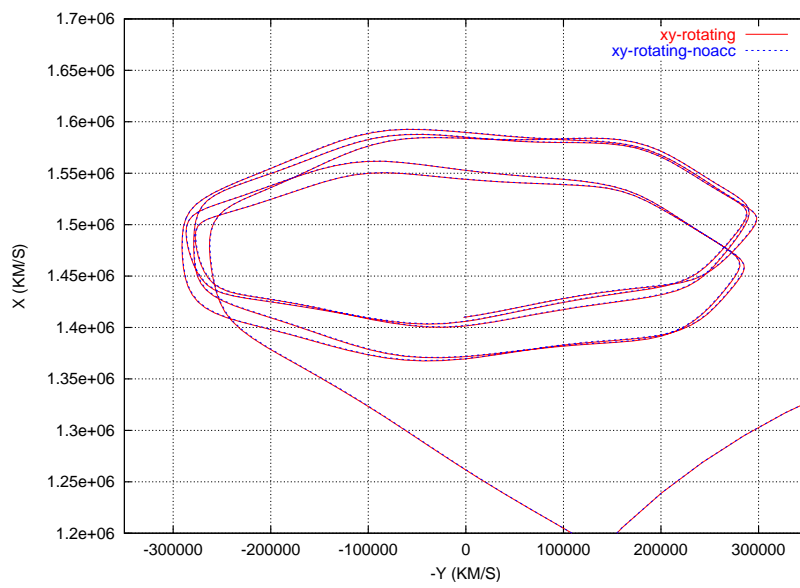


Figure 4.20: Orbit with non-gravitational perturbations

## 5 Conclusions

### 5.1 $\Delta V$ Budget

The  $\Delta V$  budget for the reference Herschel and Planck mission design is given in table 5.1. Sums should not be made because the propellant budget will depend on other system level assumptions, like the manoeuvre decomposition and the margin policy for nominal and extended mission durations.

Table 5.1:  $\Delta V$  budget for Herschel and Planck (A5E/SV - 15° Orbit)

Man.		Herschel	Planck
1	Compensation for perigee velocity variation	26 m/s	26 m/s
2	Removal of launcher dispersion	45 m/s	45 m/s
3	Manoeuvre on day 12 from perigee	3 m/s	3 m/s
4	Mid-course Correction at $T_{inj} - 20$ days	2 m/s	2 m/s
5	Orbit Injection and eclipse avoidance	0 m/s	215 m/s
6	Correction for injection at $T_{inj} + 2$ days	0 m/s	2 m/s
7	Orbit maintenance in operational orbit per year	3 m/s	1 m/s

The following remarks must be made on table 5.1:

- **The  $\Delta V$  budget has been changed from CReMA issue 3.0 to have only one flight program on ARIANE (increase of allocation of corresponding correction manoeuvre to 26 m/s) and to combine the required correction manoeuvre with the stochastic correction manoeuvre on day 2.**
- **the allocation of 215 m/s for the insertion manoeuvre of Planck covers the geometric losses for the current Planck thruster configuration.** This is equivalent to 195 m/s with 91% manoeuvre efficiency as used in the propellant budget of Alcatel. So a 9% reduction has been achieved, due to an improved optimisation allowing for a deviation of the Planck transfer orbit from the Herschel transfer orbit by a small change of the orbit correction manoeuvre on day 2. All deterministic manoeuvres done by Planck during the transfer will use the flat thrusters only (sun aspect angle = 128°).
- An updated launcher dispersion has been provided by Arianespace after the PMAR [10] for the updated launch scenario. The allocation for the manoeuvre on day 2 is 45 m/s. The preferred sun aspect angle of this first stochastic orbit correction (number 2) is shown in figure 3.28, it has been verified that this manoeuvre will be close to along the velocity or opposite with same probability. According to figure 3.28, in the current launch window, Sun aspect angles as low as 10° are possible (180° - 170°). They happen at the opening of the daily slot near equinoxes.
- Manoeuvre 6 corrects the error of the large injection manoeuvre in addition to the station keeping from table 4.8. An allocation has been made though it can be assumed that the insertion manoeuvre will be done in two steps separated by e.g. one day of orbit determination, starting with an "undershoot" such that the manoeuvre in total can be executed quite accurately.
- The target orbit has been chosen as part of the new optimisation such that there will be no more eclipse avoidance manoeuvres on Planck.
- The lifetime for Planck (allocation manoeuvre no 7) will be 21 months from launch for the nominal mission and 30 months for the extended mission. Different margin policies apply for nominal or extended mission, therefore a sum is not given. The Herschel lifetime is 3.5 years nominal and 4.5 years extended, also from launch. The allocation has been increased to 3 m/s per year assuming an orbit maintenance strategy not freezing a reference orbit (strategy 5 in section 4), but also covering the effects of the Helium venting and the wheel-offloading manoeuvres.

## 5.2 Summary of Results

- Different families of Lissajous orbits around  $L_2$  in the sun Earth system were preferred for Herschel and Planck, one specific type for each of the projects, depending on its particular requirements.
- Small orbit corrections along the escape direction (of the linear problem) have been used to numerically generate a variety of non-escape orbits around  $L_2$  (in the exact problem with moon etc.) and also for stochastic orbit maintenance.
- For Herschel/Planck (double launch) the transfer orbit has been selected along the stable manifold of a Lissajous orbit with large amplitudes such that the Herschel spacecraft will reach its destination without deterministic maneuvers after perigee. ARIANE5E/CA will directly deliver the two spacecraft into this orbit. The launch orbit has the same parameters at spacecraft delivery for all launch dates and times. An allocation of 26 m/s has been made for a deterministic correction manoeuvre to compensate for variations in the required perigee velocity relative to the velocity delivered by ARIANE, assuming only one flight program will be available on ARIANE.
- The manoeuvre on day 2 to correct for the launcher dispersion was estimated to require 45 m/s (99-percentile).
- The Planck transfer will slightly deviate from the Herschel stable manifold, from the first orbit correction manoeuvre on day 2. The spacecraft will be injected to an orbit with a smaller size (defined by the maximum sun-spacecraft-Earth angle) by one or two manoeuvres. For each launch date the combination of the amplitudes  $A_y$  and  $A_z$  for a given size (sun-spacecraft Earth angle  $\leq 15^\circ$ ), and the initial phase  $\phi_z$  on the Planck orbit are chosen differently to minimise the insertion  $\Delta V$  from the transfer orbit which is chosen to maximise the launch mass for ARIANE, and to ascertain that the reached orbit is free of eclipse for both spacecraft.
- Several orbit maintenance strategies have been compared for the Lissajous orbits around  $L_2$ . A propellant allocation of 0.5 m/s per year has been found sufficient for Planck to maintain the orbit if a method which does not prescribe a reference orbit is used. The size of the orbit correction manoeuvres mainly depends on the noise in the orbit dynamics of the spacecraft. Orbit predictability then is to the order of 500 km over one year. 1 m/s per year has been allocated for Planck. Manoeuvres will be required about once per month.
- For Herschel, orbit predictability and the orbit maintenance requirements will be strongly influenced by the wheel off-loading and helium venting effects, and the unknown radiation pressure component depending on the spacecraft attitude. An allocation of 3 m/s per year will be necessary for orbit maintenance manoeuvres, and orbit predictability will be not better than to about 3000 km over 6 months in case the free propagation maintenance strategy is selected. Maintaining the orbit along a reference trajectory will give a predictability to the order of magnitude of 100 km, however the maintenance  $\Delta V$  has then to be increased to about 5 m/s per year.
- The orbit determination accuracy, or short term predictability, with 1 range point per day and Doppler tracking will be better than 20 km in position and 1.5 cm/s in velocity. For Herschel it may be up to 3 times worse depending on the knowledge of the helium venting and wheel off loading effects.
- The maximum sun-spacecraft-Earth angle for Herschel will be less than  $36^\circ$  for all cases in the launch window.
- Ground station coverage from New Norcia will be longer than 6 hours per day for Herschel, for all launch dates and throughout the extended mission, and 8 hours for Planck.  $5^\circ$  minimum elevation from the Ground station has to be acceptable for that.

Based on the above, launch windows and propellant budgets were derived for Herschel and Planck:

- The common launch window for 2007 as given in table 3.4 is mainly determined by the propellant limit on Planck. A 159 days launch window per year, with a slot of at least 45 minutes every day (except for a reduction to at least 30 minutes for 3 weeks in February/March), is reached with an allocation of 297 m/s (with geometric losses) on Planck including the stochastic orbit corrections and

the orbit maintenance for 2 years. This is for the 15° target Lissajous orbit and for an ARIANE5E/CA optimum ascent, and only one flight program on ARIANE. The dates in the launch window in 2008 are the same as for 2007, with some minor modifications. An increase of the propellant allocation to avoid sensor blinding by the moon during the first orbit correction manoeuvre is not included in this sum.

- The  $\Delta V$  allocation (just sum of  $\Delta V$ s without decomposition losses !) on Herschel is 92 m/s assuming 4.5 years lifetime.
- 

### 5.3 Open Issues

- The effect of the helium venting on Herschel has been studied in terms of propellant allocation for orbit maintenance. However the orbit determination study has been updated to cover that effect only in a preliminary way. This will have to be revisited.

## References

- [1] M. Hechler, J. Boissieres, On the Midcourse Navigation for the GIOTTO Comet Halley Mission, MAO WP 129, ESOC, June 1980
- [2] M. Hechler, SOHO Mission Analysis, L1-Transfer Trajectory, MAO WP 202, ESOC, March 1984
- [3] R. Farquhar, Halo Orbits and Lunar Swing-by Missions of the 1990's, Acta Astronautica, Vol 24, 1991, pp. 227-234
- [4] G. Gómez, A. Jorba, J. Masdemont, C. Simó, Study Refinement of Semi-Analytical Halo Orbit Theory, Final Report ESOC Contract 8625/89/D/MD(SC), Barcelona, April 1991
- [5] M. Hechler, GAIA/FIRST Mission Analysis: ARIANE and the Orbits around  $L_2$ , MAS WP 393, ESOC February 1997
- [6] M. Hechler, J. Cobos, FIRST Mission Analysis: Transfers to Small Lissajous Orbits around  $L_2$ , MAS WP 398, ESOC July 1997
- [7] M. Hechler, J. Cobos, FIRST/PLANCK and GAIA Mission Analysis: Launch Windows with Eclipse Avoidance Manoeuvres, MAS WP 402, ESOC December 1997
- [8] J. Cobos, M. Hechler, FIRST/PLANCK Mission Analysis: Transfer to Lissajous Orbit Using the Stable Manifold, MAS WP 412, ESOC December 1998
- [9] M. Belló Mora, F. Blesa Moreno, Study on Navigation for Earth Libration Points, Final Report ESA Contract No. 12571/97/D/IM(SC), 1999
- [10] Arianespace, Preliminary Mission Analysis Trajectory and Performance Study Herschel-Planck, Ariane 5-ECA Dedicated Mission, dual launch configuration, A5E-DAMP-TRAJ-HERSCHEL-PLANCK (A4/DP/DS/LM no 2256/2004) issue 1, March 2004
- [11] Herschel DCI 10/501 31, Issue 1, Rev.0, Arianespace, June 2005
- [12] A. Yanez, M. Hechler, HERSCHEL/PLANCK Mission Analysis: Herschel Orbit Maintenance and Wheel Off-loading, MAO WP 467, ESOC March 2004
- [13] M. Hechler, HERSCHEL/PLANCK Mission Analysis: Launch Window, MAO WP 473, ESOC June 2004
- [14] M. Hechler, A. Yanez, HERSCHEL/PLANCK Mission Analysis: Orbit Determination and Control, MAO WP 474, ESOC June 2004
- [15] Calculations of Herschel Solar Forces and Torques ALCATEL SPACE HPP-2-ASPI-TN-0088
- [16] Reaction Wheel System Requirements Specification. Dutch Space H-P-4-DS-SP-0014
- [17] Nozzle position definition and performance EADS Astrium Technical note. HP-2-ASED-TN-0075
- [18] J. Pulido, J. Schoenmaekers, Herschel/Planck Transfer Optimisation, PT-CMOC-FD-TN-2702-OPS-GFI, Issue 1.0, ESOC, June 2005